

UNCLASSIFIED

AD NUMBER

AD856918

LIMITATION CHANGES

TO:

Approved for public release; distribution is unlimited.

FROM:

Distribution authorized to U.S. Gov't. agencies and their contractors; Critical Technology; MAY 1969. Other requests shall be referred to Air Force Materials Laboratory, ATTN: MAAE, Wright-Patterson AFB, OH 45433.

AUTHORITY

AFML ltr dtd 8 Oct 1971

THIS PAGE IS UNCLASSIFIED

AD0856918

63

AFML-TR-69-108

EFFECT OF BETA PROCESSING AND FABRICATION ON AXIAL LOADING FATIGUE BEHAVIOR OF TITANIUM

Emory Beck,
Martin Marietta Corporation

Technical Report AFML-TR-69-108

1969 June

This document is subject to special export controls and each transmittal to foreign governments or foreign nationals may be made only with prior approval of the Air Force Materials Laboratory (MAAE), Wright-Patterson Air Force Base, Ohio 45433.

Air Force Materials Laboratory
Air Force Systems Command
Wright-Patterson Air Force Base, Ohio

20080819 214

NOTICE

When Government drawings, specifications, or other data are used for any purpose other than in connection with a definitely related Government procurement operation, the United States Government thereby incurs no responsibility nor any obligation whatsoever; and the fact that the Government may have formulated, furnished, or in any way supplied the said drawings, specifications, or other data, is not to be regarded by implication or otherwise as in any manner licensing the holder or any other person or corporation, or conveying any rights or permission to manufacture, use, or sell any patented invention that may in any way be related thereto.

This document is subject to special export controls and each transmittal to foreign governments or foreign nationals may be made only with prior approval of the Air Force Materials Laboratory (MAAE), Wright-Patterson Air Force Base, Ohio 45433.

Copies of this report should not be returned unless return is required by security considerations, contractual obligations, or notice on a specific document.

AD856918

EFFECT OF BETA PROCESSING AND FABRICATION ON
AXIAL LOADING FATIGUE BEHAVIOR OF TITANIUM

Emory Beck
Martin Marietta Corporation

This document is subject to special export controls and each transmittal to foreign governments or foreign nationals may be made only with prior approval of the Air Force Materials Laboratory (MAAE), Wright-Patterson Air Force Base, Ohio 45433.

FOREWORD

This final technical report was prepared by the Martin Marietta Corporation, Denver Division, Materials Science Section, under USAF Contract F33615-68-C-1351, Project No. 7381, "Materials Applications," Task No. 738106, "Engineering Design Data," and is submitted in compliance with Contract Data Requirements List Item B003. This report covers the period 1 April 1968 thru 31 March 1969. The program is administered under the direction of the Air Force Materials Laboratory, Air Force System Command, Wright Patterson Air Force Base, Ohio, with Mr. David C. Watson as Project Engineer. The manuscript was released by the author 7 June 1969 for publication.

The work was conducted under the direction of Dr. Jimmy D. Mote, Program Manager, and Emory J. Beck, Technical Director.

The Martin Marietta report number for this document is MCR-69-140.

This technical report has been reviewed and is approved.

A. Olevitch
A. Olevitch
Chief, Materials Engineering Branch
Materials Support Division
Air Force Materials Laboratory

ABSTRACT

A single heat of 6Al-4V titanium has been die forged at conventional and beta forging temperatures. These forgings have been annealed, sectioned, and subsequently machined into tensile and fatigue test specimens. Notched and smooth fatigue specimens were tested in axial-loading fatigue machines at room temperature using three stress ratios. The data presented show that beta-forged material exhibits better fatigue strength than conventionally forged material, while tensile properties are nearly unaffected. A forging temperature of 120°F above the alpha-beta/beta transus was selected as the optimum forging temperature based on initial fatigue results at a single A-ratio of 0.9. This temperature was selected as a compromise between improved forgeability and the superior fatigue results realized for forging near the transus temperature. More extensive fatigue testing at various stress ratios revealed that the beta-forged material had a lower tolerance for the reversed load cycle ($A = \infty$) than the conventional-forged material. Surface effect studies for the same heat of 6Al-4V titanium indicated that mechanical material removal in a controlled manner was not detrimental to fatigue strength but was of considerable benefit. Shot peening at an intensity of 0.010A did not improve the fatigue limit of conventional or beta-forged material.

This abstract is subject to special export controls and each transmittal to foreign governments or foreign nationals may be made only with prior approval of the Air Force Materials Laboratory (MAAE), Wright-Patterson Air Force Base, Ohio 45433.

(The reverse of this page is blank.

TABLE OF CONTENTS

	<u>Page</u>
I. Introduction	1
II. Material and Forging Technique	2
III. Program Plan	17
IV. Experimental Procedure	19
1. Test Specimen Design	19
2. Specimen Preparation	20
3. Test Description	31
V. Test Results and Discussion	34
1. Forging Effects	34
2. Surface Effects	69
VI. Conclusions and Recommendations	83
Appendix -- Tables	85
Distribution	100 thru 108

Form 1473

LIST OF ILLUSTRATIONS

<u>Figure</u>		<u>Page</u>
1	Photomacrographs of Billet Material Ti 6Al-4V, Heat 293882	3
2	Cogged Preform, Ti 6Al-4V	5
3	Photograph of Blocker Shape, Ti 6Al-4V (Mag. 2/3X)	6
4	Photographs of Finish Shape, Ti 6Al-4V (Mag. 2/3X)	7
5	R-475 Forging	8
6	Test Specimen Orientation and Location Designation	9
7	Drawing of Test Forging Showing Macro Location	11
8	Photographs of Macrostructure and Microstructure of Material Forged above the Beta Transus at $T_B + 50^\circ\text{F}$	12
9	Photograph of Macrostructure of Material Forged above the Beta Transus at $T_B + 120^\circ\text{F}$	13
10	Photographs of Macrostructure and Microstructure of Material Forged above the Beta Transus at $T_B + 270^\circ\text{F}$	14
11	Photographs of Macrostructure and Microstructure of Two-Stage Forged Material, Blocking at $T_B + 270^\circ\text{F}$ and Finishing at $T_B - 80^\circ\text{F}$	15
12	Photographs of Macrostructure and Microstructure of Material Conventionally Forged Below the Beta Transus at $T_B - 80^\circ\text{F}$	16
13	Round Tension and Notched Tension Specimen Designs	21
14	Smooth and Notched Fatigue Specimen Designs	22
15	Notched Profiles Before and After Polishing, Magnification 30X	24
16	Surface Profile Photographs of Lathe-Turned 6Al-4V Titanium Alloy	25
17	Surface Profile Photographs of Chemically Milled 6Al-4V Titanium Alloy	26

18	Surface Profile Photographs of Ground 6Al-4V Titanium Alloy	27
19	Surface Profile Photographs of Lathe-Turned and Shot-Peened 6Al-4V Titanium Alloy	28
20	Surface Profile Photographs of Ground and Shot-Peened 6Al-4V Titanium Alloy	29
21	Fatigue Laboratory at Martin Marietta	32
22	Smooth Fatigue Specimens, Adapters, and Alignment Cell	33
23	S-N Curve for 6Al-4V Titanium Alloy Finish Forged at 1750°F ($T_B - 80^\circ\text{F}$)	36
24	S-N Curve for 6Al-4V Titanium Alloy Finish Forged at 1750°F ($T_B - 80^\circ\text{F}$)	37
25	S-N Curve for 6Al-4V Titanium Alloy Finish Forged at 1750°F ($T_B - 80^\circ\text{F}$)	38
26	S-N Curve for 6Al-4V Titanium Alloy Finish Forged at 1750°F ($T_B - 80^\circ\text{F}$)	39
27	S-N Curve for 6Al-4V Titanium Alloy Finish Forged at 1750°F ($T_B - 80^\circ\text{F}$)	40
28	S-N Curve for 6Al-4V Titanium Alloy Finish Forged at 1750°F ($T_B - 80^\circ\text{F}$)	41
29	S-N Curve for 6Al-4V Titanium Alloy Finish Forged at 1880°F ($T_B + 50^\circ\text{F}$)	42
30	S-N Curve for 6Al-4V Titanium Alloy Finish Forged at 1880°F ($T_B + 50^\circ\text{F}$)	43
31	S-N Curve for 6Al-4V Titanium Alloy Finish Forged at 1950°F ($T_B + 120^\circ\text{F}$)	44
32	S-N Curve for 6Al-4V Titanium Alloy Finish Forged at 1950°F ($T_B + 120^\circ\text{F}$)	45
33	S-N Curve for 6Al-4V Titanium Alloy Finish Forged at 1950°F ($T_B + 120^\circ\text{F}$)	46
34	S-N Curve for 6Al-4V Titanium Alloy Finish Forged at 1950°F ($T_B + 120^\circ\text{F}$)	47
35	S-N Curve for 6Al-4V Titanium Alloy Finish Forged at 1950°F ($T_B + 120^\circ\text{F}$)	48
36	S-N Curve for 6Al-4V Titanium Alloy Finish Forged at 1950°F ($T_B + 120^\circ\text{F}$)	49

37	S-N Curve for 6Al-4V Titanium Alloy Finish Forged at 2100°F ($T_B + 270^\circ\text{F}$)	50
38	S-N Curve for 6Al-4V Titanium Alloy Finish Forged at 2100°F ($T_B + 270^\circ\text{F}$)	51
39	S-N Curve for 6Al-4V Titanium Alloy Finish Forged at 1750°F (Blocked at $T_B + 270^\circ\text{F}$ and Finished at $T_B - 80^\circ\text{F}$)	52
40	S-N Curve for 6Al-4V Titanium Alloy Finish Forged at 1750°F (Blocked at $T_B + 270^\circ\text{F}$ and Finished at $T_B - 80^\circ\text{F}$)	53
41	S-N Curve for 6Al-4V Titanium Alloy Finish Forged at 1750°F (Blocked at $T_B + 270^\circ\text{F}$ and Finished at $T_B - 80^\circ\text{F}$)	54
42	S-N Curve for 6Al-4V Titanium Alloy Finish Forged at 1750°F (Blocked at $T_B + 270^\circ\text{F}$ and Finished at $T_B - 80^\circ\text{F}$)	55
43	S-N Curve for 6Al-4V Titanium Alloy Finish Forged at 1750°F (Blocked at $T_B + 270^\circ\text{F}$ and Finished at $T_B - 80^\circ\text{F}$)	56
44	S-N Curve for 6Al-4V Titanium Alloy Finish Forged at 1750°F (Blocked at $T_B + 270^\circ\text{F}$ and Finished at $T_B - 80^\circ\text{F}$)	57
45	S-N Curve for STA 6Al-4V Alloy Finish Forged at 1880°F ($T_B + 50^\circ\text{F}$)	58
46	S-N Curve for STA 6Al-4V Alloy Finish Forged at 1880°F ($T_B + 50^\circ\text{F}$)	59
47	Fatigue Properties of Solution-Treated and Aged Parent Metal 6Al-4V Titanium Alloy	60
48	Constant-Life Diagram for Conventionally Forged 6Al-4V Titanium Alloy in Annealed Condition . . .	61
49	Constant-Life Diagram for Beta-Forged ($T_B + 120^\circ\text{F}$) 6Al-4V Titanium Alloy in Annealed Condition	62
50	Constant-Life Diagram for Two-Stage Forged 6Al-4V Titanium Alloy in Annealed Condition . . .	63
51	Summary of Forging Temperature Effects on Smooth Fatigue Strength of 6Al-4V Titanium Alloy ($A = 0.9$)	66

52	Summary of Forging Temperature Effects on Notched Fatigue Strength of 6Al-4V Titanium Alloy ($K_t = 3.0$, $A = 0.9$)	67
53	S-N Curve for Chemically Milled 6Al-4V Titanium Alloy Finish Forged at 1750°F ($T_B - 80^\circ\text{F}$)	70
54	S-N Curve for Lathe-Turned 6Al-4V Titanium Alloy Finish Forged at 1750°F ($T_B - 80^\circ\text{F}$)	71
55	S-N Curve for Ground 6Al-4V Titanium Alloy Finish Forged at 1750°F ($T_B - 80^\circ\text{F}$)	72
56	S-N Curve for Lathe-Turned and Shot-Peened 6Al-4V Titanium Alloy Finish Forged at 1750°F ($T_B - 80^\circ\text{F}$)	73
57	S-N Curve for Ground and Shot-Peened 6Al-4V Titanium Alloy Finish Forged at 1750°F ($T_B - 80^\circ\text{F}$)	74
58	S-N Curve for Chemically Milled 6Al-4V Titanium Alloy Finish Forged at 1950°F ($T_B + 120^\circ\text{F}$)	75
59	S-N Curve for Lathe-Turned 6Al-4V Titanium Alloy Finish Forged at 1950°F ($T_B + 120^\circ\text{F}$)	76
60	S-N Curve for Ground 6Al-4V Titanium Alloy Finish Forged at 1950°F ($T_B + 120^\circ\text{F}$)	77
61	S-N Curve for Lathe-Turned and Shot-Peened 6Al-4V Titanium Alloy Finish Forged at 1950°F ($T_B + 120^\circ\text{F}$)	78
62	Summary of Surface Effects on Fatigue Strength of 6Al-4V Titanium Alloy Finish Forged at 1750°F ($T_B - 80^\circ\text{F}$, $A = 0.9$)	80
63	Summary of Surface Effects on Fatigue Strength of 6Al-4V Titanium Alloy Finish Forged at 1950°F ($T_B + 120^\circ\text{F}$, $A = 0.9$)	81

LIST OF TABLES

<u>Table</u>		<u>Page</u>
I	Chemical Analysis of Ti-6Al-4V Billet Stock . . .	2
II	Test Plan	18
III	Mechanical Properties of 6Al-4V Titanium for Five Forging Conditions, Heat No. 293882	35
IV	Summary of Forging Effects Fatigue Data	64
V	Summary of Fatigue Data for Conventional, Beta Two-Stage-Forged 6Al-4V Titanium Alloy	65
VI	Summary of Fatigue Data for Surface Effect Studies of Conventional and Beta-Forged 6Al-4V Titanium Alloy	79
VII	Cross Reference between Forging Serial Number and Material Condition	86
VIII	Fatigue Data for Conventional-Forged ($T_B - 80^\circ\text{F}$) and Annealed 6Al-4V Titanium Alloy	87
IX	Notched Fatigue Data for Conventional-Forged ($T_B - 80^\circ\text{F}$) and Annealed 6Al-4V Titanium Alloy .	88
X	Fatigue Data for Beta-Forged ($T_B + 50^\circ\text{F}$) and Annealed 6Al-4V Titanium Alloy	89
XI	Fatigue Data for Beta-Forged ($T_B + 50^\circ\text{F}$) and Solution-Treated and Aged 6Al-4V Titanium Alloy	90
XII	Fatigue Data for Beta-Forged ($T_B + 120^\circ\text{F}$) and Annealed 6Al-4V Titanium Alloy	91
XIII	Notched Fatigue Data for Beta-Forged ($T_B + 120^\circ\text{F}$) and Annealed 6Al-4V Titanium Alloy	92
XIV	Fatigue Data for Beta-Forged ($T_B + 270^\circ\text{F}$) and Annealed 6Al-4V Titanium Alloy	93
XV	Fatigue Data for Two-Stage-Forged and Annealed 6Al-4V Titanium Alloy	94
XVI	Notched Fatigue Data for Two-Stage-Forged and Annealed 6Al-4V Titanium Alloy	95

XVII	Fatigue Data for Conventionally Forged 6Al-4V Titanium Alloy with the Indicated Surface Condition	96
XVIII	Fatigue Data for Conventionally Forged 6Al-4V Titanium Alloy with the Indicated Surface Condition	97
XIX	Fatigue Data for Beta-Forged ($T_B + 120^\circ\text{F}$) 6Al-4V Titanium Alloy with the Indicated Surface Condition	98
XX	Fatigue Data for Beta-Forged ($T_B + 120^\circ\text{F}$) 6Al-4V Titanium Alloy with the Indicated Surface Condition	99

SECTION I

INTRODUCTION

The traditional approach to titanium alloy forging has been to heat the forging stock to some temperature below the alpha-beta/beta transus and work the material to the desired shape. This practice has been required because material heated to temperatures above the beta transus transforms and becomes rather brittle.

Designers of aerospace structural components frequently desire a high level of sophistication in the parts they design. Working with aluminum and alloy steels, these shapes have been feasible. With titanium, less shape sophistication has been possible. The necessity for forging at relatively low temperatures has been a primary reason for this limitation.

It was found that titanium that had been extensively and continuously worked above the beta transus rather than just heated into this range, exhibited a significant improvement in fracture toughness without adversely affecting other mechanical properties.

Wyman-Gordon, our subcontractor on this program, took advantage of this interesting potential and performed the necessary work to demonstrate that beta forging would improve shape sophistication, reduce costs, and in some cases improve mechanical properties.

The evaluations of beta forged titanium have shown that strength properties are relatively unaffected, ductility decreases slightly, and toughness increases. The largest void in our property information associated with the process is the effect on fatigue behavior.

The objectives of this research are to study two specific and distinct areas of fatigue technology that require design information data. These are:

- 1) Effect of forging history (beta forging);
- 2) Effect of surface condition.

SECTION II

MATERIAL AND FORGING TECHNIQUE

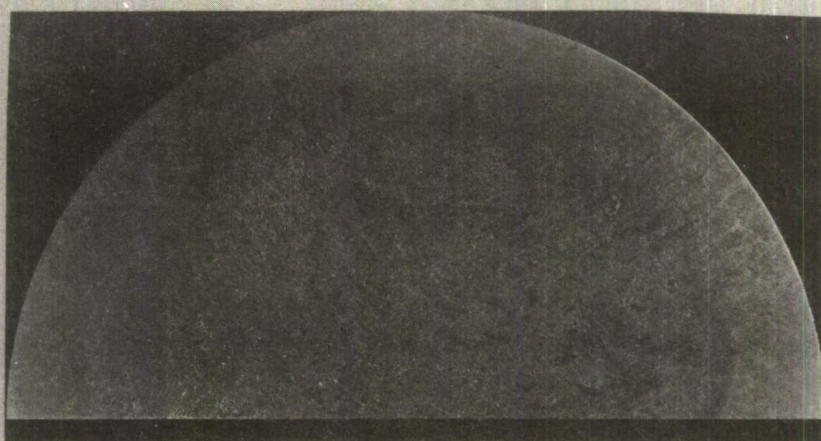
In the selection of a forged shape, two courses were considered. The first was to forge a pancake shape using the open-die technique. This permits all of the required specimens to be obtained from a single uniform property section. However, the pancake is not sufficiently representative of the aerospace components for which the beta forging process will be used.

The alternative was to use a closed die to forge a simple typical aerospace component. Closed-die forgings are attractive because they are normally made in two stages using different dies. Initial working is performed in a blocker die; subsequent working is performed in a final finish die. The forging selected for this work was a small component shape frequently used by Wyman-Gordon for forging evaluation. This shape incorporates a rectangular solid section approximately $6\frac{1}{2} \times 3\frac{1}{2} \times 2$ in., which should exhibit good uniformity of working history and mechanical properties. The rectangular section is ideally suited to provide the required test specimen blanks. To provide a sufficient number of specimens for each testing condition, a number of forgings must be prepared. This presented another attractive feature in favor of press forging where high reproducibility can be obtained from part to part and test results that accurately reflect typical behavior can be obtained.

All forgings for this program are made from 6Al-4V titanium alloy stock, 6-in. diameter, Heat Number 293882. The source of the material was Reactive Metals, Inc. Chemical analysis of this stock is shown in Table I. The billet macrostructure is shown in Figure 1. The alpha-beta/beta transus (T_B) of this heat of material was found to be 1830°F.

Table I Chemical Analysis of Ti-6Al-4V Billet Stock

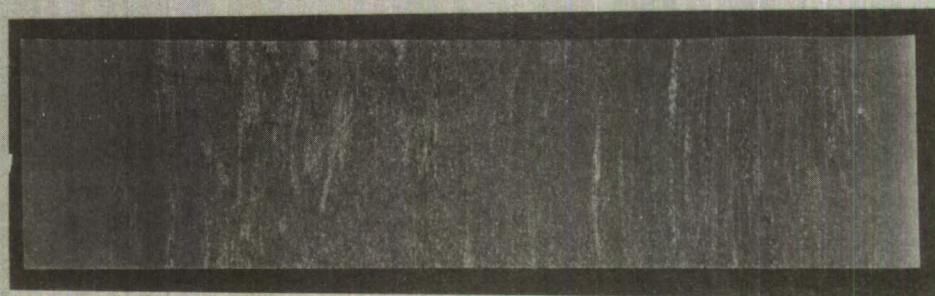
	Chemical composition (weight %)						
	Al	V	Fe	C	N ₂	H ₂	O ₂
293822 Mill cut	6.2	4.3	0.09	0.010	0.010	0.0057	0.182
W-G Analysis C-5422	6.18	4.19	0.09	0.009	0.009	0.0043	0.187



Neg. 5635

Transverse

3/4X



Neg. 5636

Longitudinal

3/4X

Figure 1 Photomicrographs of Billet Material Ti 6Al-4V,
Heat 293882

All material was forged in two steps, blocker and finish, from a cogged preform shape. The small dies used for forging are designated R-475. All forging operations were conducted on a 1500-ton hydraulic press. Approximate dimensions of the cogged preform are shown in Figure 2(a). A photograph of the cogged preform is shown in Figure 2(b). Blocker and finish shape are shown in Figure 3 and 4, respectively. Drawings showing the blocker and final forging dimensions are given in Figures 5(a) and 5(b), respectively.

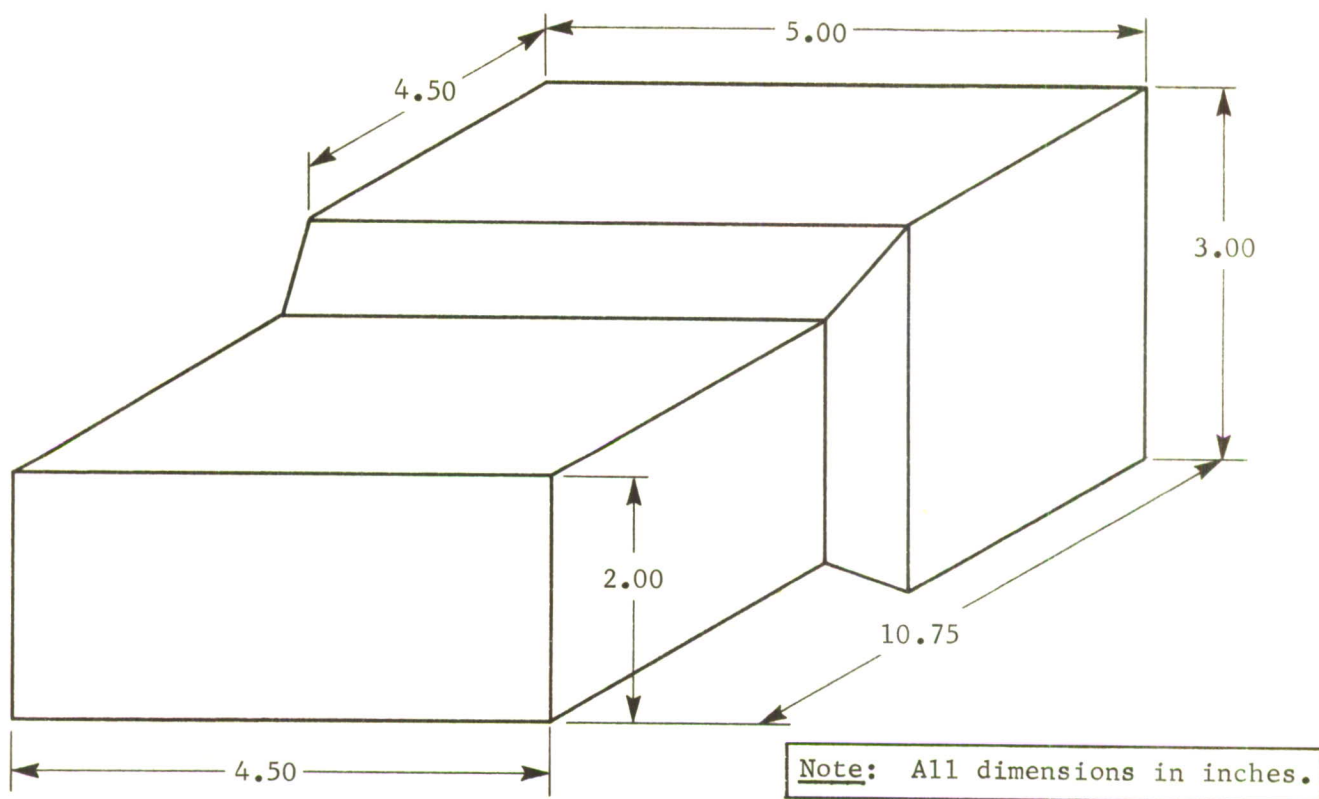
The cogging operation was performed at 1750°F. The cogged preform was then heated to the specified forging temperature, and held at this temperature for 30 minutes to obtain thermal equilibrium throughout the mass. The preform was then quickly removed from the furnace into the preheated dies (720 to 740°F) and forged. It takes less than 30 sec to move the part from the furnace into the dies and forge.

The five forging conditions selected for evaluation are listed below:

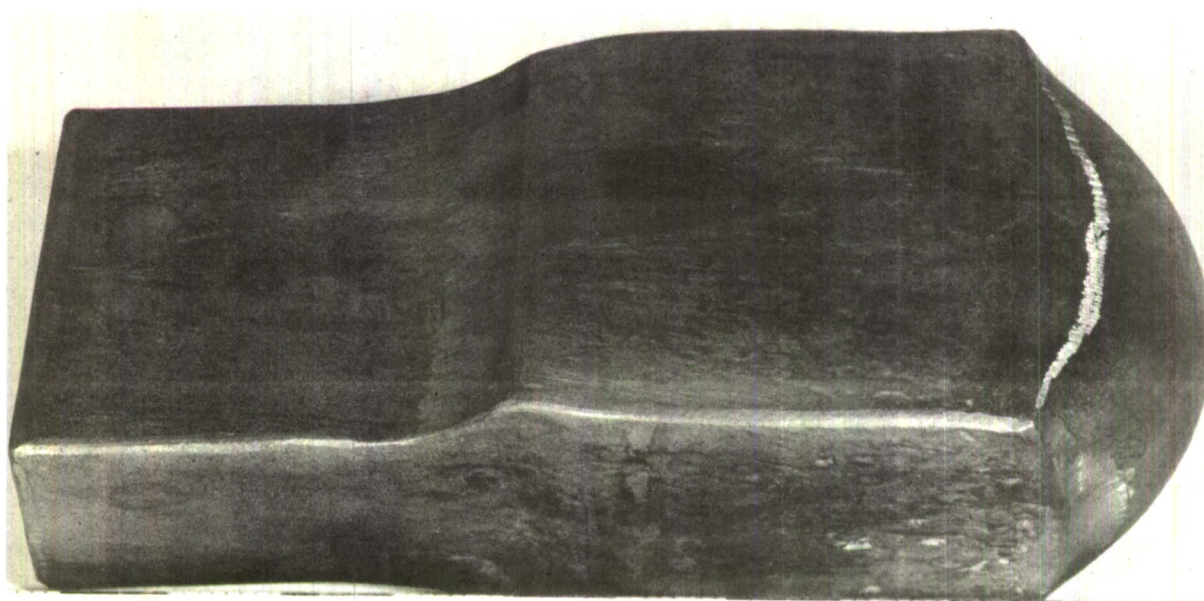
- 1) Conventionally forged in alpha-beta range at $T_B - 80^\circ\text{F}$ (1750°F);
- 2) Beta forged at $T_B + 50^\circ\text{F}$ (1880°F);
- 3) Beta forged at $T_B + 120^\circ\text{F}$ (1950°F);
- 4) Beta forged at $T_B + 270^\circ\text{F}$ (2100°F);
- 5) Two-stage forging, blocked at $T_B + 270^\circ\text{F}$ (2100°F) and finished at $T_B - 80^\circ\text{F}$ (1750°F).

Blocker and finish forging is performed at the same temperature with the exception of the two-stage forging. After forging, all material was annealed (1300°F - 2 hr, AC) except for two $T_B + 50^\circ\text{F}$ forgings which were solution-treated and aged (1725°F - 1 hr, H₂O quench, 1000°F - 4 hr, AC).

All forgings are identified with a serial number and sectioned into 12 specimen blanks as shown in Figure 6. A cross reference between forging condition and serial number is shown in the appendix, Table VII. Each specimen blank is stamped on the end with the appropriate forging serial number and location designation so that mechanical behavior can be checked against specimen location in the forging.



(a) Dimension of Cogged Preform



(b) Photograph of Cogged Preform

Figure 2 Cogged Preform, Ti 6Al-4V

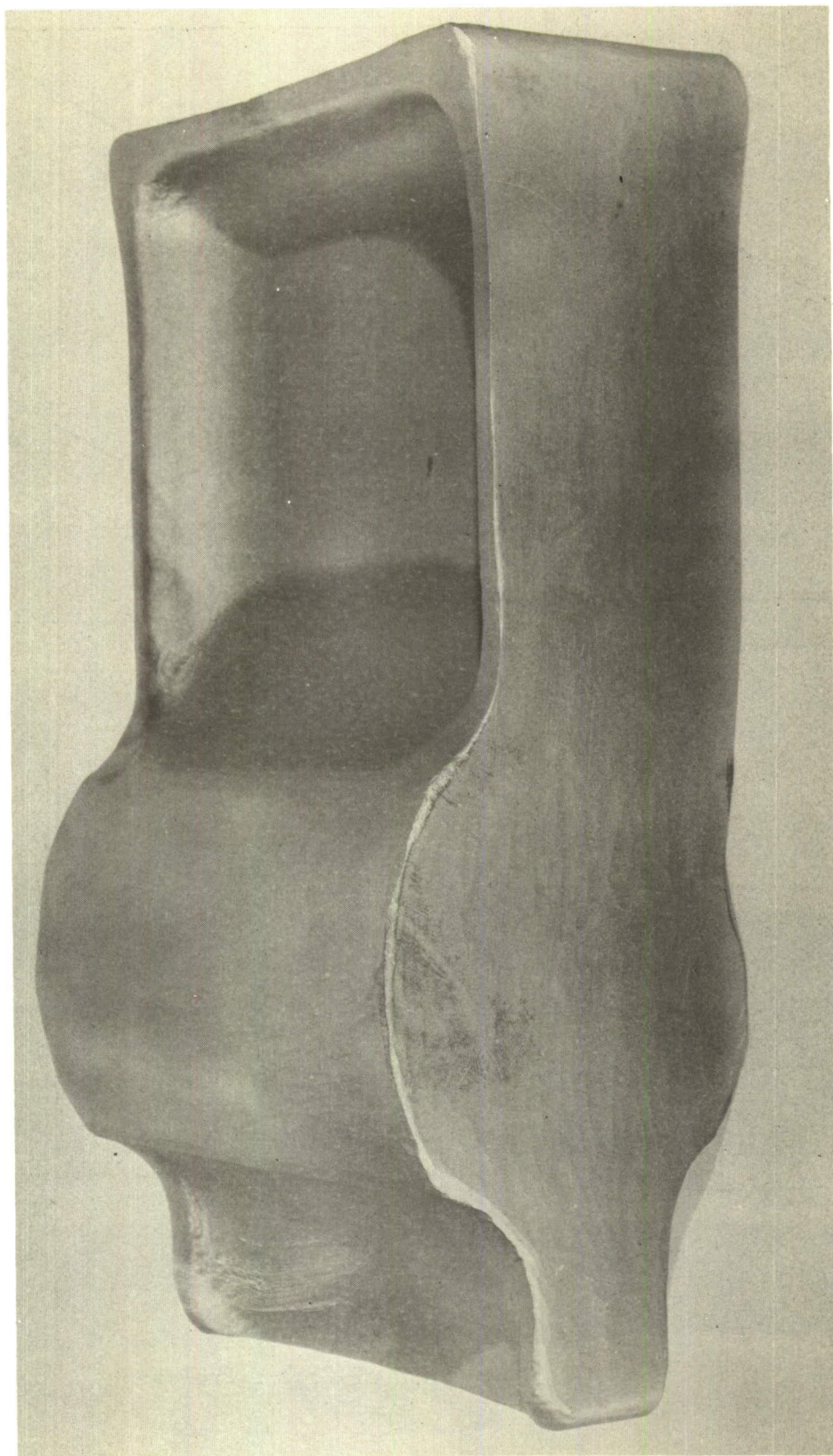


Figure 3 Photograph of Blocker Shape, Ti 6Al-4V (Mag. 2/3X)

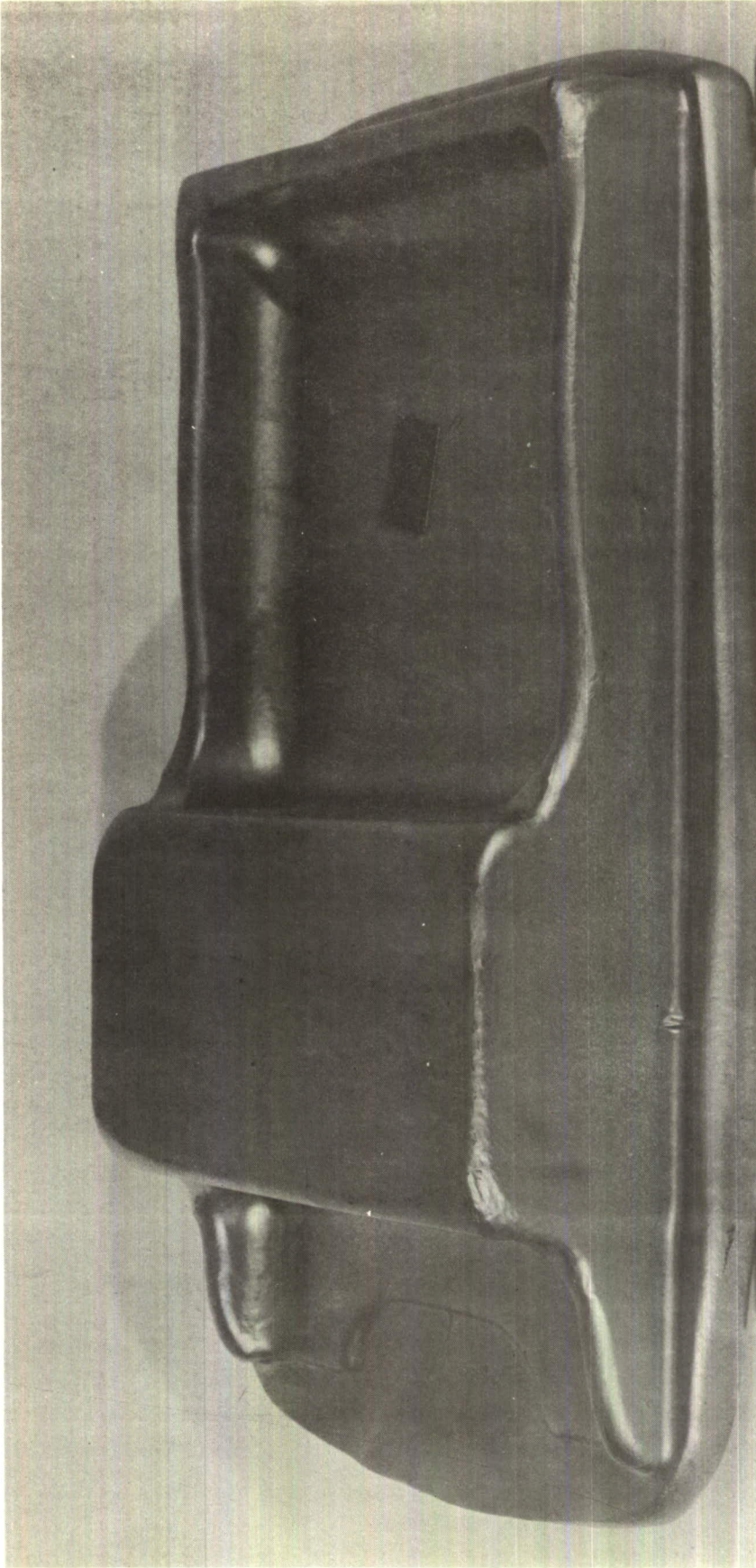


Figure 4 Photograph of Finish Shape, Ti 6Al-4V (Mag. 2/3X)

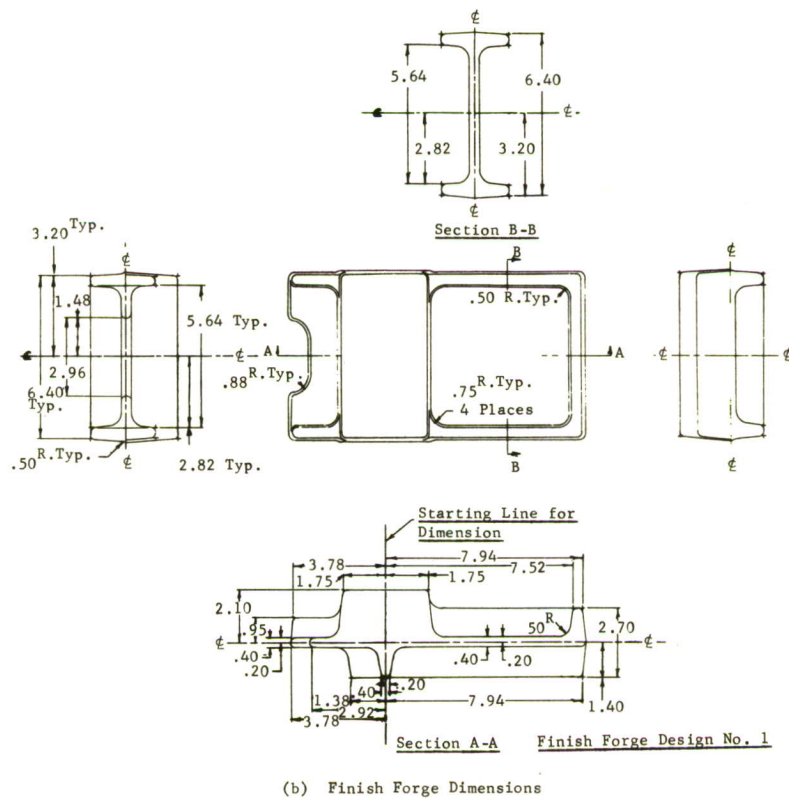
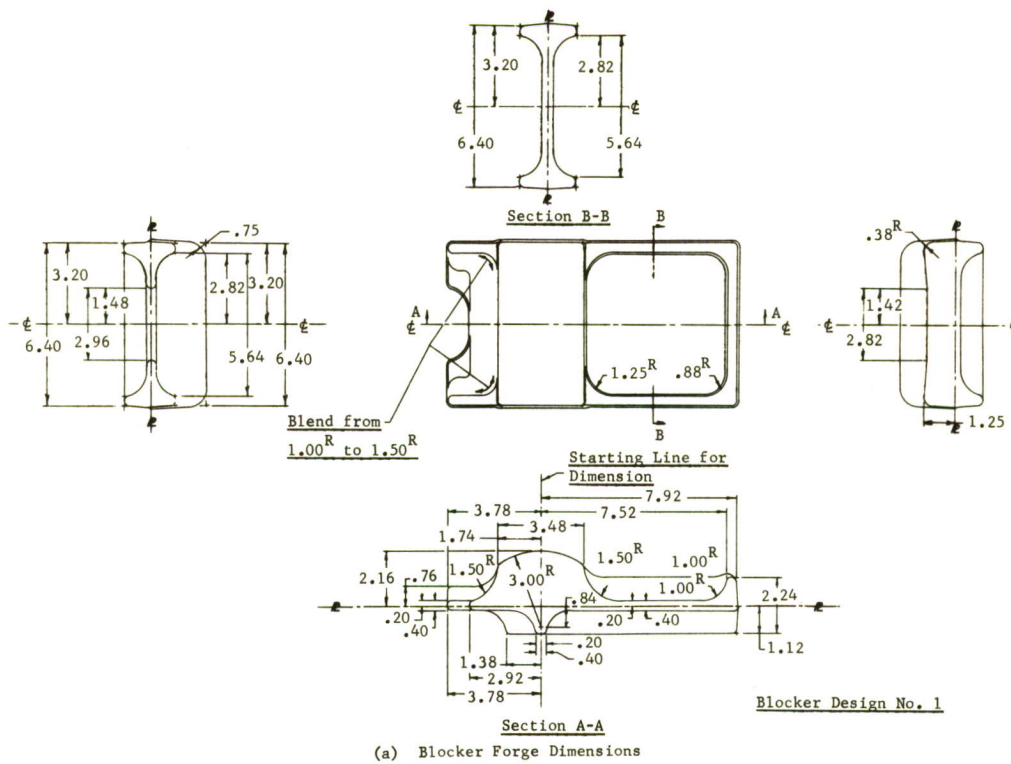


Figure 5 R-475 Forging

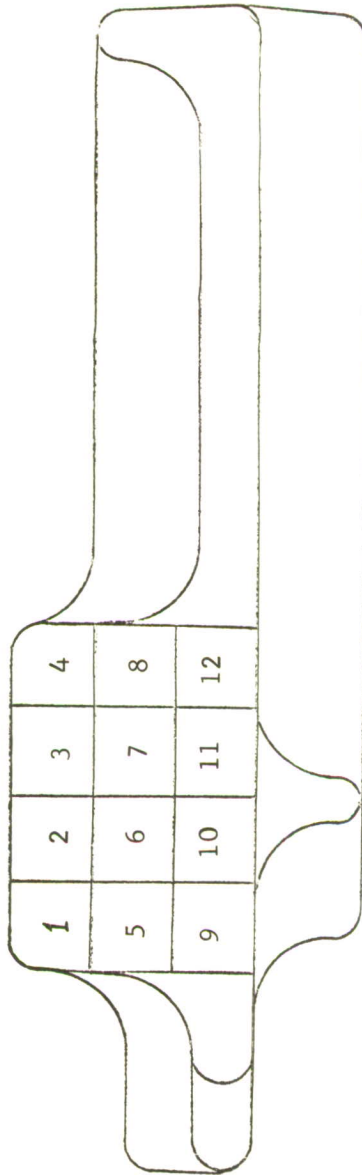


Figure 6 Test Specimen Orientation and Location Designation

One forging representative of each forging condition has been sectioned for metallurgical examination. These sample forgings were sectioned as shown in Figure 7. The etched macrostructures and microstructures for all forging conditions are shown in Figures 8 thru 12. Notice the larger-grain structure in the beta forgings when compared to the conventional forging in Figure 12. The flow lines are quite distinct in the conventional and two-stage-forged material but are not easily discerned in the three beta-forged photomacrographs. This indicates that this forging configuration has produced uniform working of the beta grain and should yield uniform properties in the bulk of the forged mass. This worked grain structure is very desirable in beta forged material, which would otherwise be brittle; and is of little significance in the alpha-beta-forged material.

The photomacrographs also show an equiaxed layer of grains on the top and side surfaces of the beta finished forgings. When the beta-forged blocker is reheated into the beta temperature range for the finish forging operation the entire forging is recrystallized. When the forging is placed in the die and the die is closed, the surface of the part in contact with the die face cools very rapidly and does not flow in the die. This results in a "dead metal" zone at the surface of the forging. This region of nonuniformity, i.e., the dead zone, does not extend too far into the material block and is subsequently machined away when the reduced section of the specimen is made.

The shape of the alpha platelets in the completely beta-forged parts are very similar. However, the alpha platelets in the two-stage forging are thicker than in the beta forgings. This change in shape is a result of heating in the alpha-rich region of the phase diagram during the finish-forging operation.

It was also decided to evaluate the effect of beta forging on 6Al-4V titanium in the solution-treated and aged condition (STA). Material used for this evaluation was beta forged at 1880°F in the usual manner, cut into specimen blanks, and heat treated. Heat treating these small blanks helped assure uniform hardening that could not be obtained if heat treating was performed on the forged block.

The STA condition was achieved by solution treating at 1725°F for 1 hr, water quenching, and aging at 1000°F for 4 hr.

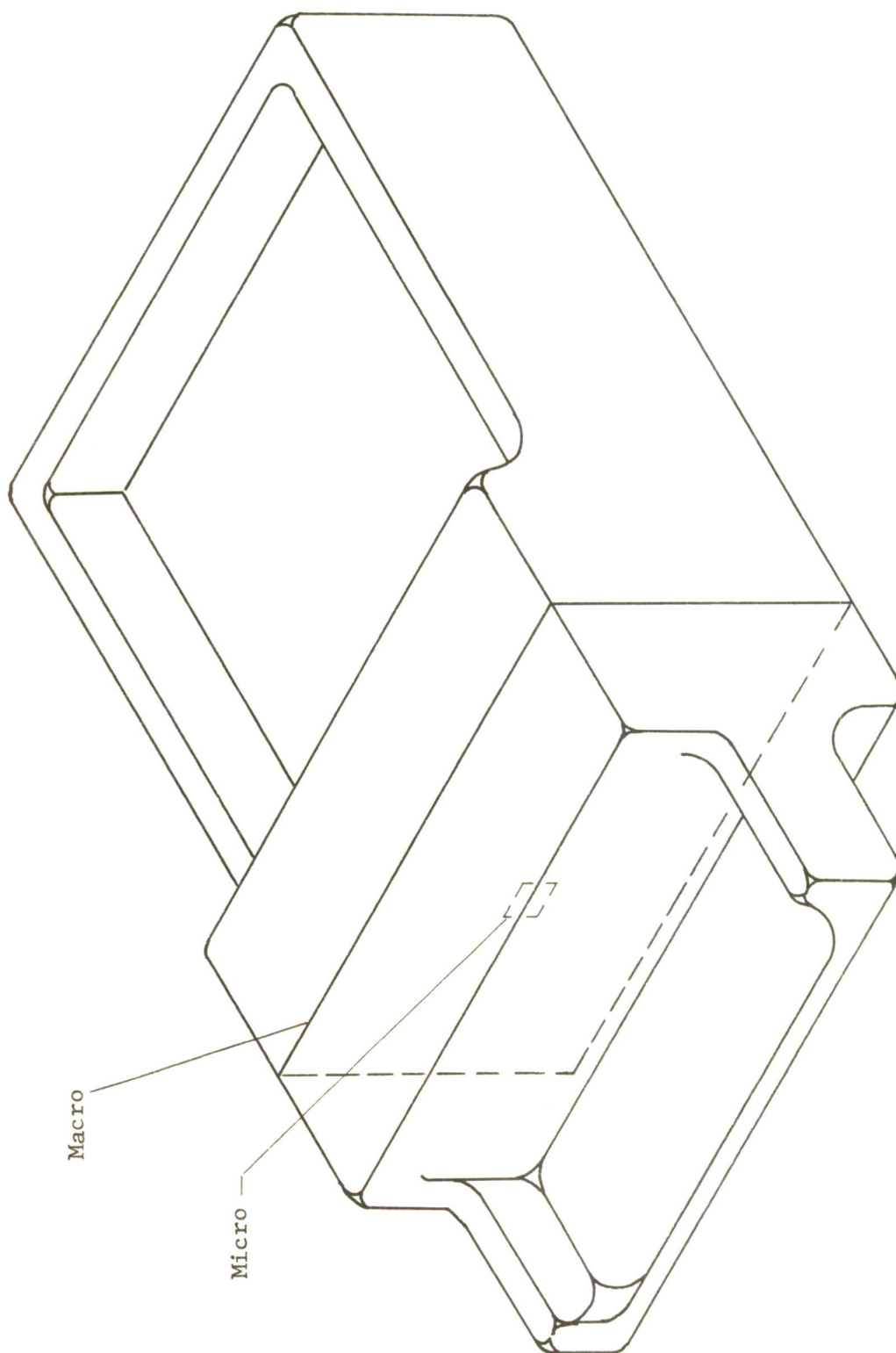


Figure 7 Drawing of Test Forging Showing Macro and Micro Location

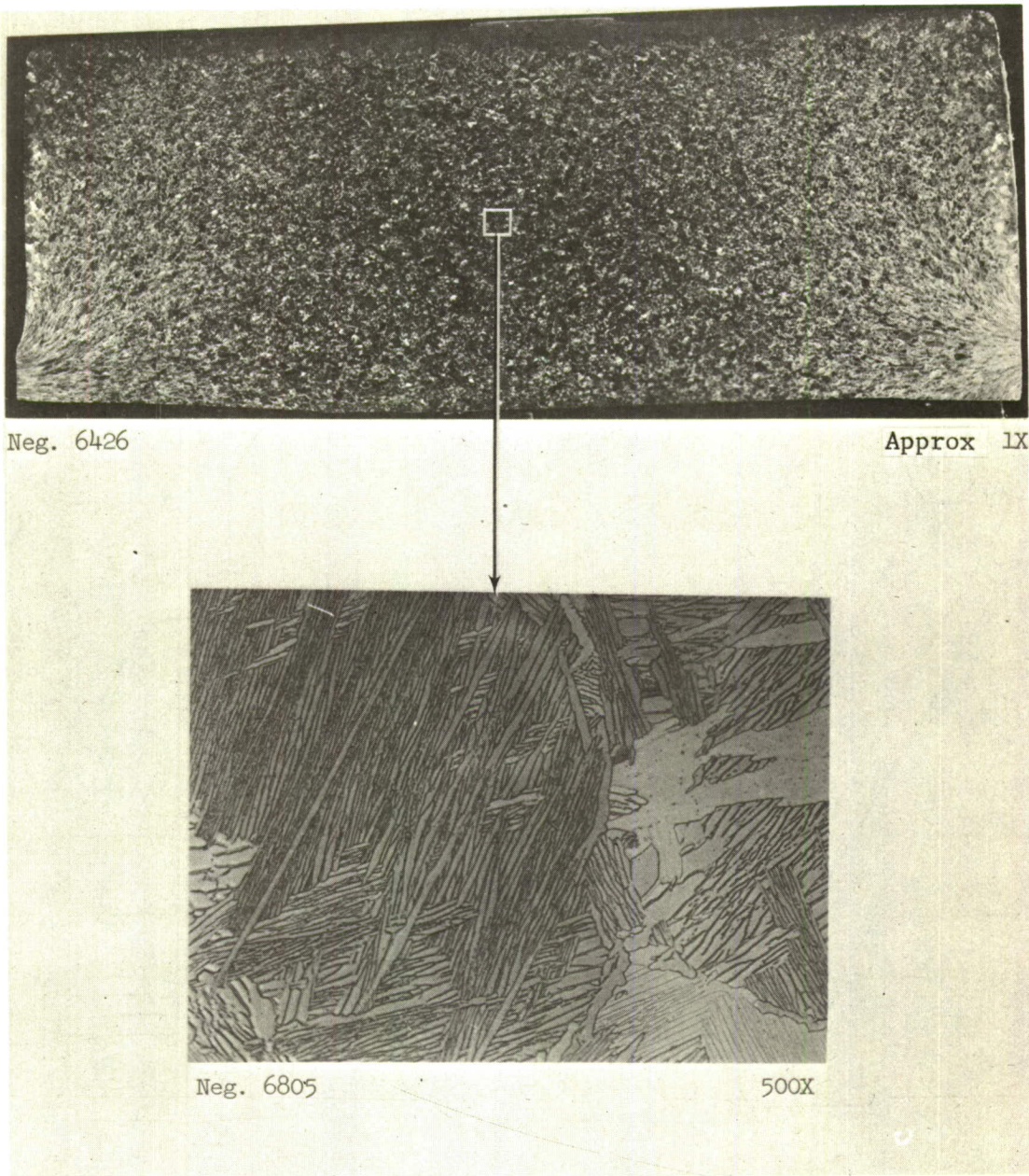
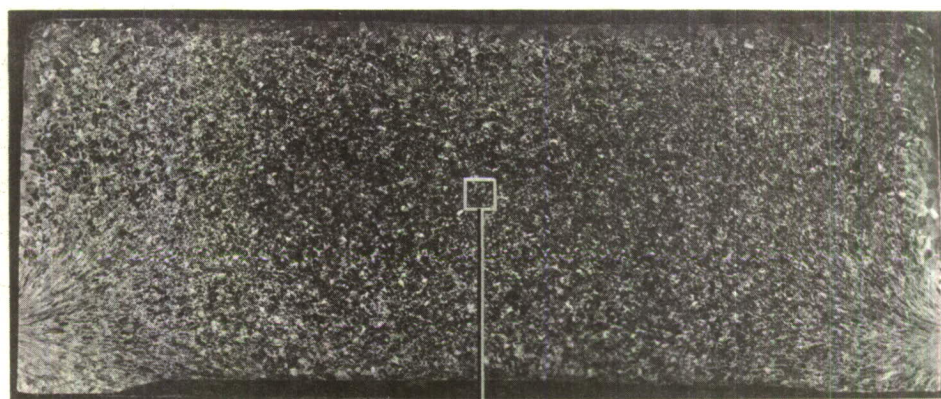
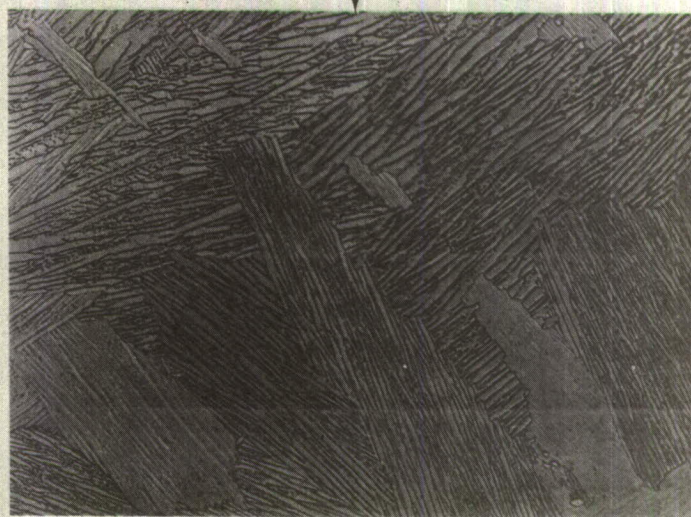


Figure 8 Photographs of Macrostructure and Microstructure of Material Forged above the Beta Transus at $T_B + 50^\circ\text{F}$



Neg. 6798

Approx 1X



Neg. 6807

500X

Figure 9 Photographs of Macrostructure of Material Forged above the Beta Transus at $T_B + 120^\circ\text{F}$

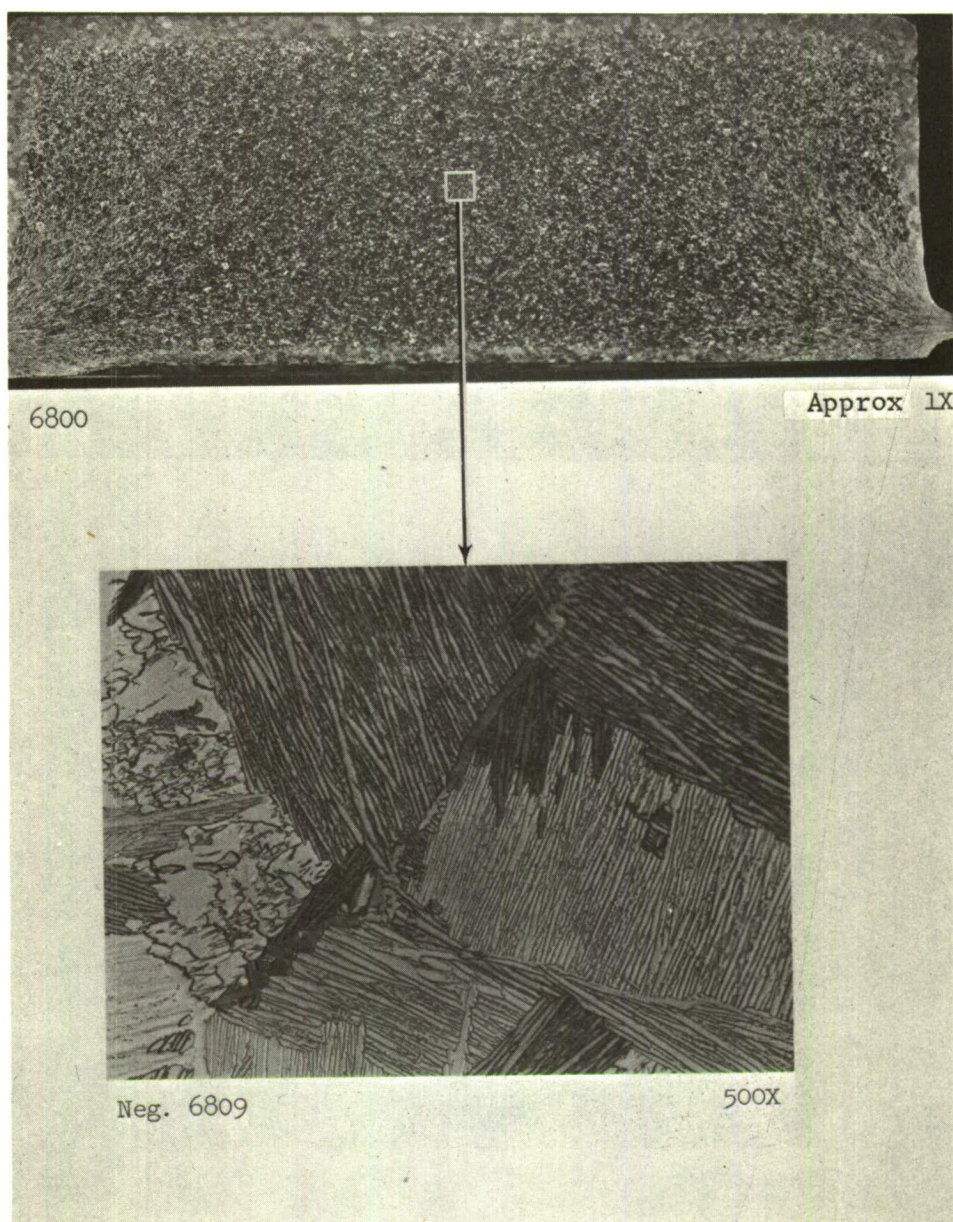


Figure 10 Photographs of Macrostructure and Microstructure of Material Forged above the Beta Transus at $T_B + 270^\circ\text{F}$



Neg. 6799

Approx 1X



Neg. 6811

500X

Figure 11 Photographs of Macrostructure and Microstructure of Two-Stage Forged Material, Blocking at $T_B + 270^\circ\text{F}$ and Finishing at $T_B - 80^\circ\text{F}$

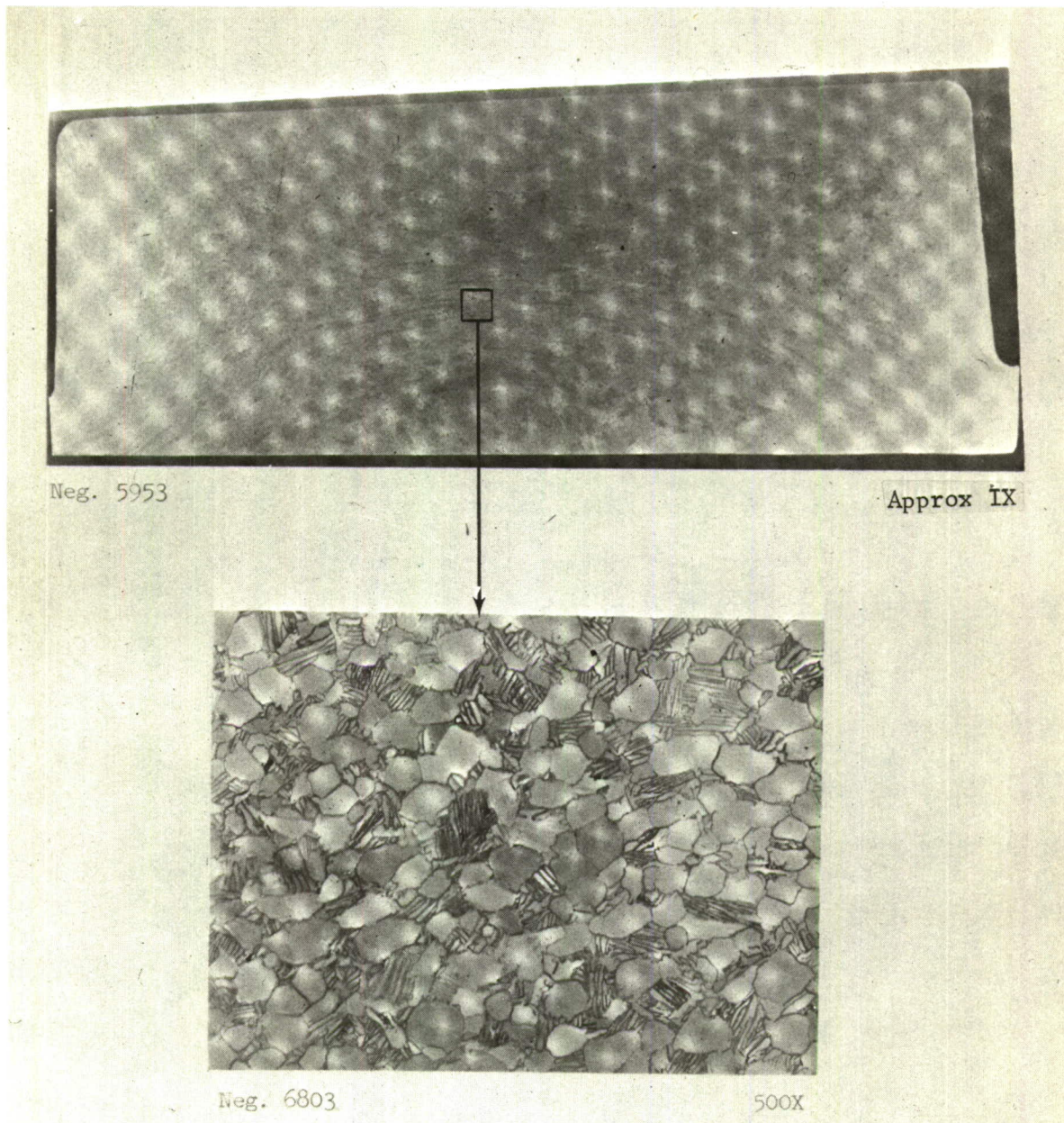


Figure 12 Photographs of Macrostructure and Microstructure of Material Conventionally Forged Below the Beta Transus at $T_B - 80^\circ\text{F}$

SECTION III

PROGRAM PLAN

The test plan prepared for this program was designed to provide a rather extensive evaluation of processing and fabrication variables within the framework of a limited number of experimental determinations. This was accomplished by separating the evaluation into two distinct areas of study: forging temperature effects and surface preparation effects. Room temperature fatigue strength was used as the major criterion for establishing relative performance. Axial loading was employed to permit evaluation at different stress ratios and because this loading mode is the most common and can be easily correlated to other loading environments. Table II summarizes the test plan.

Conventional-alpha-beta-forged material was evaluated to provide a baseline of comparison for the other forging conditions. The effect of forging, blocking and finishing, above the beta transus was determined at three temperatures. In addition, some material was blocked above the beta transus and finished below the beta transus. The optimum forging temperature was then selected from these five forging procedures for further evaluation. One group of beta forgings was solution treated and aged to determine the effect of heat treatment.

The fatigue evaluation was performed using notched and unnotched test specimens at three A^1 -ratios (∞ , 0.9, 0.33). Cycle life was controlled within the range of 10^4 to 10^7 cycles to failure. At least 10 tests were performed for each set of conditions and a corresponding best fit S-N curve was drawn. These curves were then used to construct constant life diagrams.

The effect of machining or processing was studied by determining the fatigue properties after imposing a variety of controlled surface finishes on conventional and optimum forged 6Al-4V titanium material.

$A^1 = \frac{S_a}{S_m}$, where S_a = stress amplitude, and S_m = mean stress.

Table II Test Plan

Forging condition	Heat treatment	Number of specimens for indicated condition						
		Tension	Notched tension	Smooth fatigue A-ratio		Notched fatigue A-ratio		
				∞	0.9	0.33	∞	0.9
Forging Effects								
Conventional Alpha-Beta ($T_B^* - 80^\circ\text{F}$)	Annealed	3	3	10	10	10	10	10
Beta ($T_B + 50^\circ\text{F}$)	Annealed	3			10		10	
Beta ($T_B + 120^\circ\text{F}$)	Annealed	3			10		10	
Beta ($T_B + 270^\circ\text{F}$)	Annealed	3			10		10	
2-Stage ($T_B + 270^\circ\text{F}$ and $T_B - 80^\circ\text{F}$)	Annealed	3	3	10	10	10	10	10
Beta optimum, ($T_B + 120^\circ\text{F}$)	Annealed		3	10	10	10	10	10
Beta ($T_B + 50^\circ\text{F}$)	Solution-treated and aged	<u>3</u>	<u> </u>	<u>10</u>	<u>10</u>	<u> </u>	<u> </u>	<u> </u>
Total tests		18	9	130	130	110	110	
Surface effects								
Surface condition		Number of specimens for indicated material						
		Alpha-Beta ($T_B - 80^\circ\text{F}$)			Optimum-Beta ($T_B + 120^\circ\text{F}$)			
		10	10	10	10	10	10	10
Lathe-turned (63 rms, nominal)								
Ground (32 rms nominal)								
Chemically milled (125 rms or better)								
Late-turned and shot peened								
Ground and shot peened								
Total tests			50					40
*Alpha-Beta/Beta transformation temperature.								

SECTION IV

EXPERIMENTAL PROCEDURE

1. TEST SPECIMEN DESIGN

Round bar specimens were selected for both static and dynamic testing. The round bars were selected primarily because they are somewhat more amenable to surface conditioning. For axial loading, smooth specimen shape does not appear to significantly affect fatigue behavior, which is in contrast to reversed bending in which stress gradients and critical volume subjected to peak stresses appear to have an effect.

Our unnotched and notched tensile specimens were designed in general accordance with standard ASTM specifications.

Fatigue specimens were specially designed to provide simplicity of installation and accuracy of alignment. The scheme incorporates a bearing shoulder at the end of the threaded section for alignment and locking, as opposed to aligning on threads, which is commonly done. Using threads for alignment is a poor practice and should be avoided whenever possible. The advantage of this system is that only two close tolerance alignment surfaces are required. The specimen, when locked with a preloaded nut at each end of the threaded bar, can be subjected to a tension-compression loading cycle that is continuous through zero. A torque of approximately 400 in.-lb is used for preloading each nut and is applied without twisting the specimen.

The notch configuration in tensile and fatigue specimens was designed to a theoretical stress concentration factor (K_t) of 3.0. The physical relationships required to obtain the stress concentration are delineated in Peterson² and were balanced with the load capacity available for testing and manufacturing considerations to arrive at the final specimen design.

The unnotched specimen was designed with a large gage section radius, 9.0 in., which has a theoretical stress concentration of 1.0. Actually, a 3.0-in. radius is sufficient to prevent stress concentration, but a 9.0-in. radius was selected for additional

²R. E. Peterson: Stress Concentration Design Factors. John Wiley & Sons, Inc., N. Y., 1962.

assurance. This large section radius is used to preclude scatter. An advantage is gained by subjecting a smaller portion of the specimen to the maximum stress, and therefore reducing the probability that a defect or metallurgical nonhomogeneity will occur in this small area.

All test specimens were machined from 3/4-in.-square blanks cut from the forging. Specimen orientation and location designations are shown in Figure 6.

Four types of test specimens were used for this program. They are tensile, notched tensile, smooth fatigue, and notched fatigue. Specimen designs are shown in Figures 13 and 14. The smooth fatigue specimen configuration was used for all forging and surface effect studies.

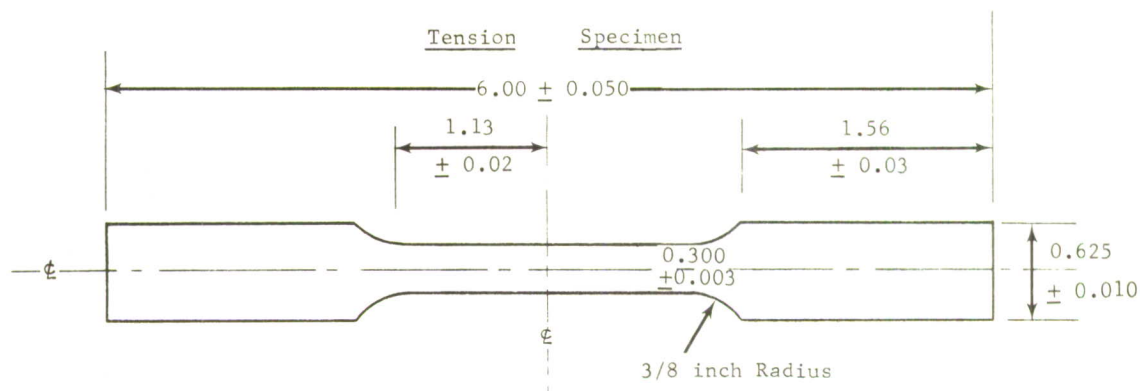
2. SPECIMEN PREPARATION

a. Forging Effect Studies. Smooth fatigue specimens were polished using techniques described in ASTM, STP-91, Section IV. These specimens must pass visual inspection that requires a surface finish classified as 4-L using visual surface roughness gages. Several specimens have been inspected with a surface profilometer. Agreement between visual and profilometer surface-roughness measurements was good.

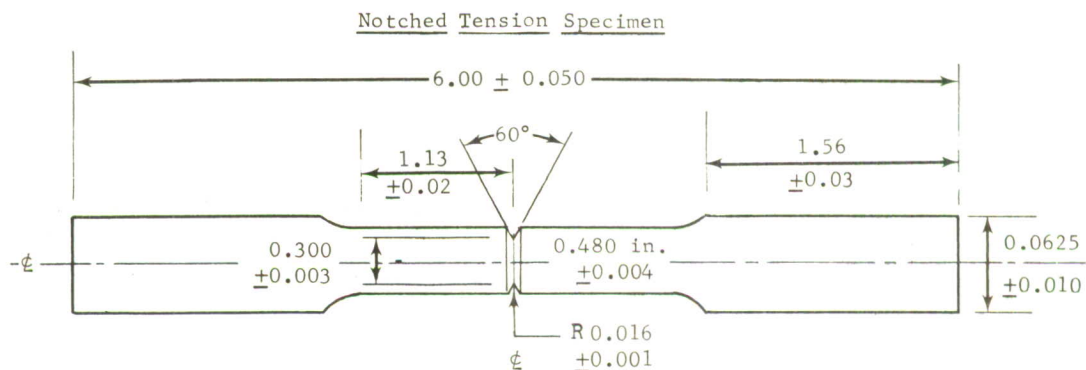
Notched fatigue specimens require notch-root polishing to obtain an accurate stress concentration and to remove scratches and worked material at the root of the notch.

The recommended procedure³ for polishing notches is to load polishing compound on a metal wire and draw the wire through the notch as the specimen is rotated. This method has proved to be effective for our notched specimens if a suitable metal wire and polishing compound is used. In the technique developed for this work, tungsten wire, 0.030-in. diameter, with DuPont 606 polishing compound, was selected for polishing the 6Al-4V titanium alloy specimens. Satisfactory polishing rates were not achieved when softer metal was used as the wire carrier. The DuPont compound contains silica as an abrasive in a water soluble carrier. The carrier is composed of kerosene, water, and calcium hydrate. This compound has the consistency of soft butter and adheres well to the metal wire.

³Manual on Fatigue Testing. ASTM, STP 91.



- Note:
1. Diameter of reduced section can taper slightly to center, 0.003 in. is acceptable.
 2. Do not under cut at reduced section radius.
 3. Polish reduced section until scratches are removed.



- Note:
1. Notch root radius is critical and must be inspected optically after machining.
 2. Root of notch should be polished to remove all scratches.
 3. Lathe turned finish is acceptable except for notch.

Figure 13 Round Tension and Notched Tension Specimen Designs

The tungsten wire is held in a coping saw frame where it can be manipulated easily. The wire is not allowed to remain in one position during polishing, but is rotated and drawn into different areas where fresh compound is present. A slight pressure is applied between the wire and specimen during polishing. The specimen is rotated in a lathe at a speed of approximately 150 rpm. After a short period of polishing the compound is washed from specimen and wire for optical inspection. A profile view of a typical notched specimen before and after polishing is shown in Figure 15. Notch tension specimens are also polished using the above procedure.

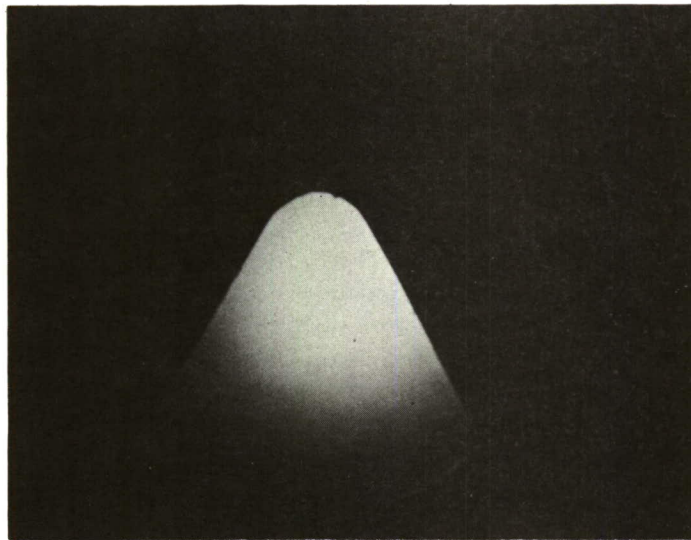
b. Surface Effect Studies.

(1) Lathe-Turned Surface. Fatigue specimens requiring a lathe-turned (nominal 63 rms) surface finish were machined using a procedure similar to that used for smooth fatigue specimens in the forging effect studies. Although these specimens required no polishing, the surface finish was controlled by using a special technique that helped eliminate variation between each specimen.

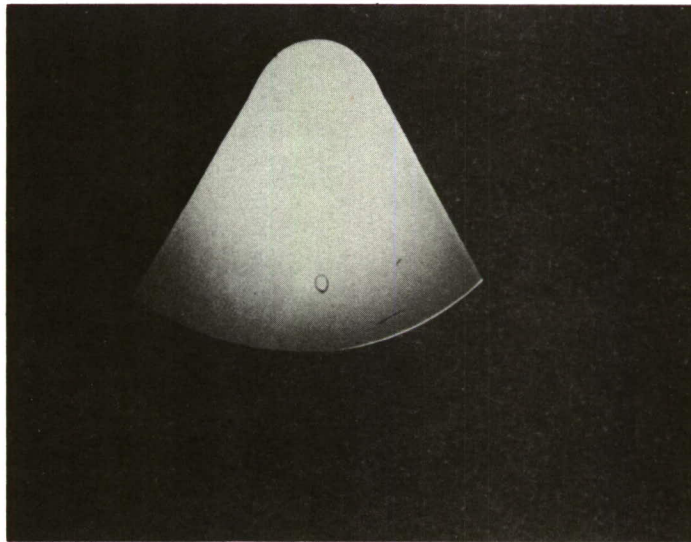
This lathe-turned finish was obtained by making the last finish lathe cut with a special tool. This tool, used only for the final cut on all specimens, remains sharp and retains its profile for a longer period of time. Rake angle and lathe speed and feed are held constant. Surface roughness readings were taken on each lathe-turned specimen. Readings on all specimens were 30 to 60 rms. A photomicrograph of a sectioned lathe-turned specimen is shown in Figure 16. Some compression and distortion of the grains near the surface can be observed in this figure.

Figures 16 thru 20 show surface profile photos before and after etching. Both conditions are presented because of the difficulty experienced in retaining edge definition after etching. To help solve this problem, a nickel coating was electro-deposited on the surface of the titanium. This procedure was quite successful if the nickel was deposited in sufficient thickness, e.g., Figure 20.

(2) Chemically Milled Surface. A chemically milled surface finish was obtained by polishing and chemically milling the reduced section of oversize (test section only) lathe-turned fatigue specimens. During chemical milling, the diameter of each fatigue specimen is reduced from 0.285 ± 0.002 to 0.250 ± 0.002 in.

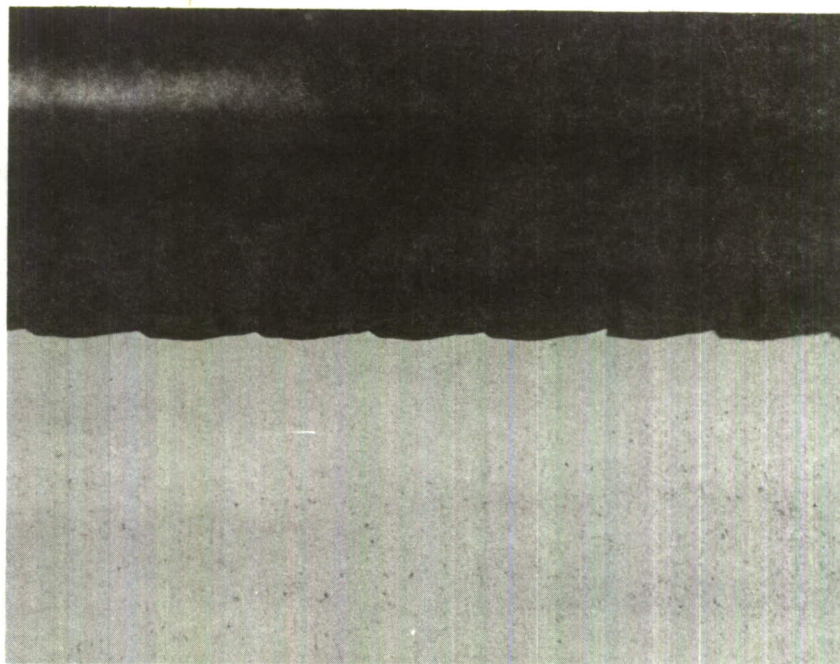


(a) Notch Profile before Polishing

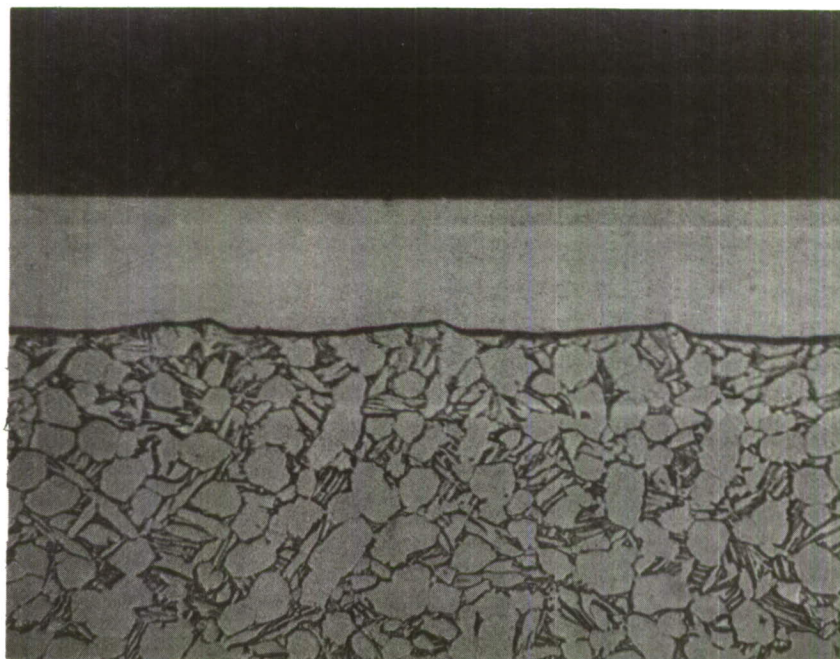


(b) Notch Profile after Polishing

Figure 15 Notched Profiles Before and After Polishing,
Magnification 30X

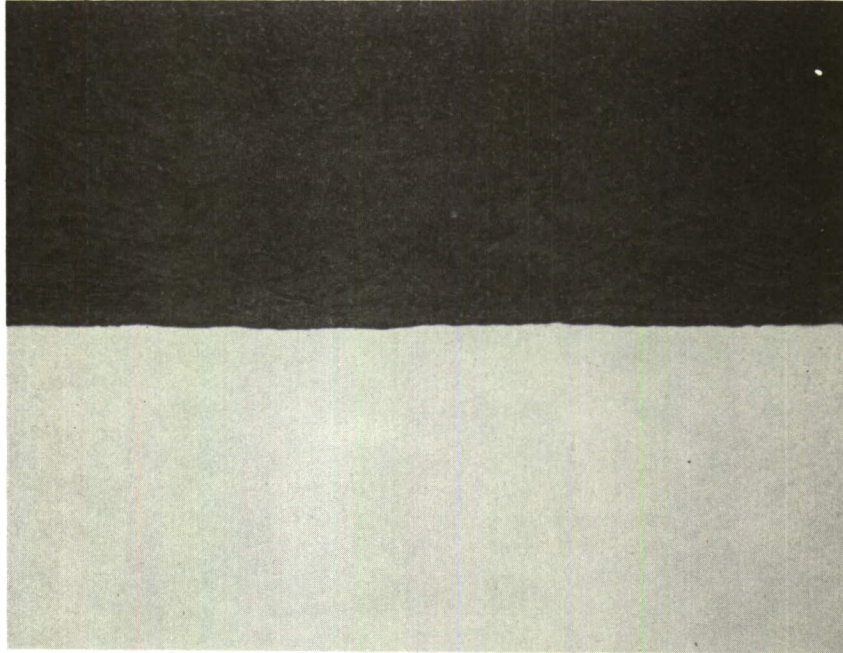


(a) Surface Profile before Etching, 200X

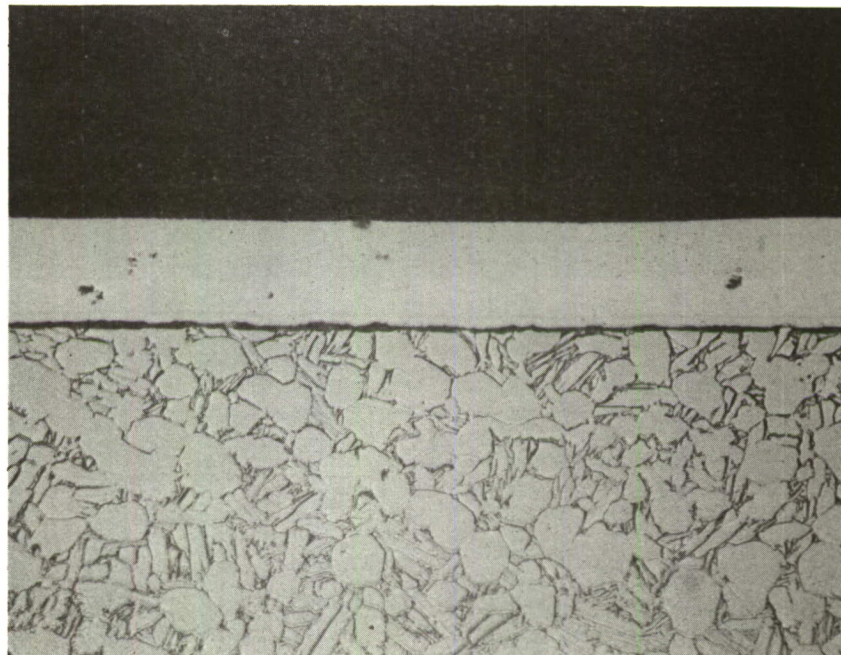


(b) Surface Profile after Etching, 400X

Figure 16 Surface Profile Photographs of Lathe-Turned 6Al-4V Titanium Alloy

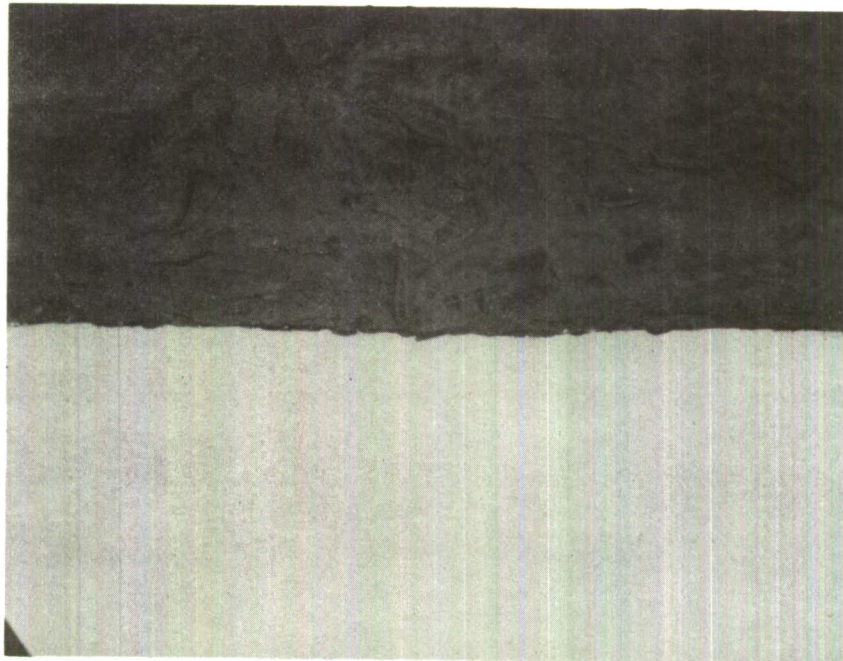


(a) Surface Profile before Etching, 200X

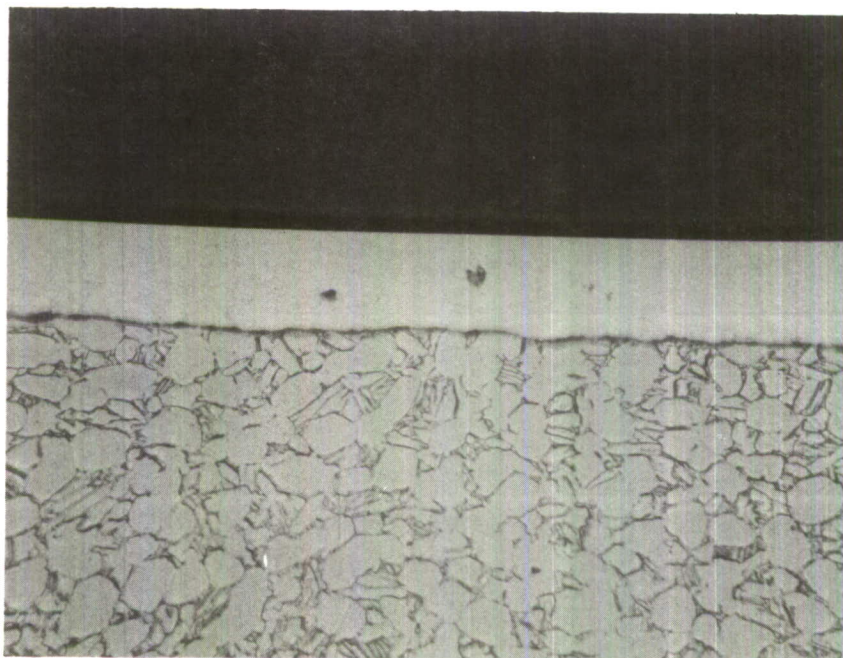


(b) Surface Profile after Etching, 400X

Figure 17 Surface Profile Photographs of Chemically Milled 6Al-4V Titanium Alloy

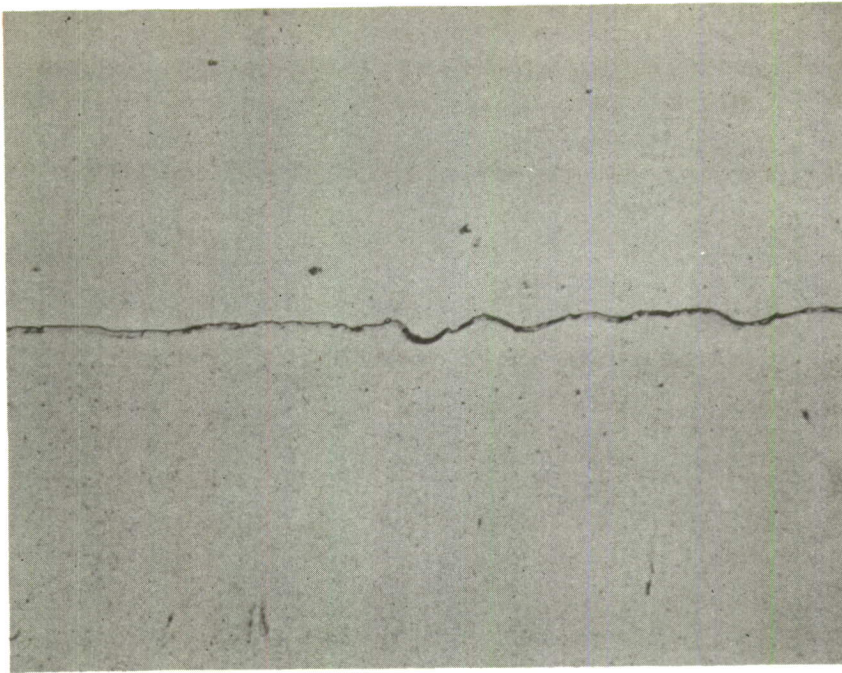


(a) Surface Profile before Etching, 400X

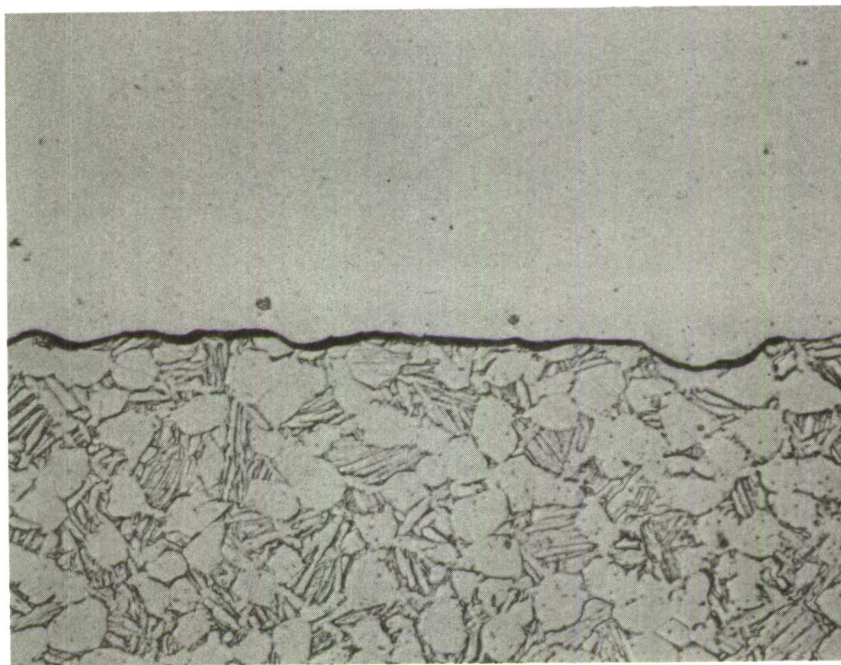


(b) Surface Profile after Etching, 400X

Figure 18 Surface Profile Photographs of Ground 6Al-4V Titanium Alloy

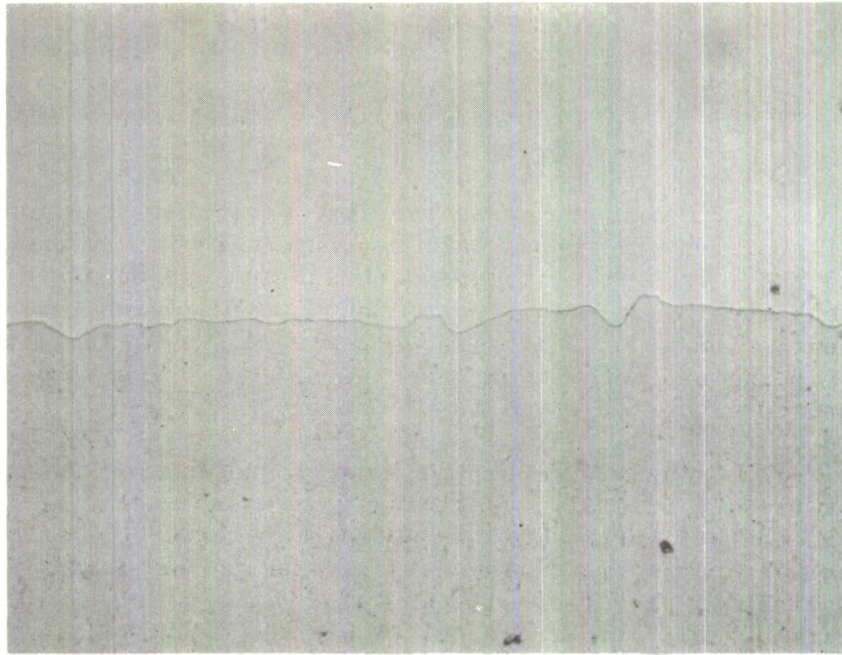


(a) Surface Profile before Etching, 400X

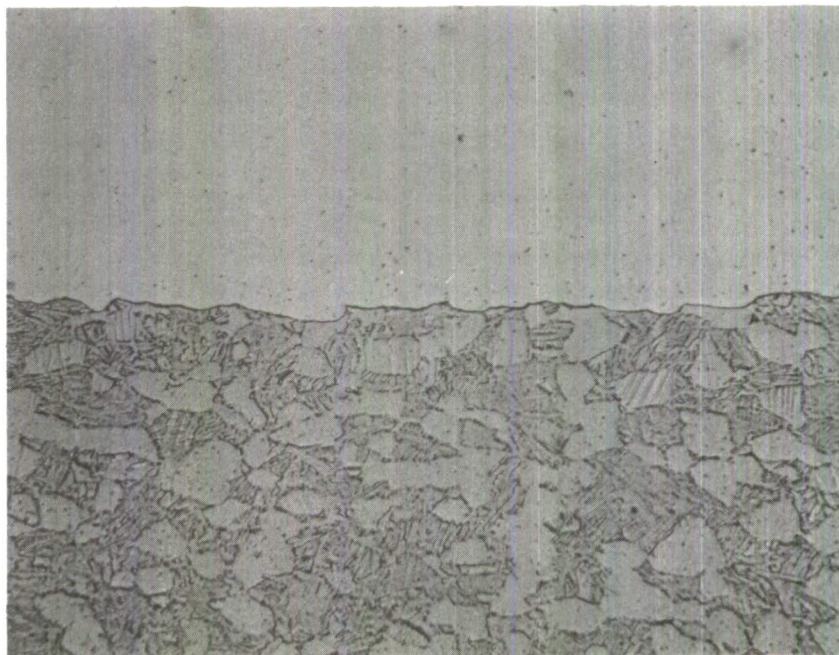


(b) Surface Profile after Etching, 400X

Figure 19 Surface Profile Photographs of Lathe Turned and Shot-Peened 6Al-4V Titanium Alloy



(a) Surface Profile before Etching, 400X



(b) Surface Profile after Etching, 400X

Figure 20 Surface Profile Photographs of Ground and Shot-Peened 6Al-4V Titanium Alloy

Surface roughness readings were also taken on these chemically milled specimens. All readings were in the range of 15 to 25 rms. This relatively smooth surface was obtained by using a weak etching solution containing HF, HNO₃ acids, and a wetting agent. The slow etching rates realized (0.005 in./min) prevented pitting and nonuniform material removal. The smooth uniform surface can be observed in Figure 17.

(3) Ground Surface. Surface-ground fatigue specimens were obtained by initially machining an oversize (test section only) smooth fatigue specimen from the as-received blank. This specimen was then surface-ground transverse to the loading axis. The grinding was performed only in the central reduced section of the specimen. The grinding wheel (1.0-in. wide by 8-in. dia), rotating at approximately 3000 rpm, is turned against the specimen. The specimen, which is rigidly held between centers, is slowly rotated as each cut is made with the grinding wheel. The central diameter of the specimen is reduced from 0.275 to 0.250 ± 0.002 in. during grinding at a rate of approximately 0.005 in. per pass.

The grinding wheel used for this operation is specially prepared with its grinding surface dressed to a radius of 4.0 in. This radius, which is mathematically determined, results in a smoothly tapered reduced section free of the dimensional irregularities that might produce stress concentration.

Surface roughness measurements obtained from these ground specimens were 20 to 30 rms, which is very close to the nominal contract requirement of 32 rms. This ground surface can be observed in Figure 18. Very little grain distortion is observed in this photograph.

(4) Shot Peened Surface. Shot peening was performed with glass shot rather than steel shot to prevent corrosion. Small particles of the material used for peening become imbedded in the surface of the part. This causes no problem if the material is chemically inert to the parent metal, but iron in the presence of a small amount of moisture would cause a galvanic corrosion site on the surface of the titanium and may be detrimental.

The smooth fatigue specimens were indexed in the shot stream to obtain a uniform shot-peening intensity over the reduced section of the specimen. All specimens were shot peened to an intensity of $0.10A \pm 0.01$. The intensity was monitored with an almen strip, which is subjected to the identical shot peening environment as the specimen.

Shot peening was always performed subsequent to lathe turning or grinding. The results of these two-step surface preparations are shown in Figures 19 and 20. Notice, these surfaces are very irregular when compared to previous surface micro-photographs.

3. TEST DESCRIPTION

a. Tension Testing. Tension tests were performed in a conventional B-L-H universal testing machine. Strain was measured on each specimen using bonded strain gages, and a strain-beam extensometer. The strain gage output was used for accurate modulus and yield strength determination, while the high elongation extensometer allowed complete measurement of the load-strain curve. Two strain gages were bonded to opposite surfaces of each specimen to cancel bending effects. Strain rate was controlled at 0.005 in./in./min to yield, and then increased and maintained at 0.05 in./in./min until failure. Our test machines are certified to an accuracy of $\pm 1.0\%$ of indicated load. The test machines are calibrated and certified on a semiannual basis. Strain recorders are calibrated immediately before each use by applying a known strain signal to the recorder, through the sensing element to be used, and noting the corresponding deflection of the record drum.

b. Notch Tension Testing. Notch tension tests were also performed in the B-L-H testing machine. All tests were conducted at a constant platen speed of 0.01 in./min to failure.

c. Axial Fatigue Testing. All fatigue testing for this program was performed using axial load, rotating-eccentric-mass machines. A photograph of the Fatigue Laboratory at the Denver Division is shown in Figure 21. Shown is a IVY-12, a Baldwin Sonntag SF-10U, and two Baldwin Sonntag SF-1U fatigue machines. All machines used are equipped with automatic static-load controllers that automatically maintain a constant static load independent of specimen elongation.

The specimen and adapters (Figure 22) have been designed to maintain and provide good specimen alignment even for a fully reversed load cycle ($A = \infty$). Alignment of fixture and specimen is maintained by periodic checking with a strain-gaged alignment cell.

All fatigue machines are load-calibrated on a routine periodic basis.

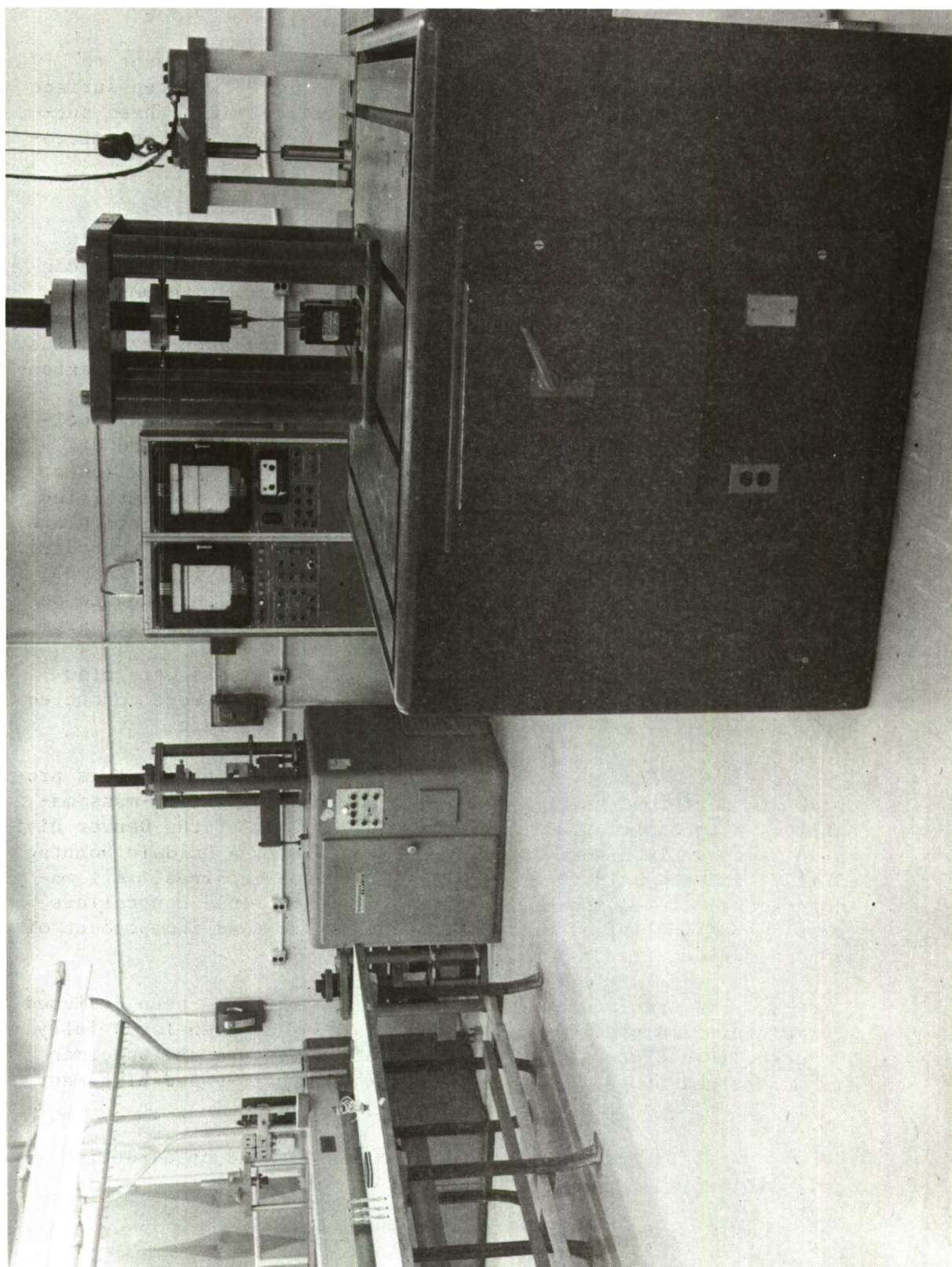


Figure 21 Fatigue Laboratory at Martin Marietta

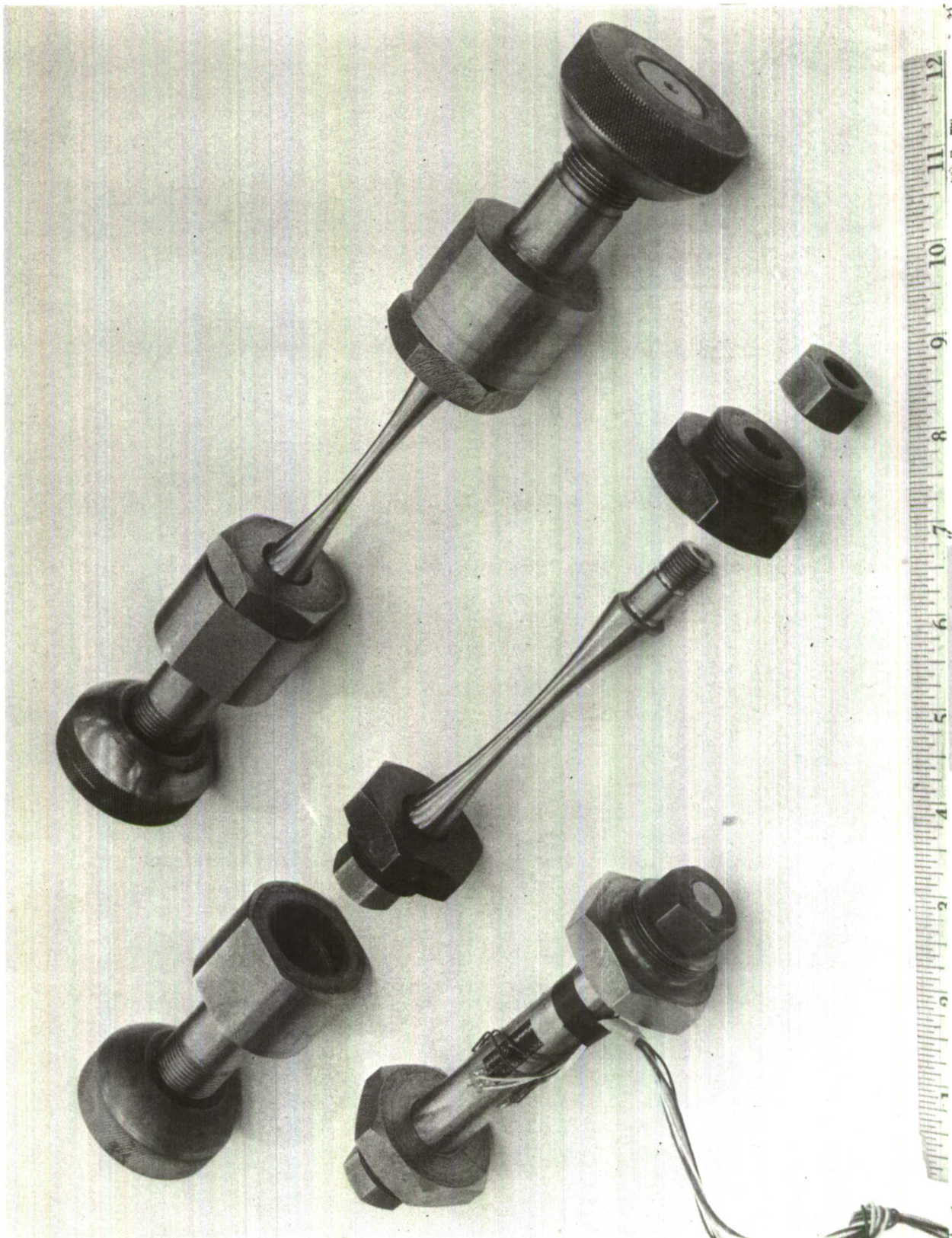


Figure 22 Smooth Fatigue Specimens, Adapters, and Alignment Cell

SECTION V

TEST RESULTS AND DISCUSSION

1. FORGING EFFECTS

Tensile data for all forging-conditions studied are presented in Table III. An examination of the data reveals that strength properties are virtually unaffected by beta forging. While some ductility has been lost during beta forging, this loss is not large enough to detract from the usefulness of the material. The two-stage forging shows a ductility level similar to that exhibited by alpha-beta forging. These data are in good agreement with the available data from the literature.

The forging-effect fatigue results are presented in tabular form in the appendix, plotted as S-N curves in Figure 23 thru 47, and summarized in Constant Life Diagrams (Figure 48, 49 and 50) and in Tables IV and V.

The effect of stress amplitude ratio (A-ratio) on the S-N curves for smooth and notched alpha-beta forged 6Al-4V titanium alloy is shown in Figures 23 thru 28. The constant-life diagram in Figure 48 is constructed from these basic S-N curves and illustrates the influence of A-ratio on fatigue life for the conventional-forged material. The trends illustrated here are in general agreement with other results on the effect of stress ratio on fatigue strength. These fatigue data are also presented in Tables IV and V as baseline data for comparison with the other forging procedures.

The effect of forging at temperatures of 50, 120, and 270°F above the beta transus is expressed by S-N curves in Figures 29 thru 44. Initially, before the optimum forging temperature was selected, specimens representing each forging condition were tested at the single A-ratio of 0.9. This was an efficient way to obtain sufficient fatigue data with which to choose the optimum forging temperature.

The effect of forging temperature can be easily seen in Figures 51 and 52 and Table IV. The two figures were constructed by group plotting the best fit S-N curves obtained at the five forging temperatures and the single A ratio, 0.9. Examining these two curves, indicates that beta forging offers no significant advantage to conventional forging except at 10^7 cycles or until the fatigue limit is approached. The better performance at the longer lifetimes is, of course, very desirable because the fatigue limit is the basis for material selection in many design applications.

Table III Mechanical Properties of 6Al-4V Titanium for Five Forging Conditions, Heat No. 293882

Forging condition	Heat treatment*	Ultimate tensile strength (ksi)	Tensile yield strength (ksi)†	Notch tensile strength (ksi)‡	Reduction of area (%)	Elongation (%) in. 1.2-in. gage length**	Modulus (psi x 10 ⁶)
Conventional Alpha-Beta (T _B - 80°F)	Annealed	141.0	127.6	219.9	26.8	9.1	16.5
		138.1	125.9	218.4	38.0	--	16.3
		137.7	127.8	215.1	41.2	14.2	17.0
		138.9 Avg	127.1 Avg	217.8 Avg	35.3 Avg	11.7 Avg	16.6 Avg
Beta (T _B + 50°F)	Annealed	142.9	131.2	--	18.5	11.0	17.1
		140.4	126.6	--	19.7	9.0	16.4
		144.3	130.5	--	16.4	9.1	16.6
		142.5	129.4	--	18.2	9.7	16.7
Beta (T _B + 120°F)	Annealed	145.6	135.8	207.2	10.7	8.1	16.9
		138.6	127.4	210.6	11.1	12.2	16.3
		147.5	134.7	210.2	15.0	8.6	16.8
		143.9	132.6	209.3	12.3	9.6	16.7
Beta (T _B + 270°F)	Annealed	135.5	120.5	--	22.1	11.0	17.4
		142.9	132.2	--	18.4	8.0	17.0
		135.1	122.9	--	18.6	10.0	16.0
		137.8	125.2	--	19.7	9.7	16.8
2 stage (T _B + 270°F and T _B - 80°F)	Annealed	138.4	129.0	222.7	32.1	13.3	16.6
		144.3	134.5	214.8	29.1	14.3	17.1
		142.8	128.0	220.8	32.1	11.2	16.5
		141.8	130.5	219.4	31.1	12.9	16.7
Beta (T _B + 50°F)	STA	161.0	146.1	--	11.0	--	16.6
		160.4	148.3	--	14.2	6.1	15.9
		161.2	144.7	--	10.2	--	16.7
		160.9	146.4	--	11.8	6.1	16.4

*Annealed, 1300°F (2 hr) AC; STA, solution-treated at 1725°F (1 hr), water quenched, aged 1000°F (4 hr).

†0.2% offset.

‡K_t = 3.0.

**Elongation obtained from extensometer strain record.

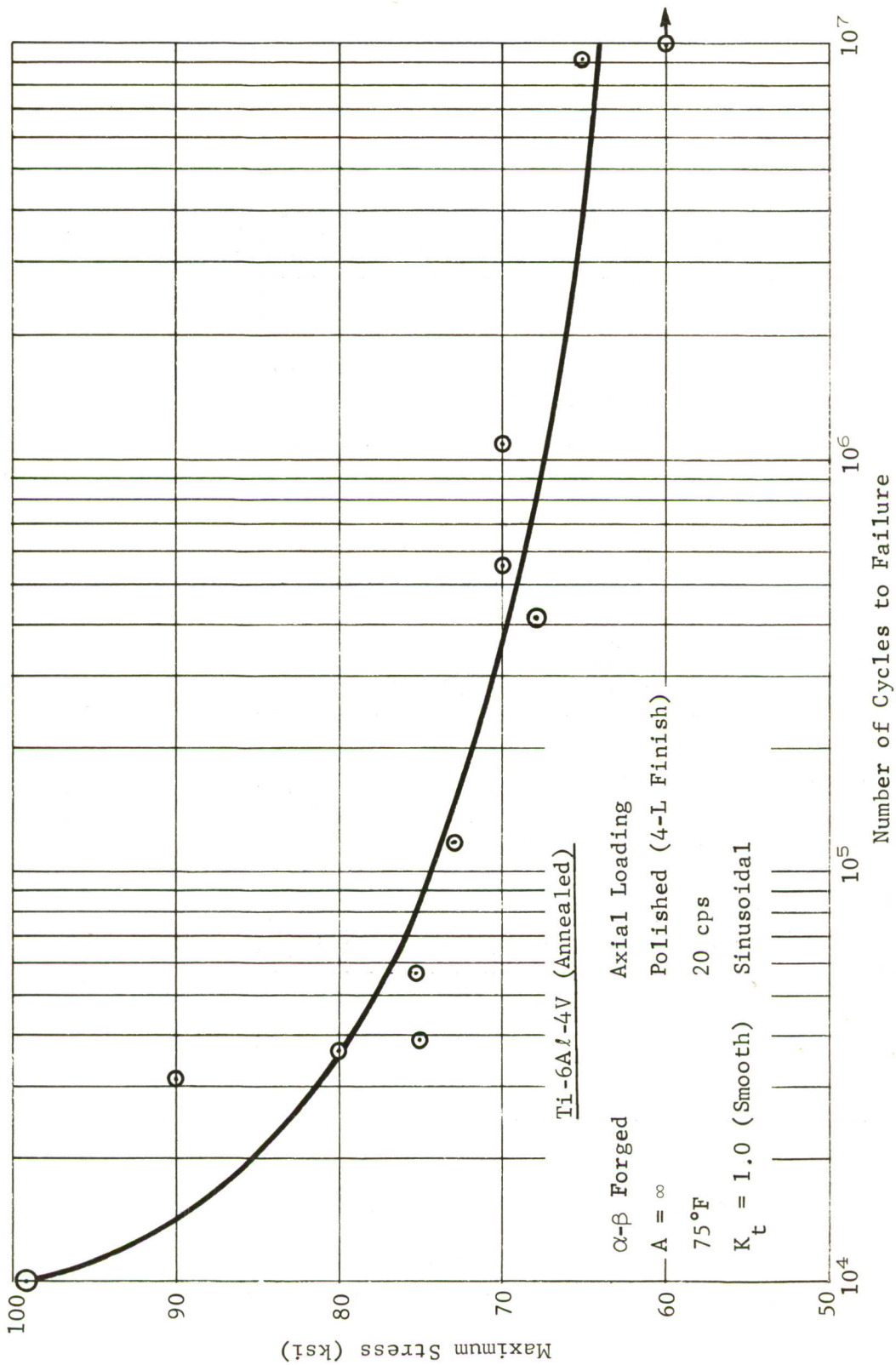


Figure 23 S-N Curve for 6Al-4V Titanium Alloy Finish Forged at 1750°F ($T_B - 80^\circ\text{F}$)

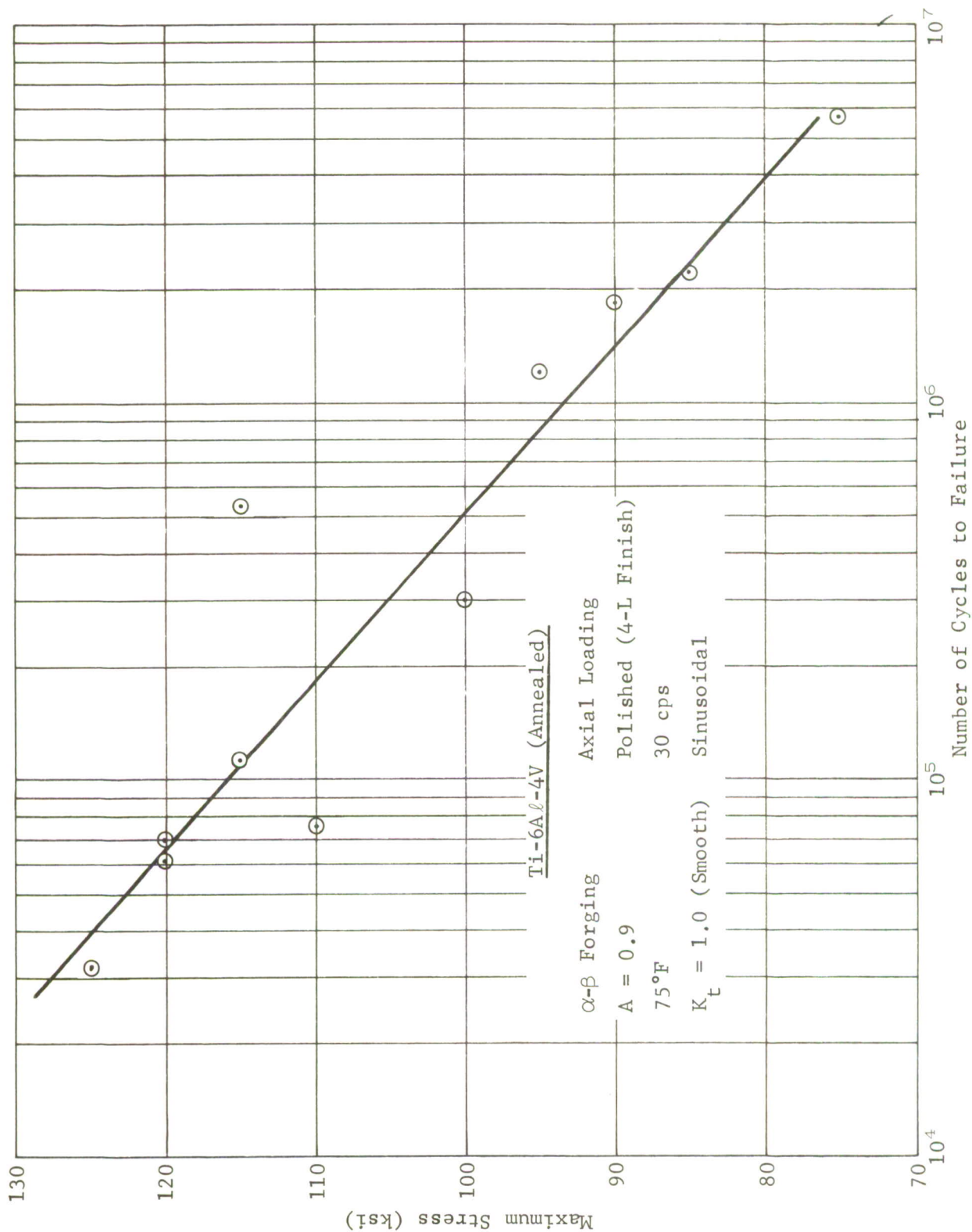


Figure 24 S-N Curve for 6Al-4V Titanium Alloy Forged at 1750°F (T_B - 80°F)

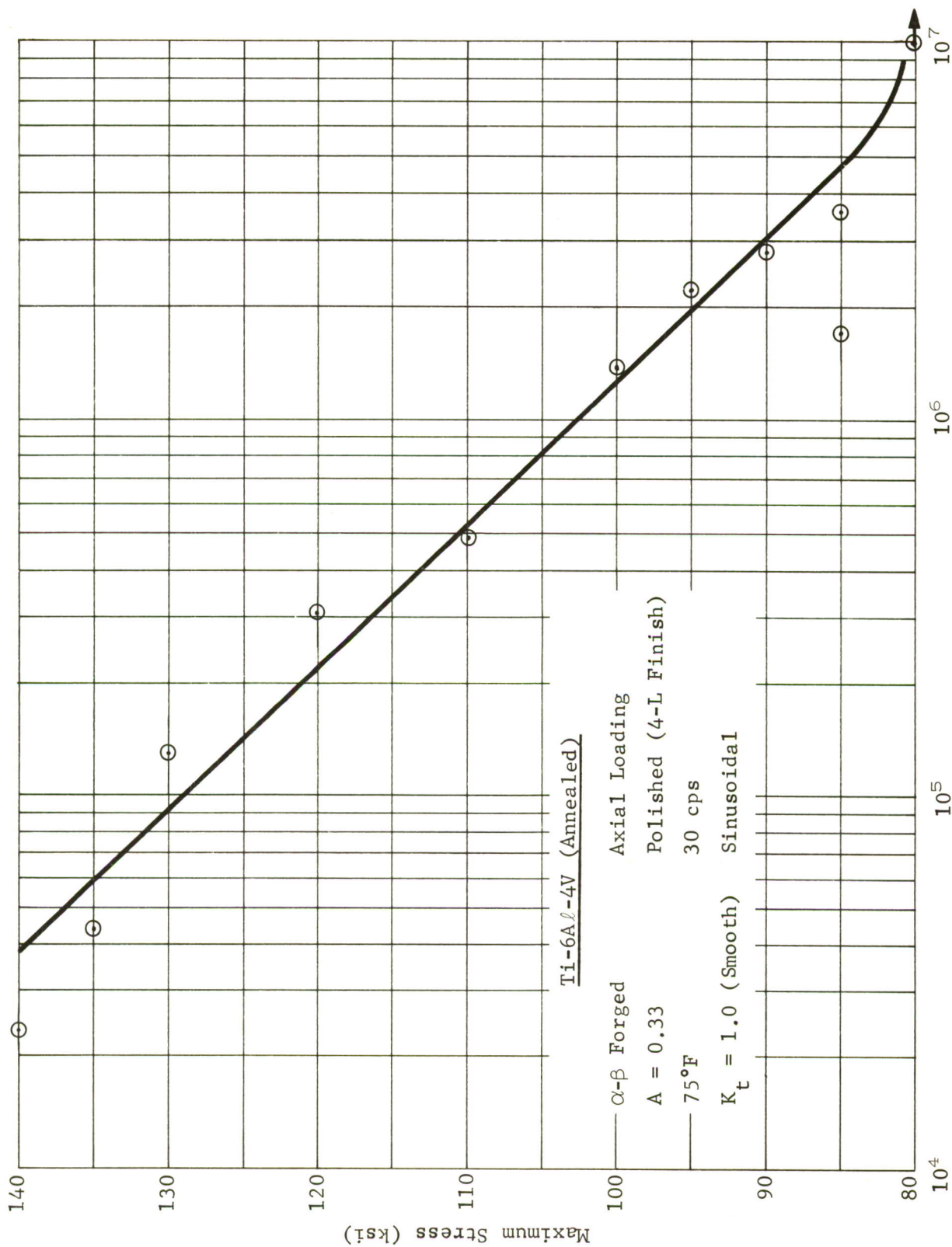


Figure 25 S-N Curve for 6Al-4V Titanium Alloy Forged at 1750°F ($T_B - 80^\circ\text{F}$)

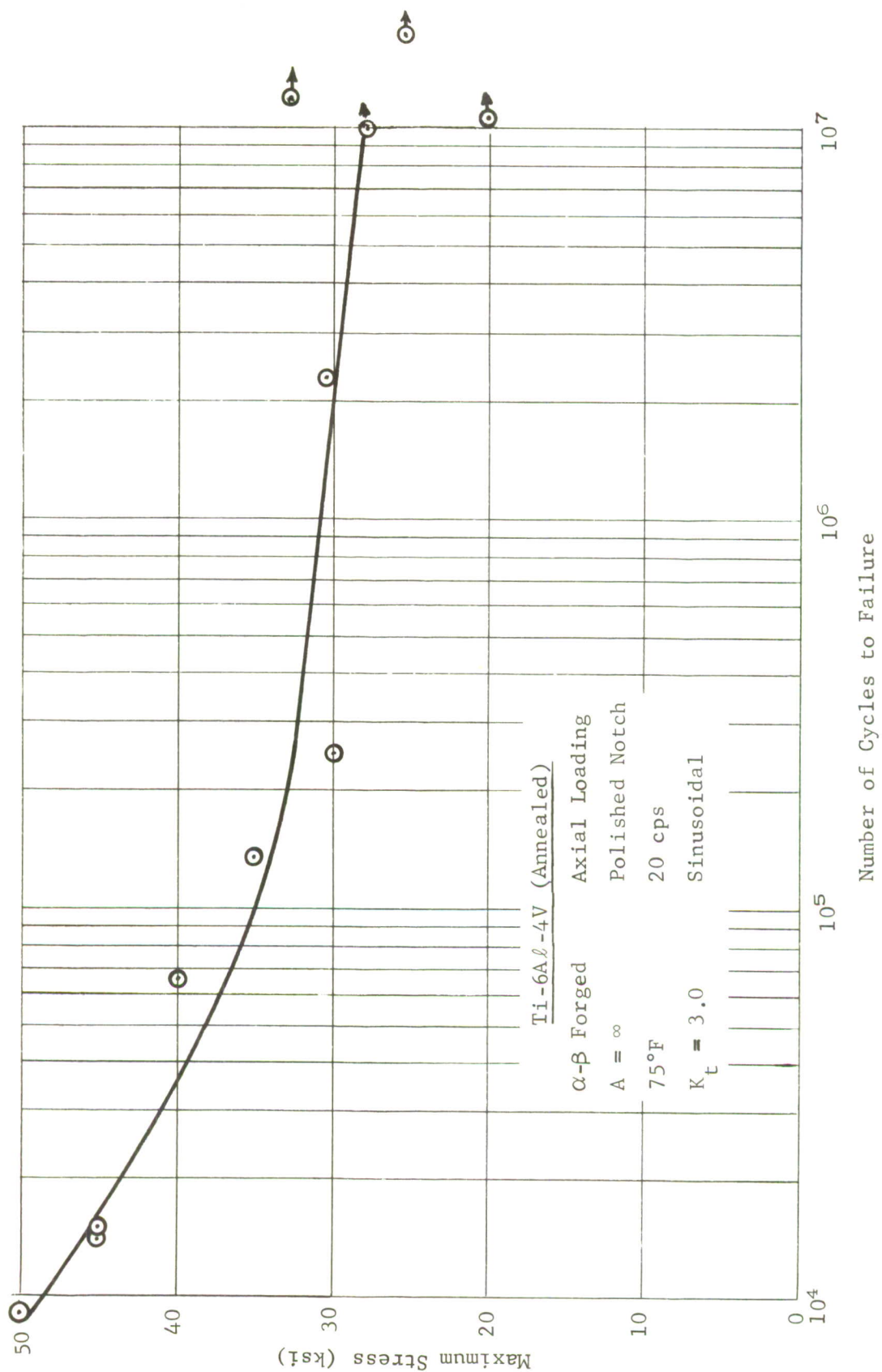


Figure 26 S-N Curve for 6Al-4V Titanium Alloy Finish Forged at 1750°F ($T_B - 80^\circ\text{F}$)

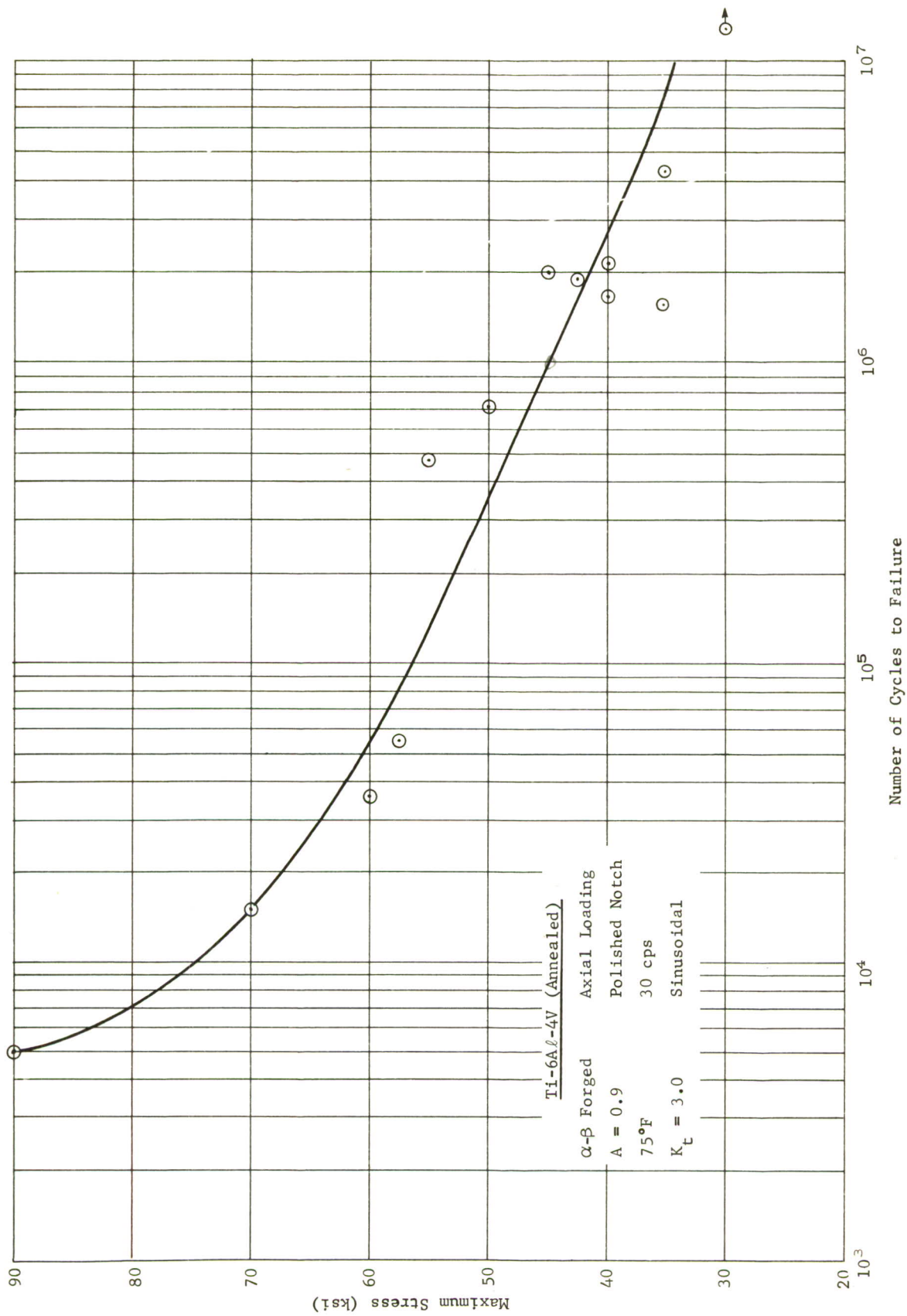


Figure 27 S-N Curve for 6Al-4V Titanium Alloy Finish Forged at 1750°F ($T_B - 80^\circ\text{F}$)

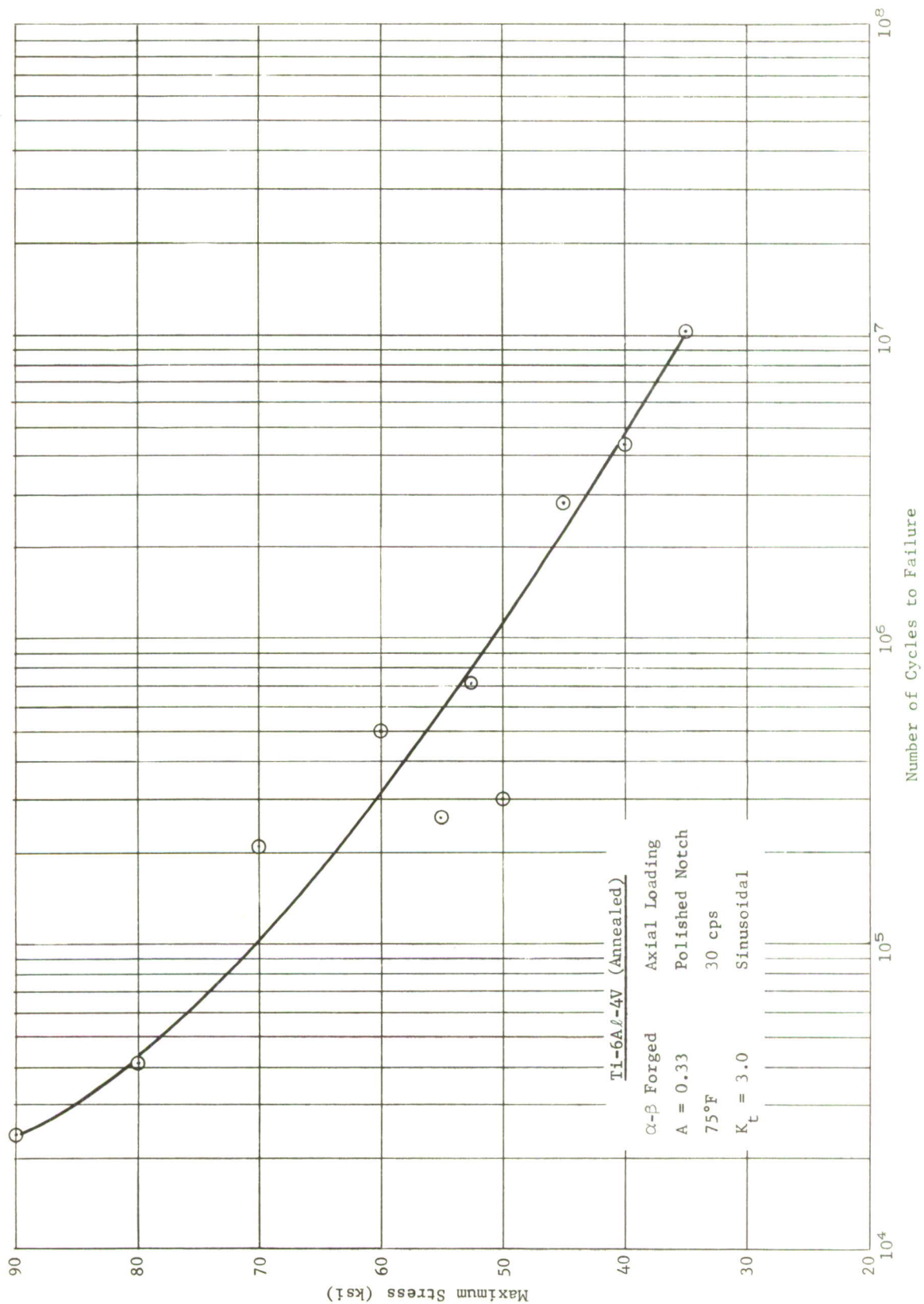


Figure 28 S-N Curve for 6Al-4V Titanium Alloy Finish Forged at 1750°F (T_B - 80°F)

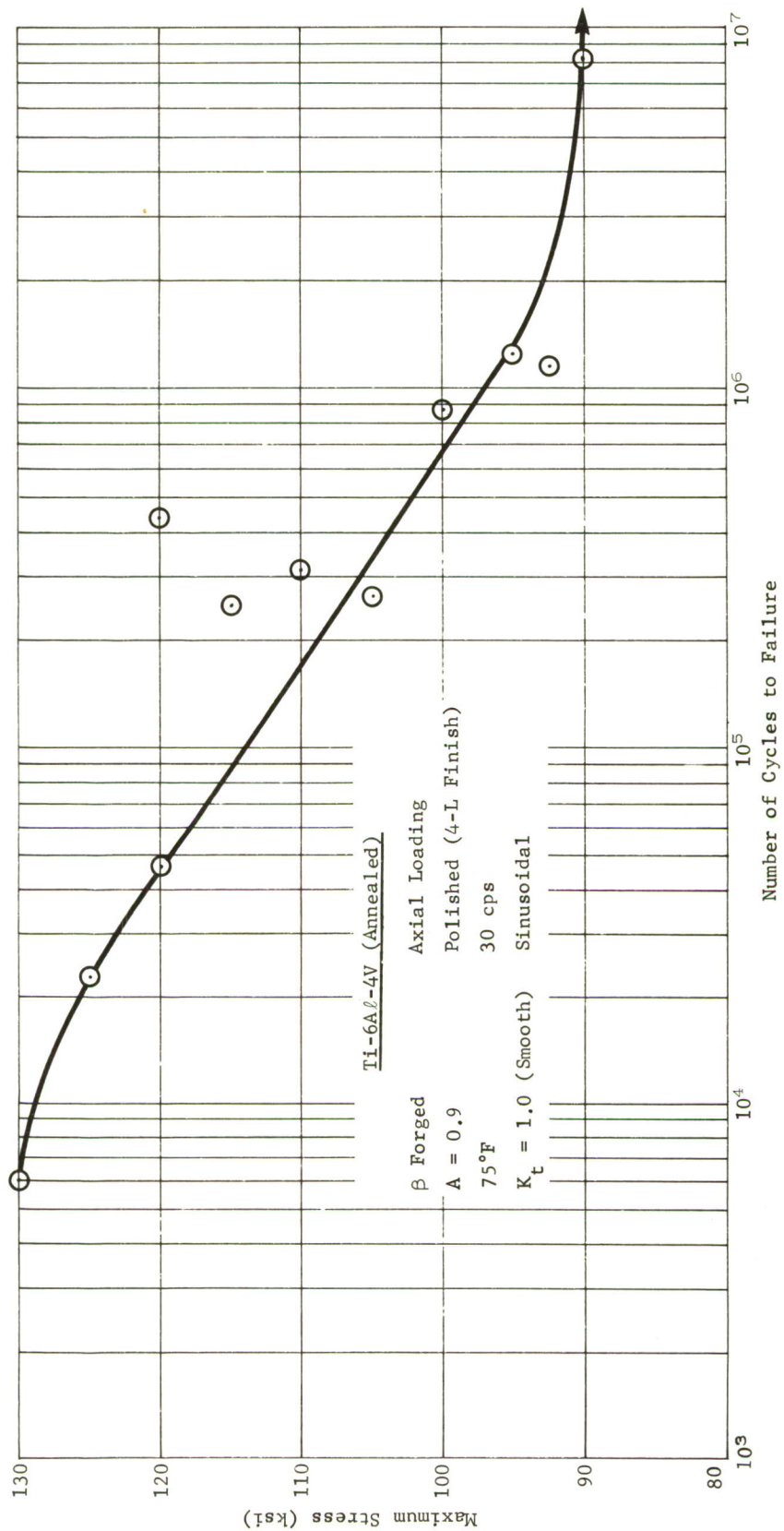


Figure 29 S-N Curve for 6Al-4V Titanium Alloy Forged at 1880°F (T_B + 50°F)

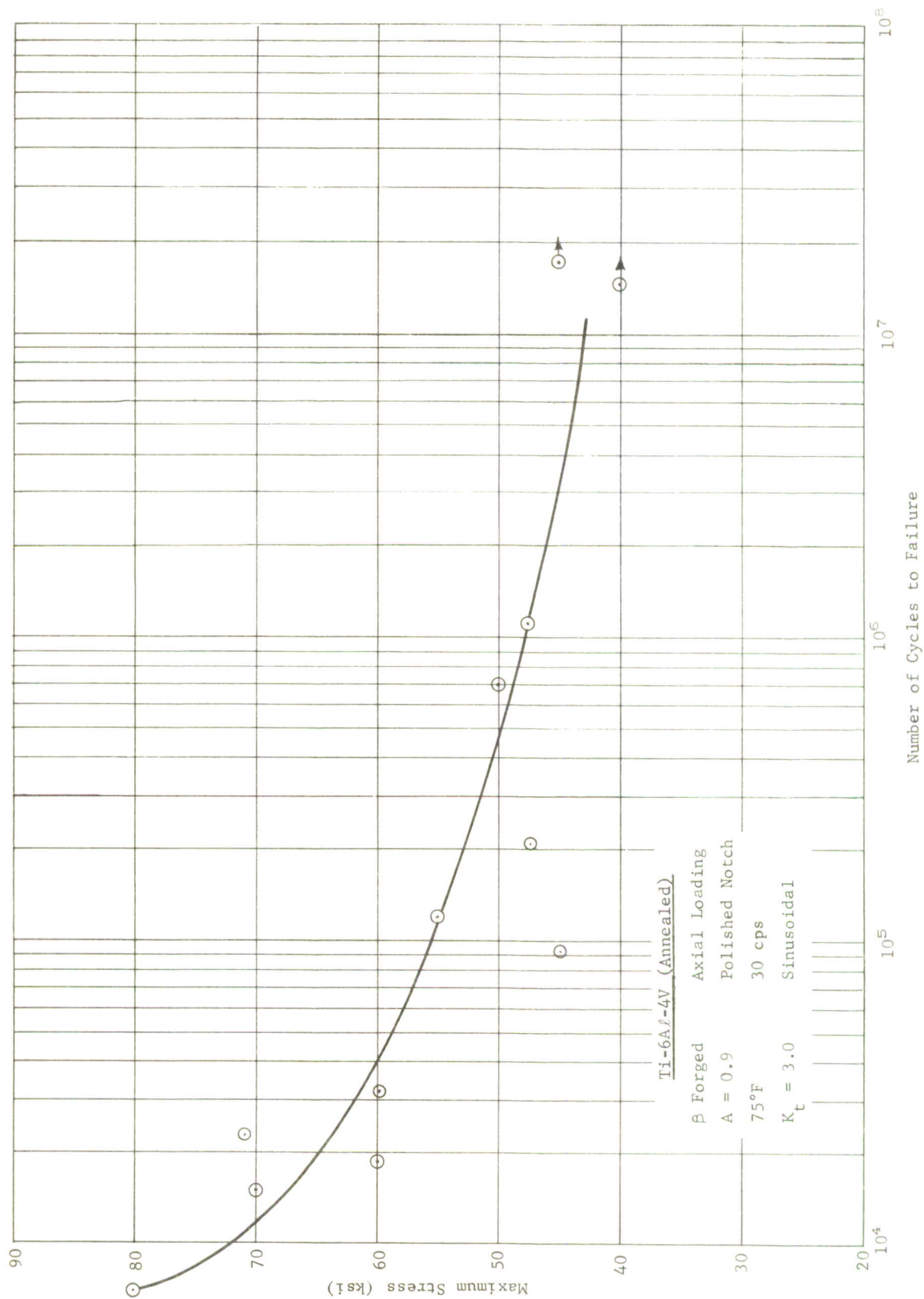


Figure 30 S-N Curve for 6Al-4V Titanium Alloy Finish Forged at 1880°F ($T_B + 50^\circ\text{F}$)

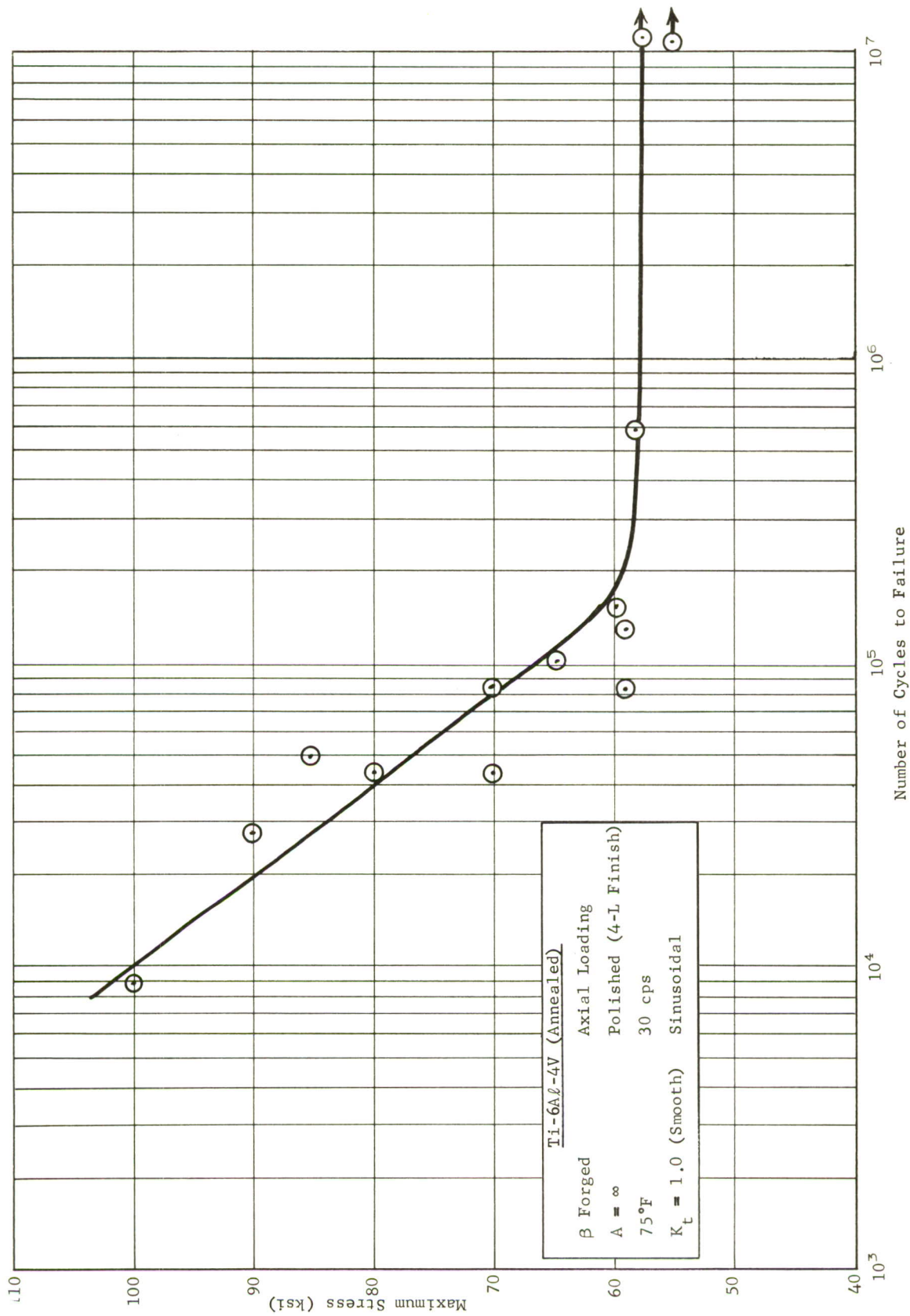


Figure 31 S-N Curve for 6Al-4V Titanium Alloy Forged at 1950°F (T_B + 120°F)

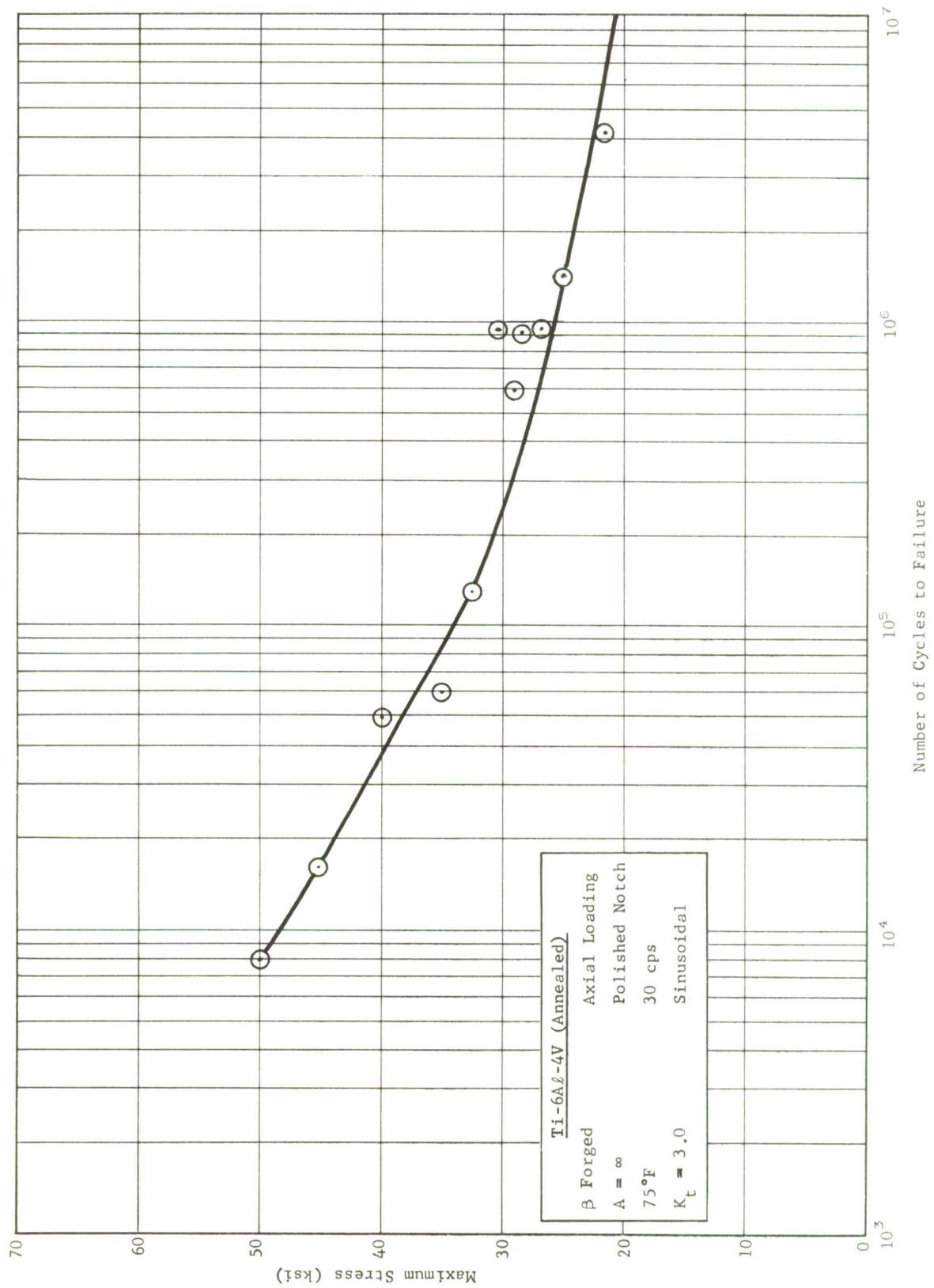


Figure 32 S-N Curve for 6Al-4V Titanium Alloy Finish Forged at 1950°F ($T_B + 120^\circ\text{F}$)

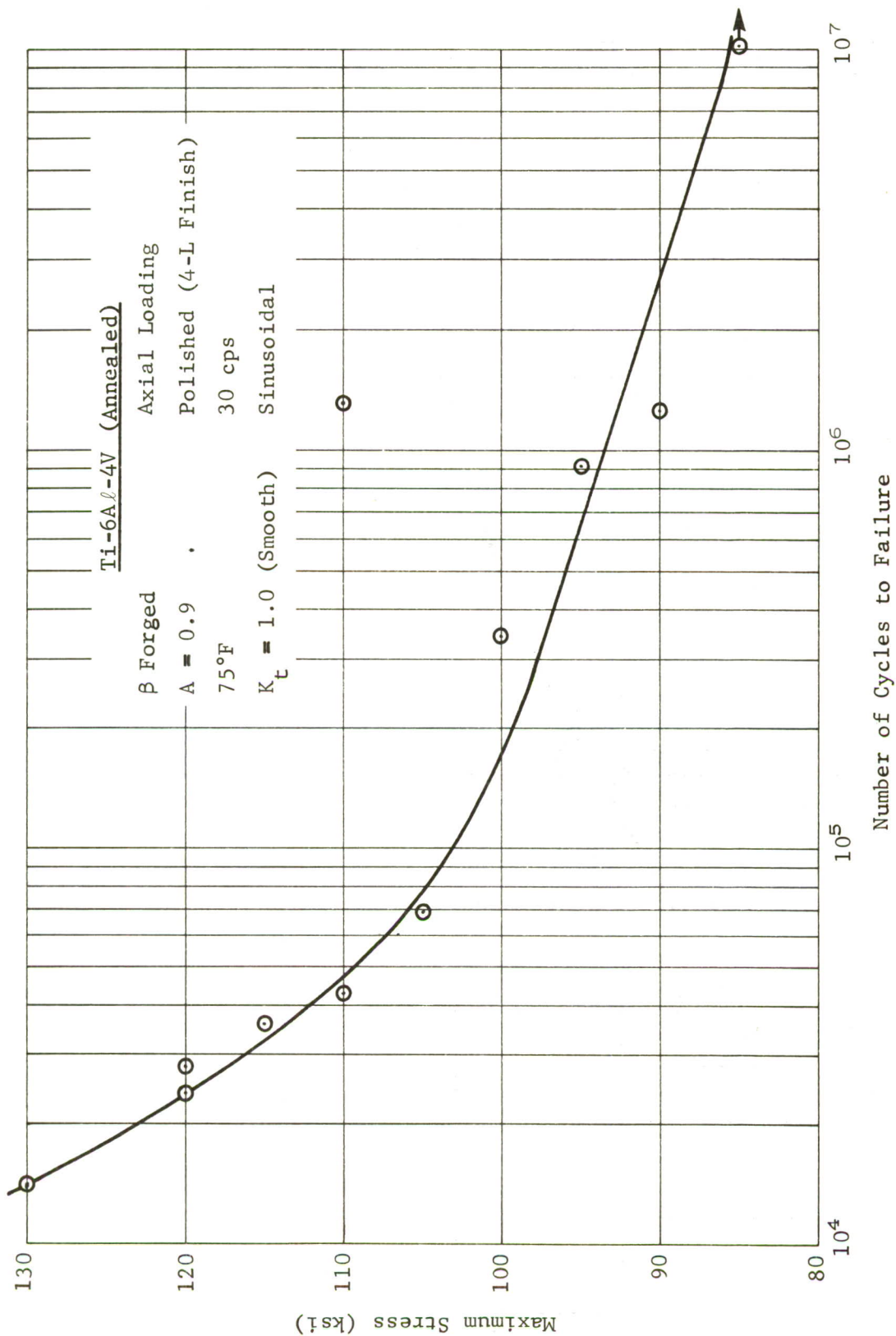


Figure 33 S-N Curve for 6Al-4V Titanium Alloy Finish Forged at 1950°F
($T_B + 120^\circ\text{F}$)

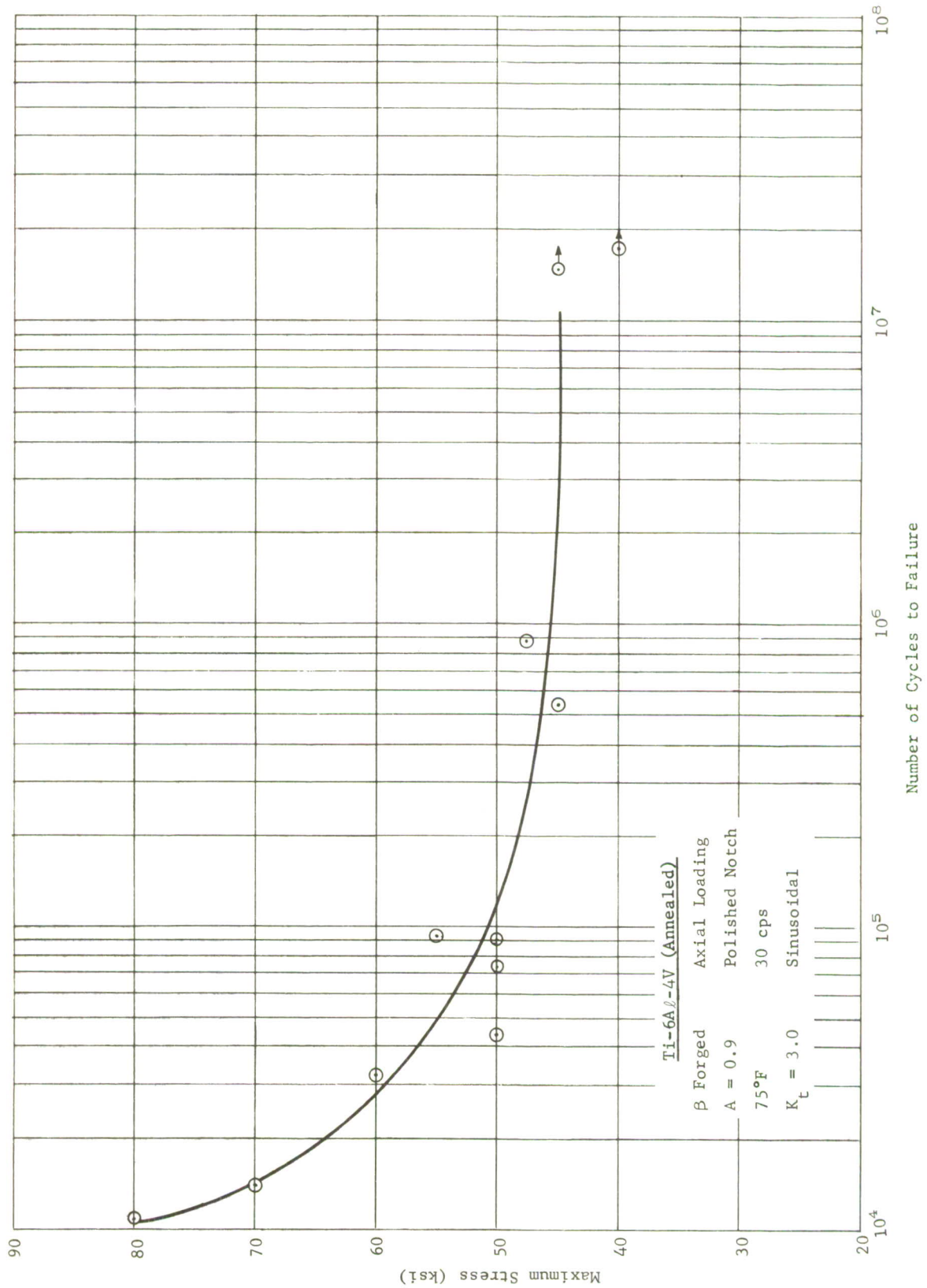


Figure 34 S-N Curve for 6Al-4V Titanium Alloy Finish Forged at 1950°F (T_B + 120°F)

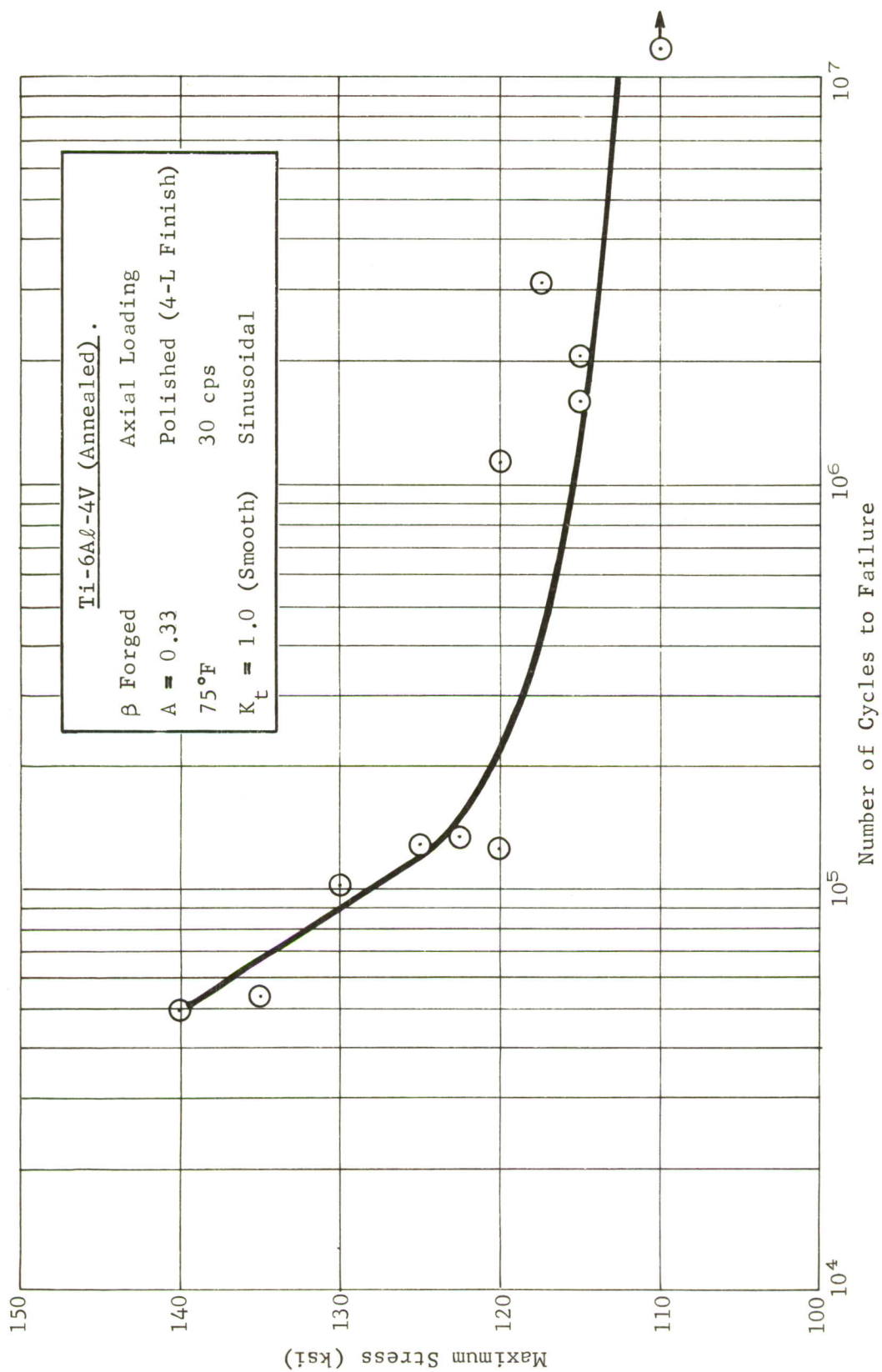


Figure 35 S-N Curve for 6Al-4V Titanium Alloy Finish-Forged at 1950°F ($T_B + 120^\circ\text{F}$)

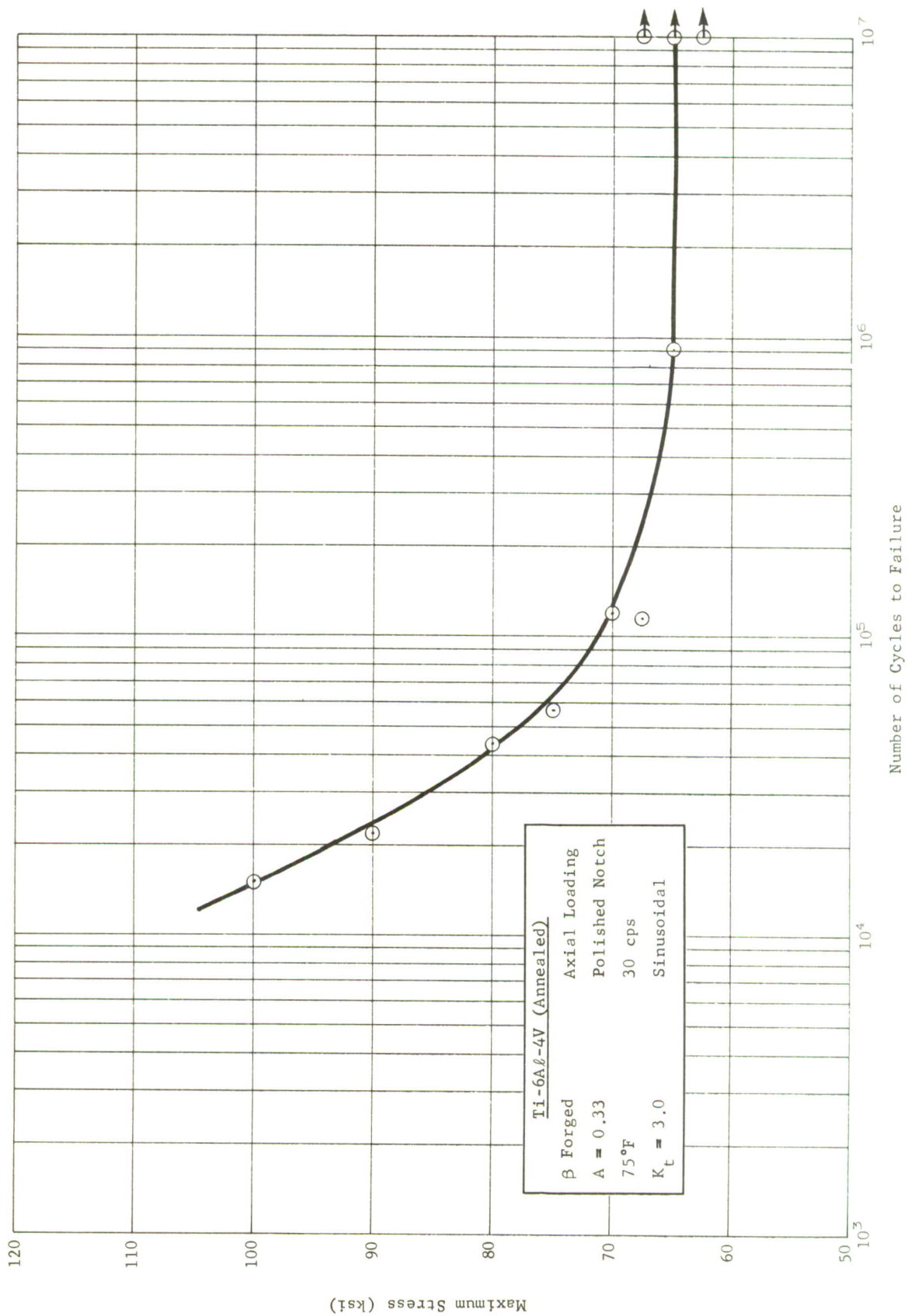


Figure 36 S-N Curve for 6Al-4V Titanium Alloy Finish Forged at 1950°F ($T_B + 120^\circ\text{F}$)

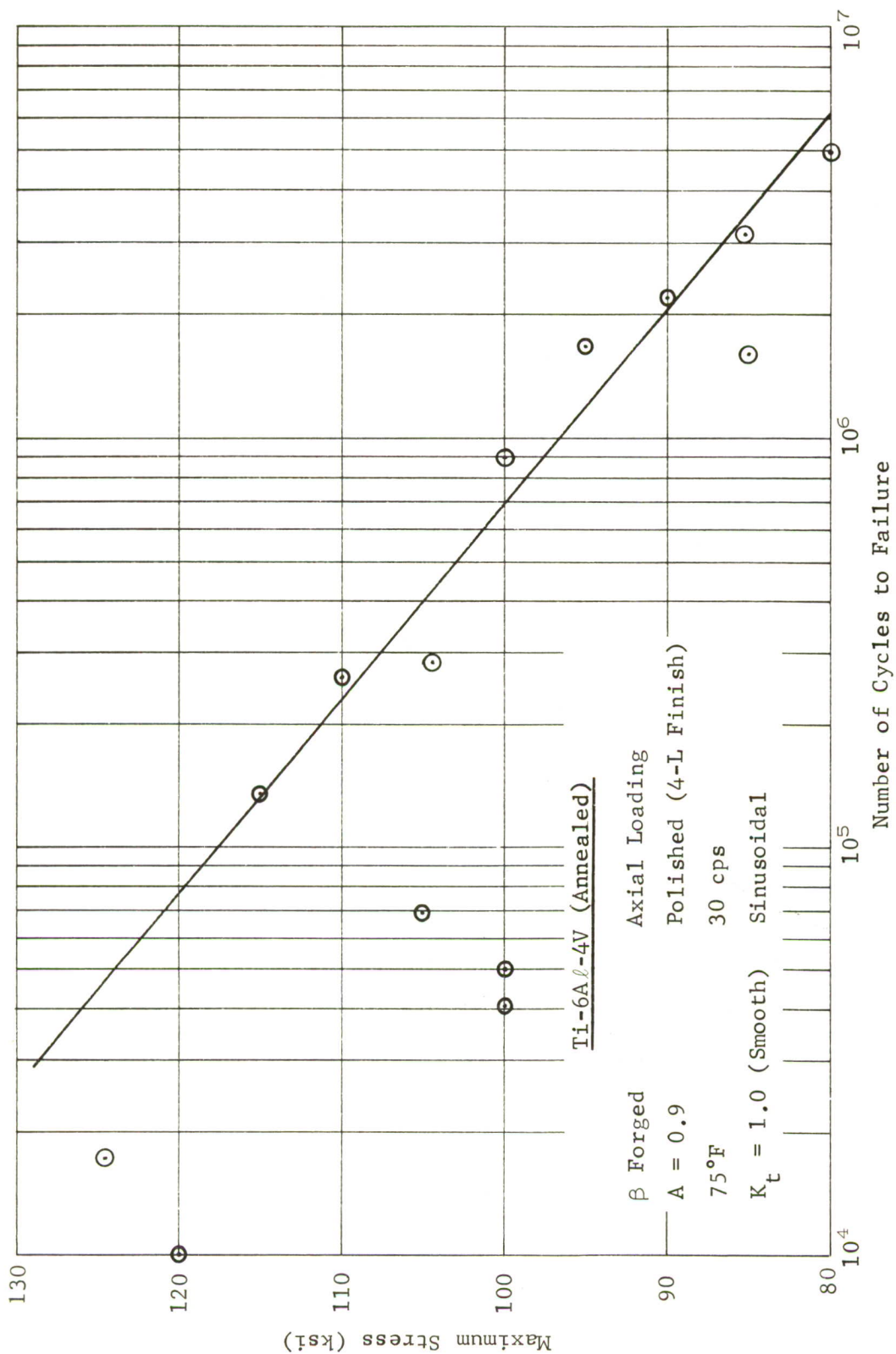


Figure 37 S-N Curve for 6Al-4V Titanium Alloy Forged at 2100°F (T_B + 270°F)

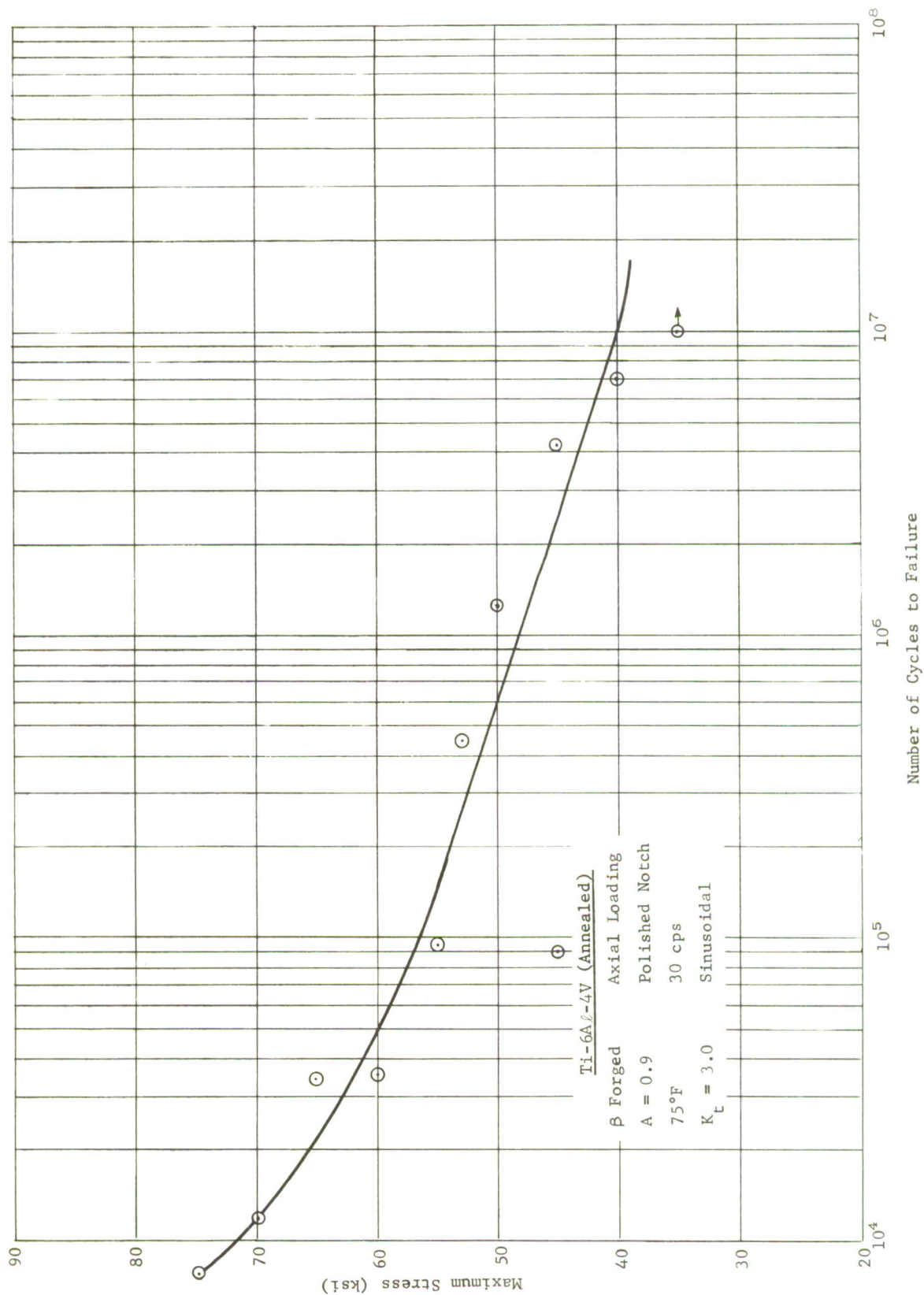


Figure 38 S-N Curve for 6Al-4V Titanium Alloy Finish Forged at 2100°F ($T_B + 270^\circ\text{F}$)

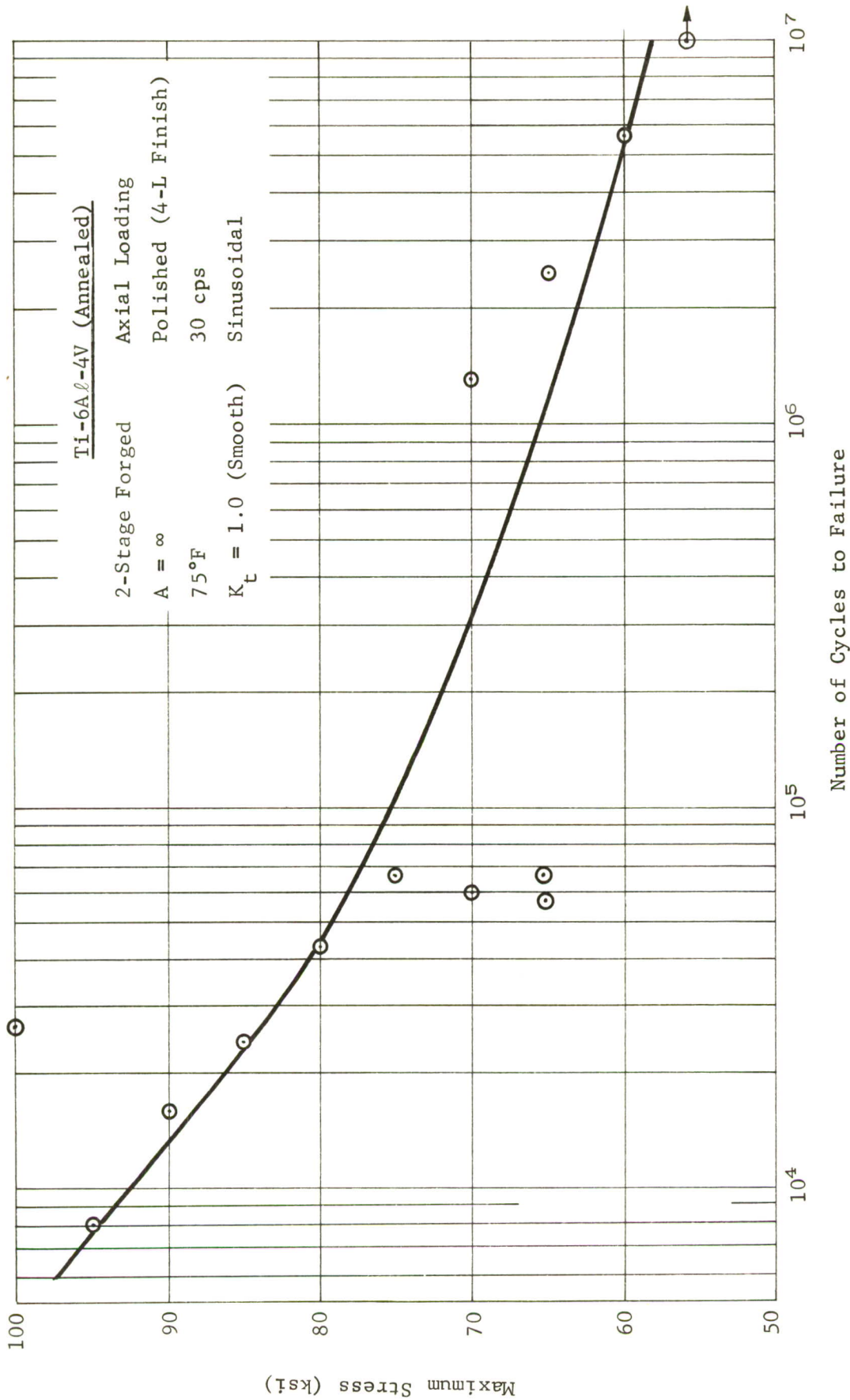


Figure 39 S-N Curve for 6Al-4V Titanium Alloy Finish Forged at 1750°F (Blocked at $T_B + 270^\circ\text{F}$ and Finished at $T_B - 80^\circ\text{F}$)

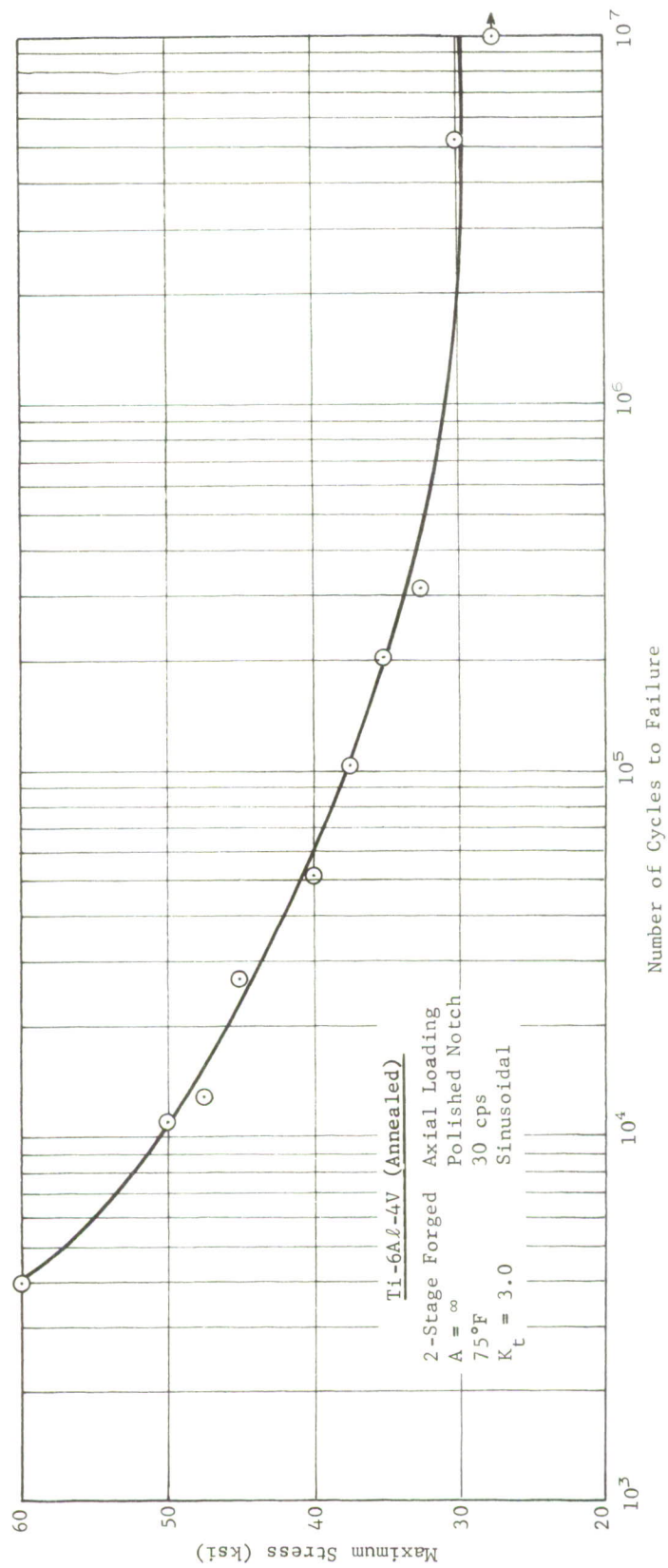


Figure 40 S-N Curve for 6Al-4V Titanium Alloy Finish Forged at 1750°F (Blocked at $T_B + 270^\circ\text{F}$ and Finished at $T_B - 80^\circ\text{F}$)

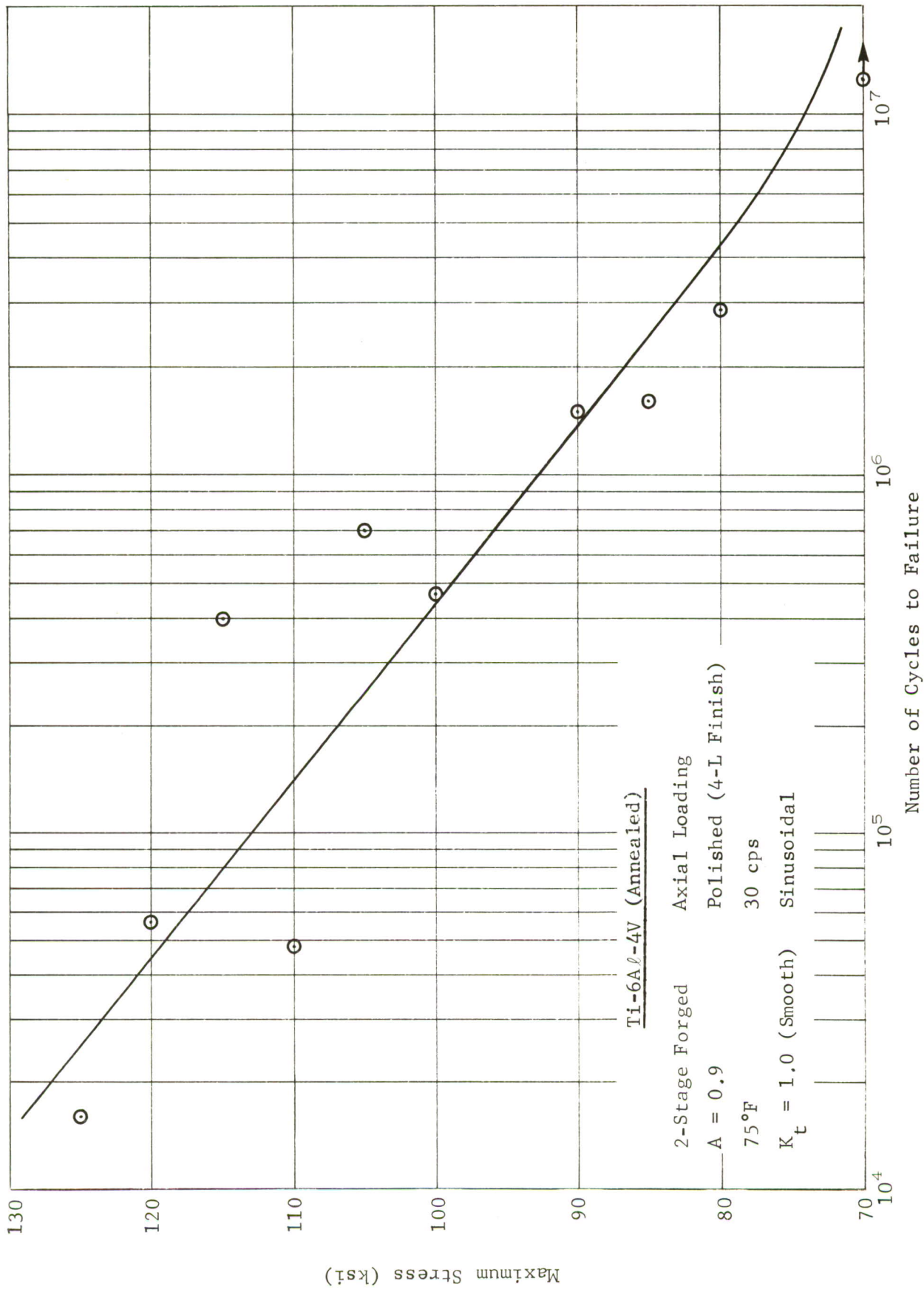


Figure 41 S-N Curve for 6Al-4V Titanium Alloy Forged at 1750°F (Blocked at $T_B + 270^{\circ}\text{F}$ and Finished at $T_B - 80^{\circ}\text{F}$)

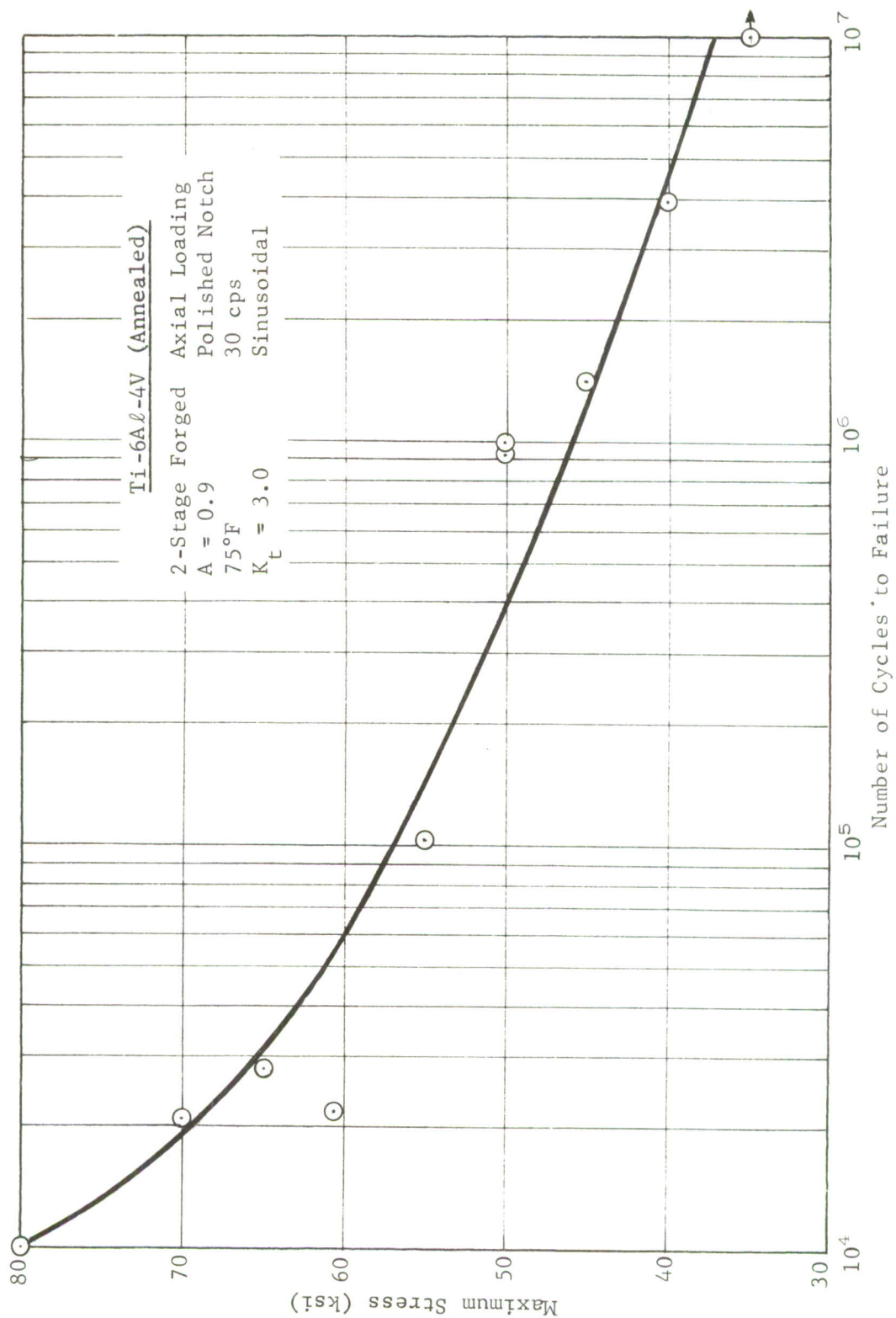


Figure 42 S-N Curve for 6Al-4V Titanium Alloy Finish Forged at 1750°F
 (Blocked at $T_B + 270^\circ\text{F}$ and Finished at $T_B - 80^\circ\text{F}$)

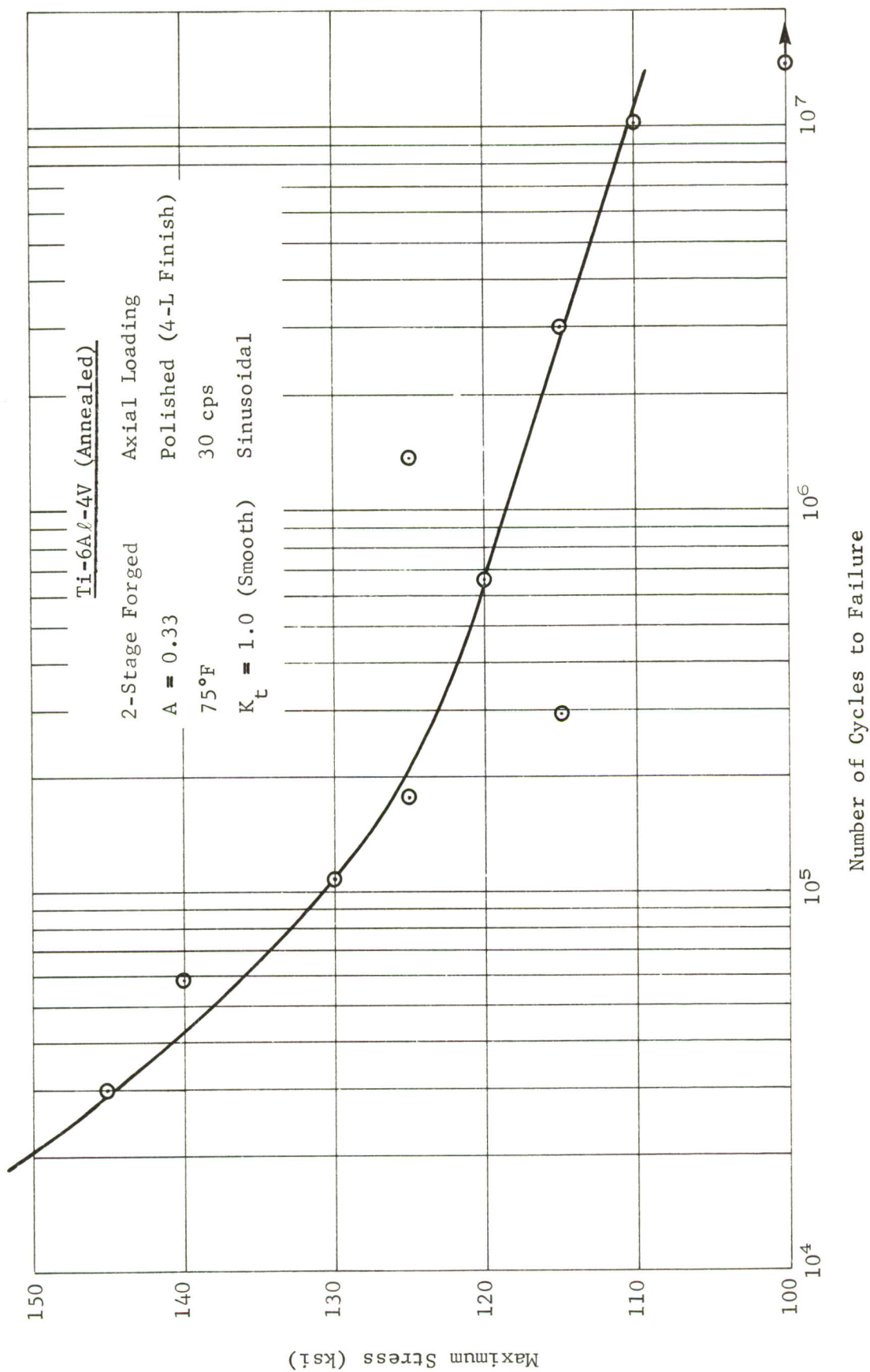


Figure 43 S-N Curve for 6Al-4V Titanium Alloy Finish Forged at 1750°F (Blocked at $T_B + 270^\circ\text{F}$ and Finished at $T_B - 80^\circ\text{F}$)

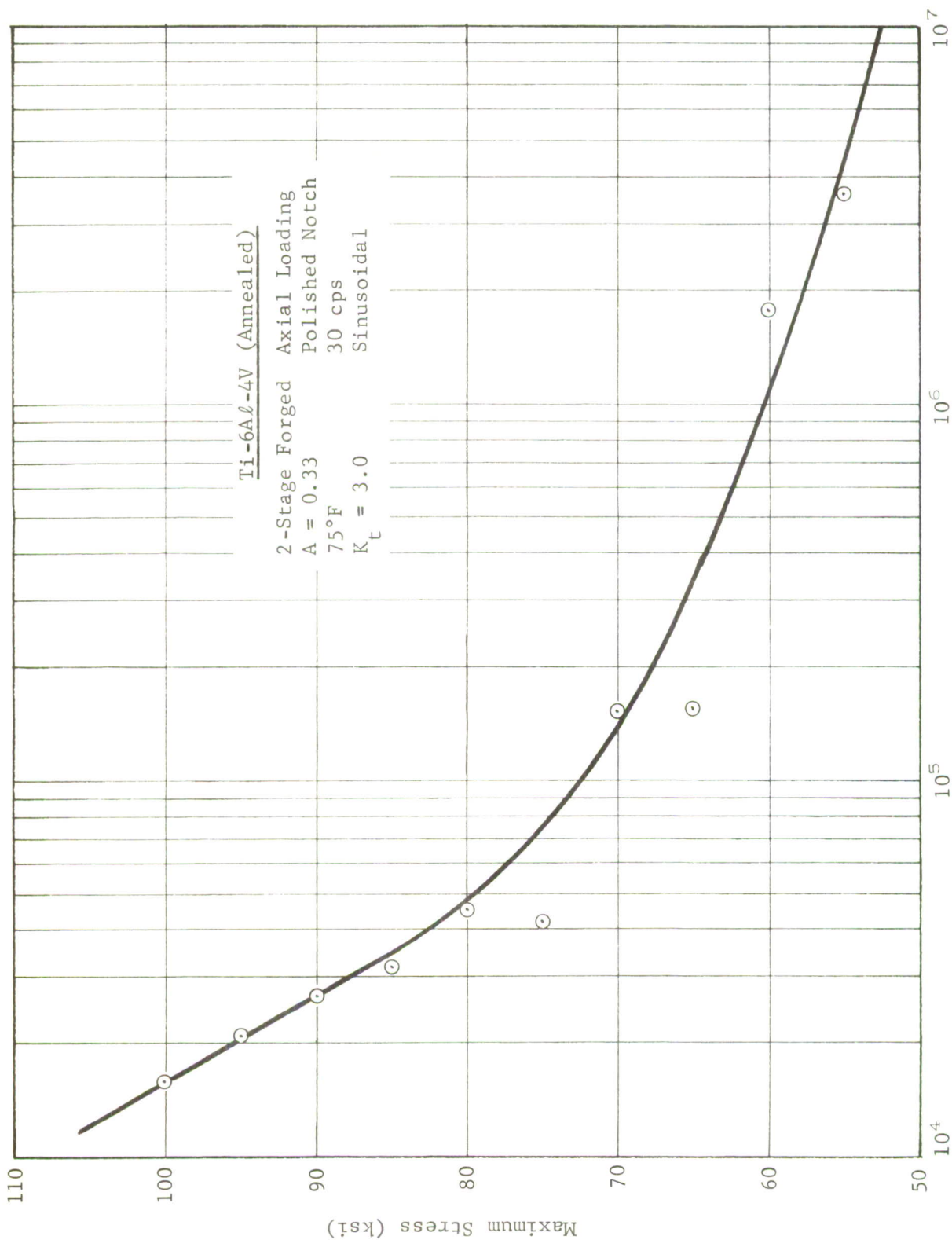


Figure 44 S-N Curve for 6Al-4V Titanium Alloy Finish Forged at 1750°F
 (Blocked at T_B + 270°F and Finished at T_B - 80°F)

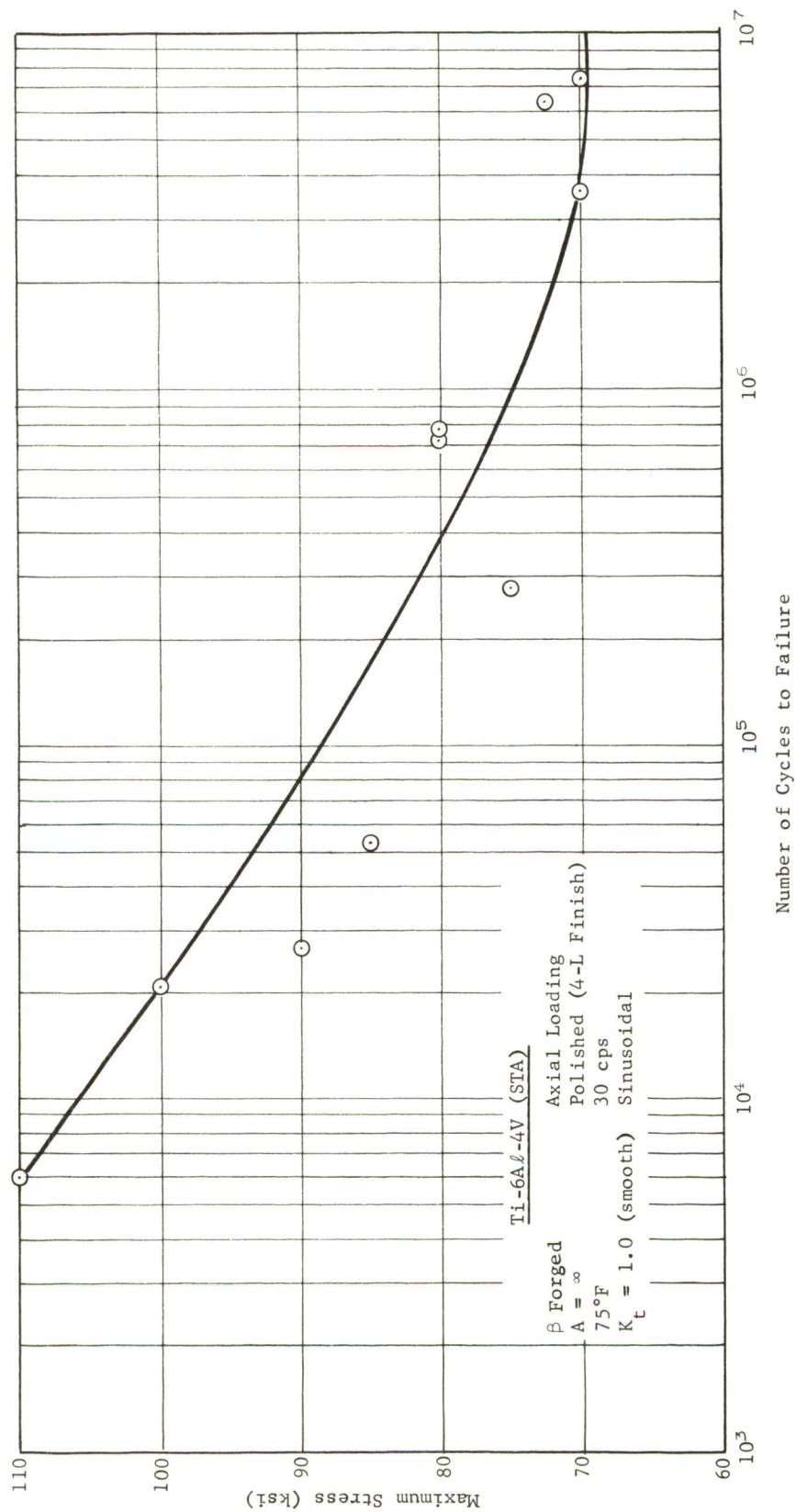


Figure 45 S-N Curve for STA 6Al-4V Titanium Alloy Finish Forged at 1880°F ($T_B + 50^\circ\text{F}$)

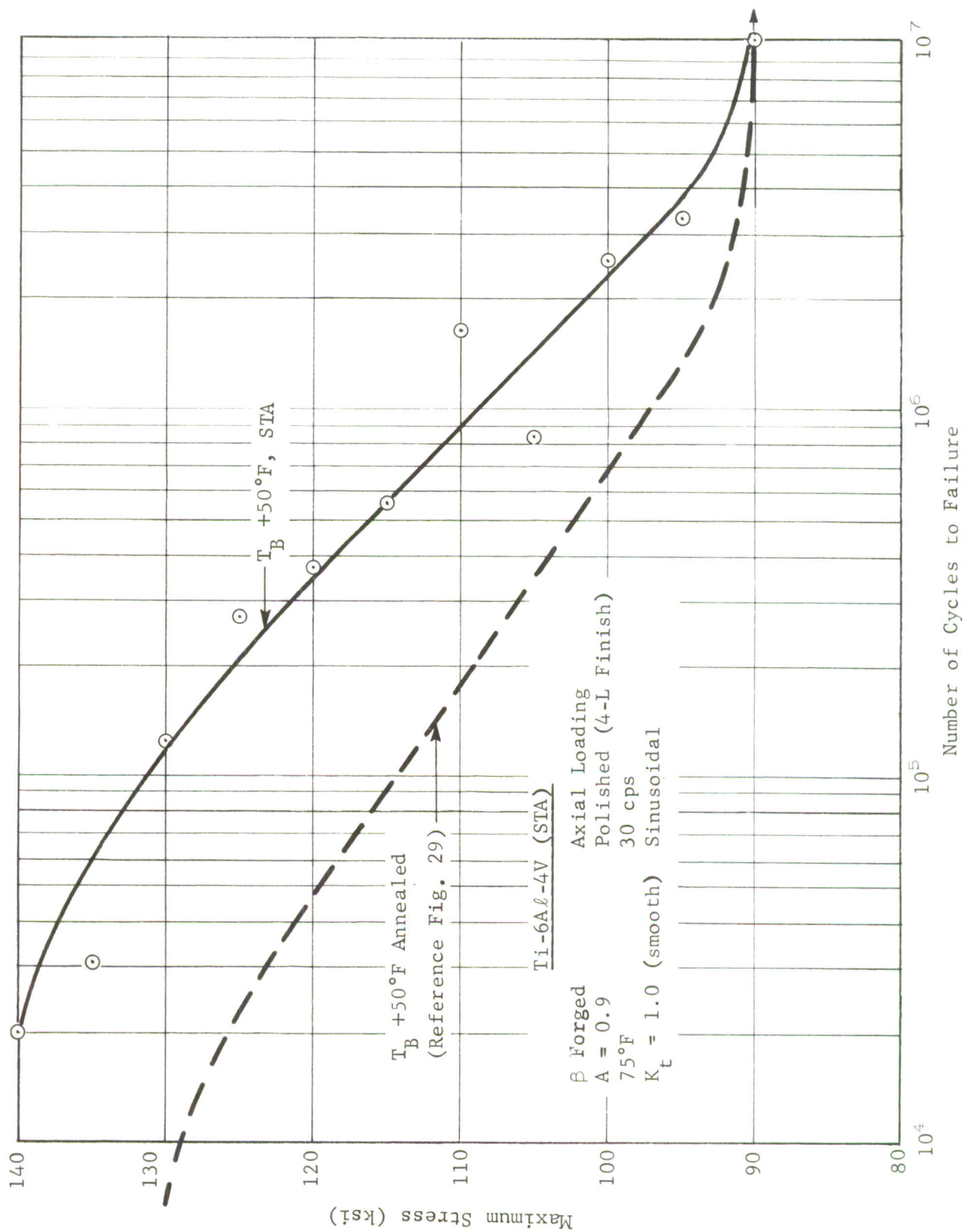


Figure 46 S-N Curve for STA 6Al-4V Titanium Alloy Finish Forged at 1880°F ($T_B + 50^\circ\text{F}$)

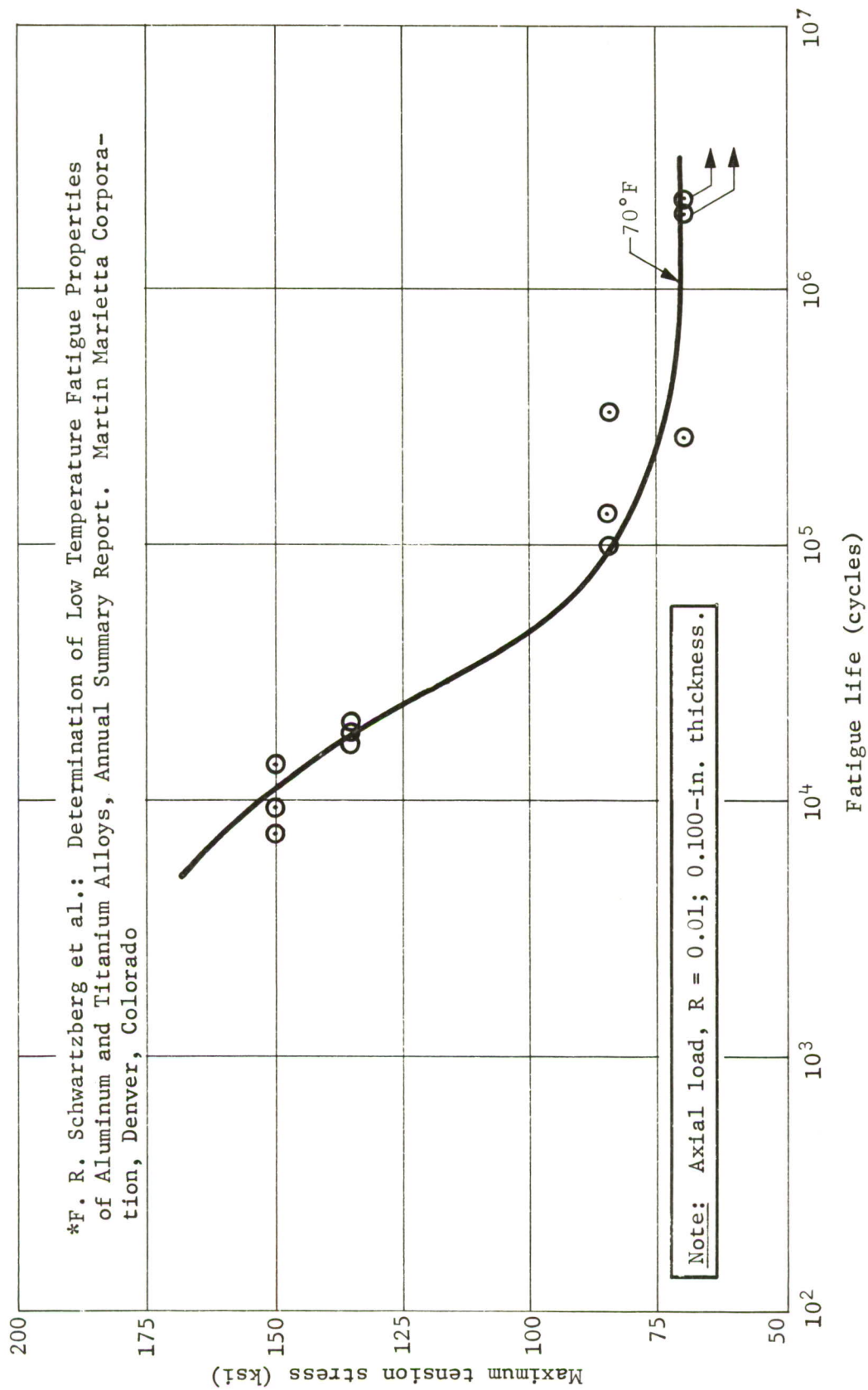


Figure 47 Fatigue Properties of Solution-Treated and Aged Parent Metal 6Al-4V Titanium Alloy*

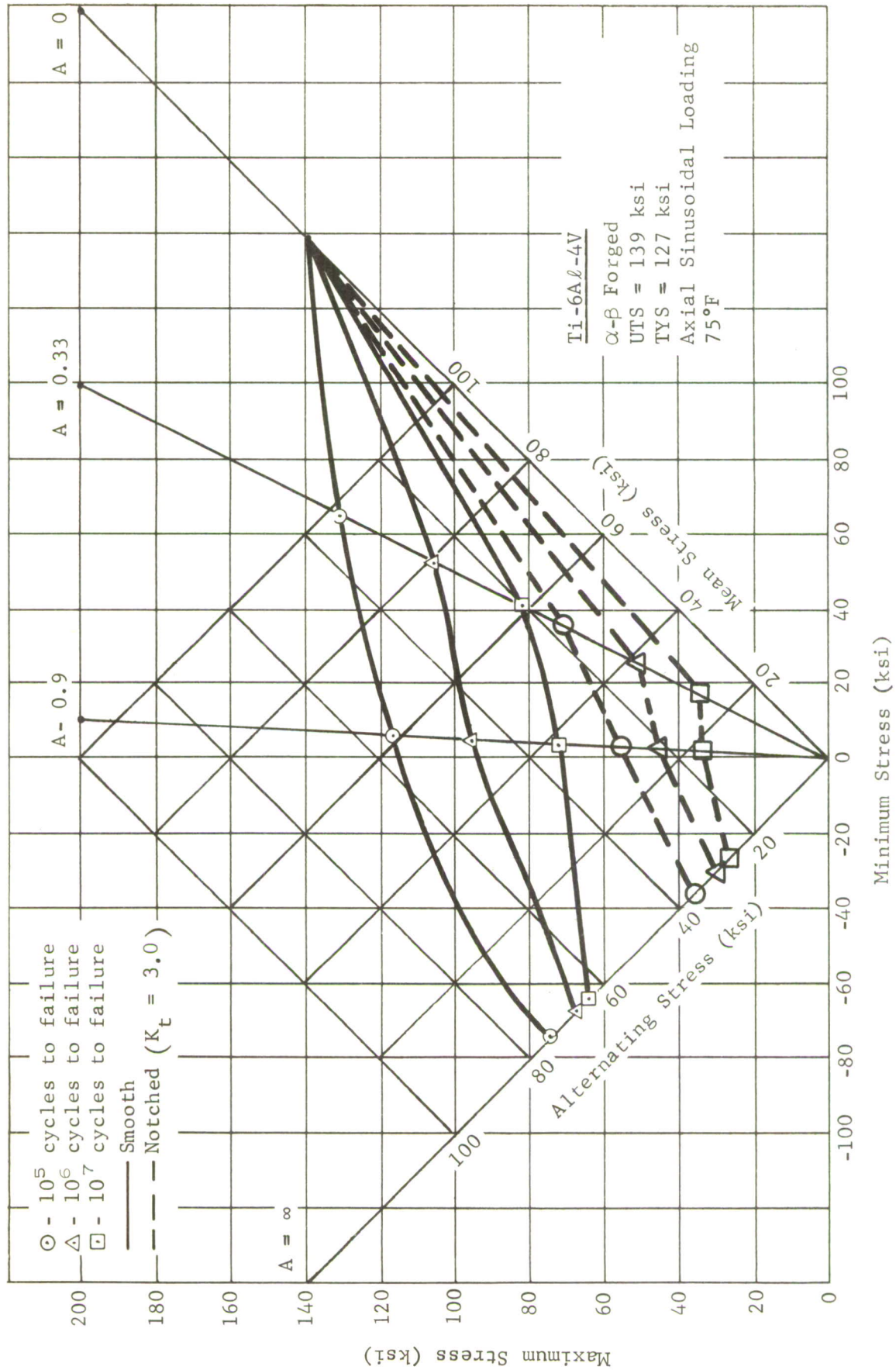


Figure 48 Constant-Life Diagram for Conventionally Forged 6Al-4V Titanium Alloy in Annealed Condition

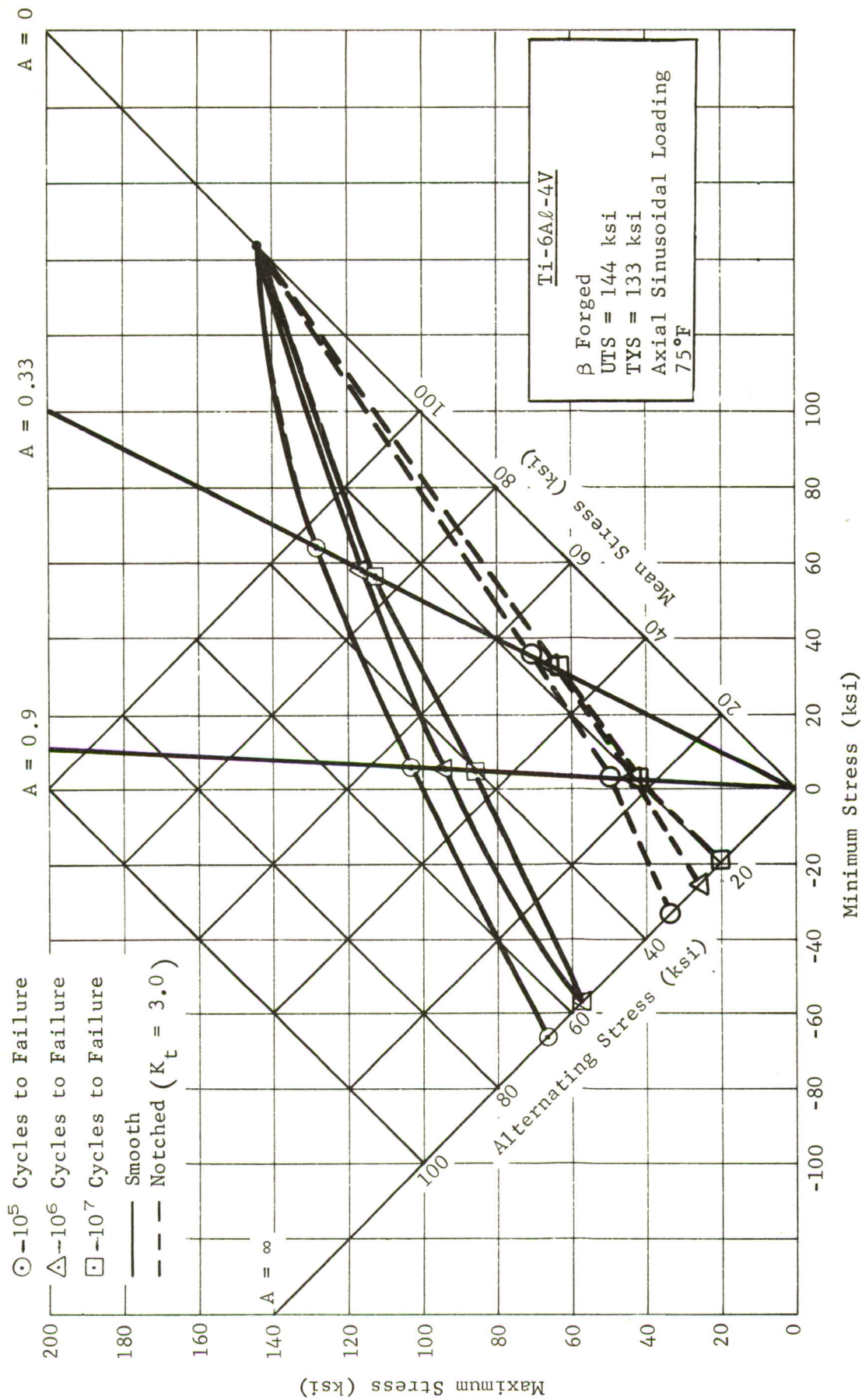


Figure 49 Constant-Life Diagram for Beta-Forged ($T_B + 120^\circ\text{F}$) 6Al-4V Titanium Alloy in Annealed Condition

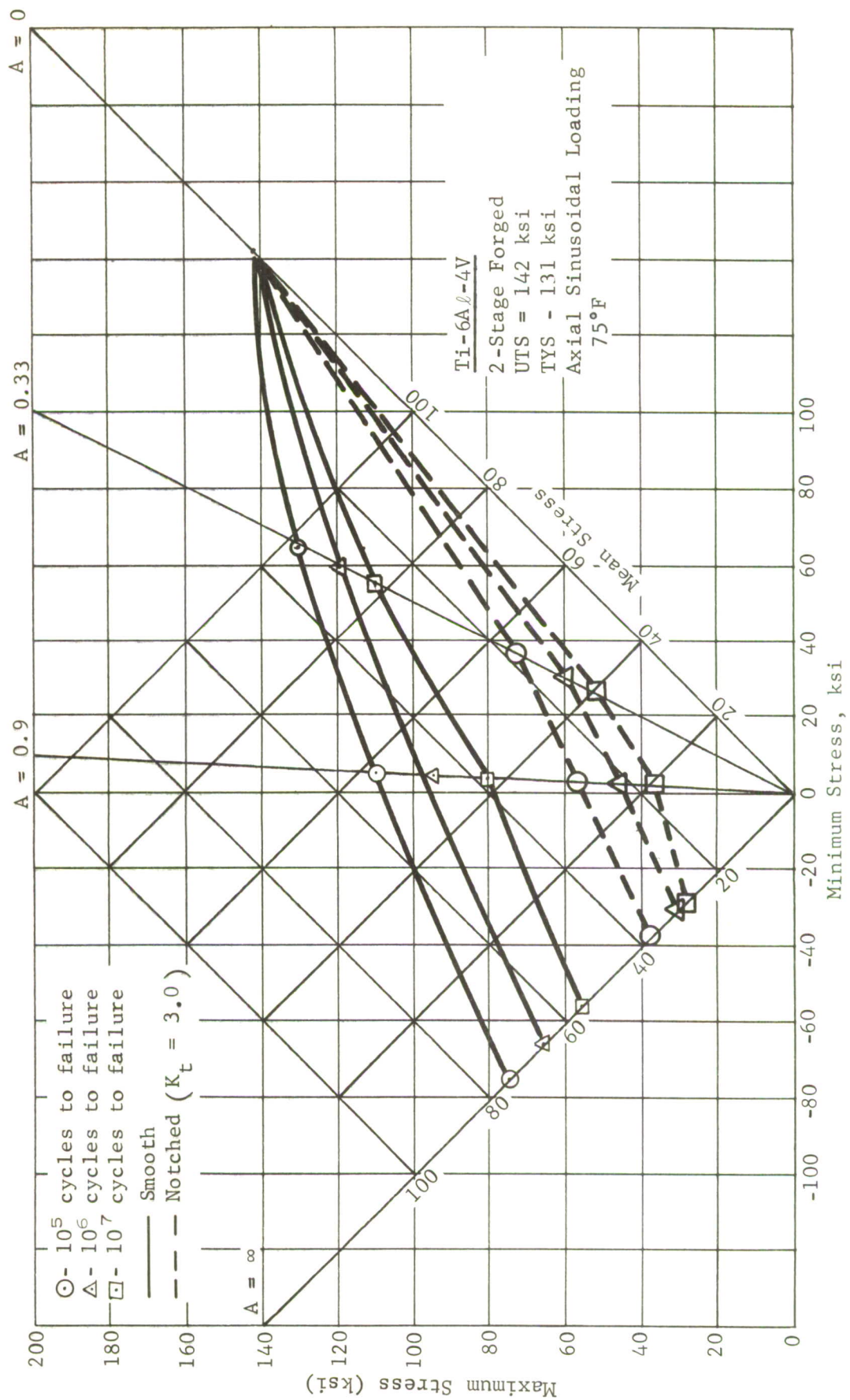


Figure 50 Constant-Life Diagram for Two-Stage Forged 6Al-4V Titanium Alloy in Annealed Condition

Table IV Summary of Forging Effects Fatigue Data

Material forging condition	Heat treatment	Fatigue strength (ksi) for indicated material and number of cycles								
		Smooth fatigue*			Notched fatigue* ($K_t = 3.0$)					
		Number of cycles								
		10^4	10^5	10^6	10^7	10^4	10^5	10^6	10^7	
Conventional Alpha-Beta ($T_B - 80^\circ\text{F}$)	Annealed	138	116	93	71	75	56	45	34	
Beta ($T_B + 50^\circ\text{F}$)	Annealed	129	114	97	90	73	56	48	43	
Beta ($T_B + 120^\circ\text{F}$)	Annealed	136	103	94	86	81	51	46	45	
Beta ($T_B + 270^\circ\text{F}$)	Annealed	126	117	97	77	72	57	48	40	
2-Stage ($T_B + 270^\circ\text{F}$ and $T_B - 80^\circ\text{F}$)	Annealed	130	109	93	77	80	57	46	37	
Beta ($T_B + 50^\circ\text{F}$)	STA	141	131	109	91					

*A = 0.9.

*A = 0.9.

Table V Summary of Fatigue Data for Conventional, Beta ($T_B + 120^\circ\text{F}$), and Two-Stage-Forged 6Al-4V Titanium Alloy

Material forging condition	A-ratio	Fatigue strength (ksi) for indicated material and number of cycles									
		Smooth fatigue					Notched fatigue (K _t = 3.0)				
		Number of cycles									
		10 ⁴	10 ⁵	10 ⁶	10 ⁷	10 ⁴	10 ⁵	10 ⁶	10 ⁷		
Conventional (T _B - 80°F)	0.33	---	129	103	81	---	70	51	35		
Beta (T _B + 120°F)	0.33	---	128	116	113	110	71	67	67		
Two stage	0.33	---	131	118	110	109	72	60	52		
Conventional (T _B - 80°F)	0.90	138	116	93	71	75	56	45	34		
Beta (T _B + 120°F)	0.90	136	103	94	86	81	51	46	43		
Two stage	0.90	130	109	93	77	80	57	46	37		
Conventional (T _B - 80°F)	∞	100	74	68	64	48	35	31	28		
Beta (T _B + 120°F)	∞	100	66	57	57	48	34	26	21		
Two stage	∞	93	75	66	58	51	38	31	29		

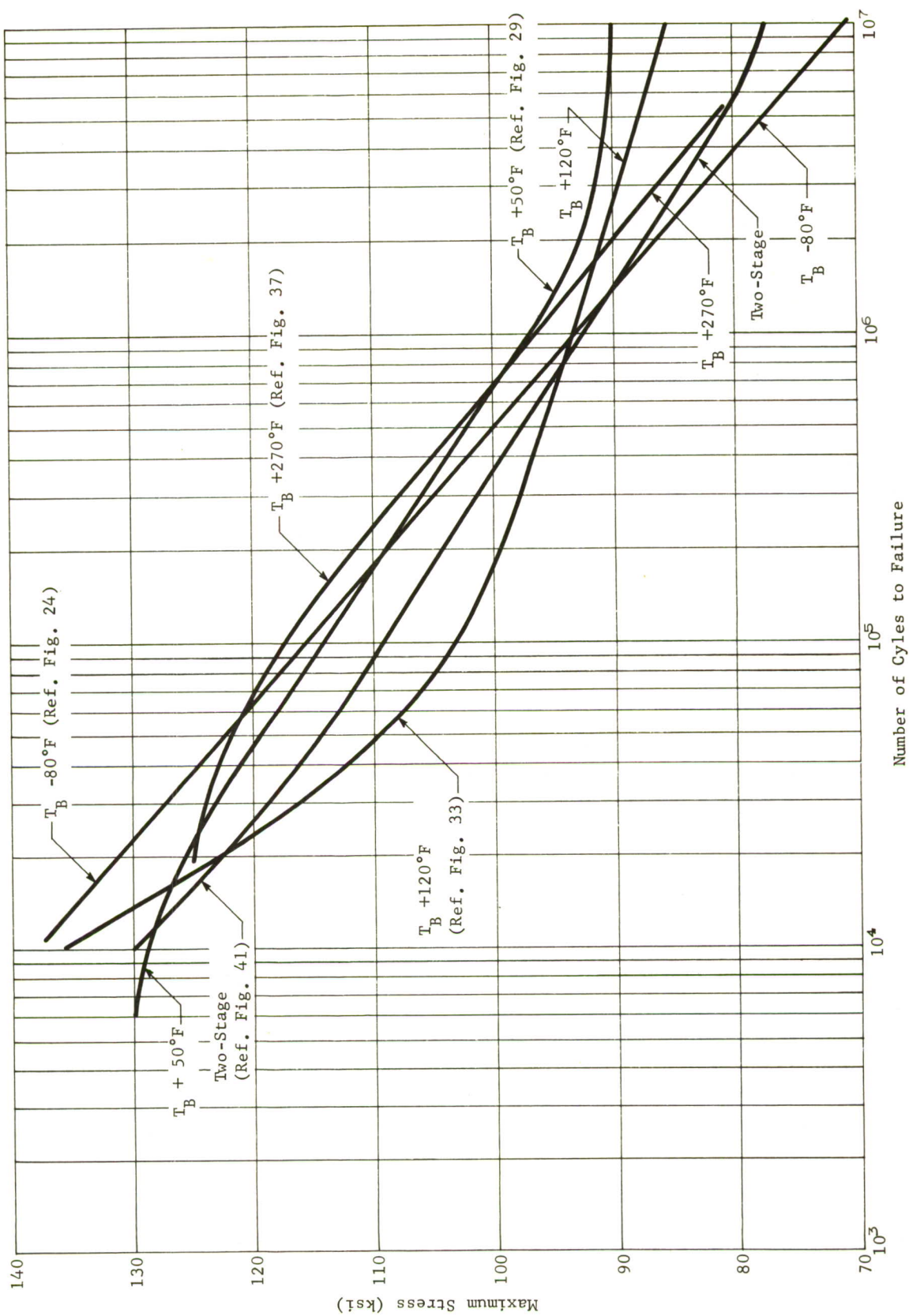


Figure 51 Summary of Forging Temperature Effects on Smooth Fatigue Strength of 6Al-4V Titanium Alloy ($A = 0.9$)

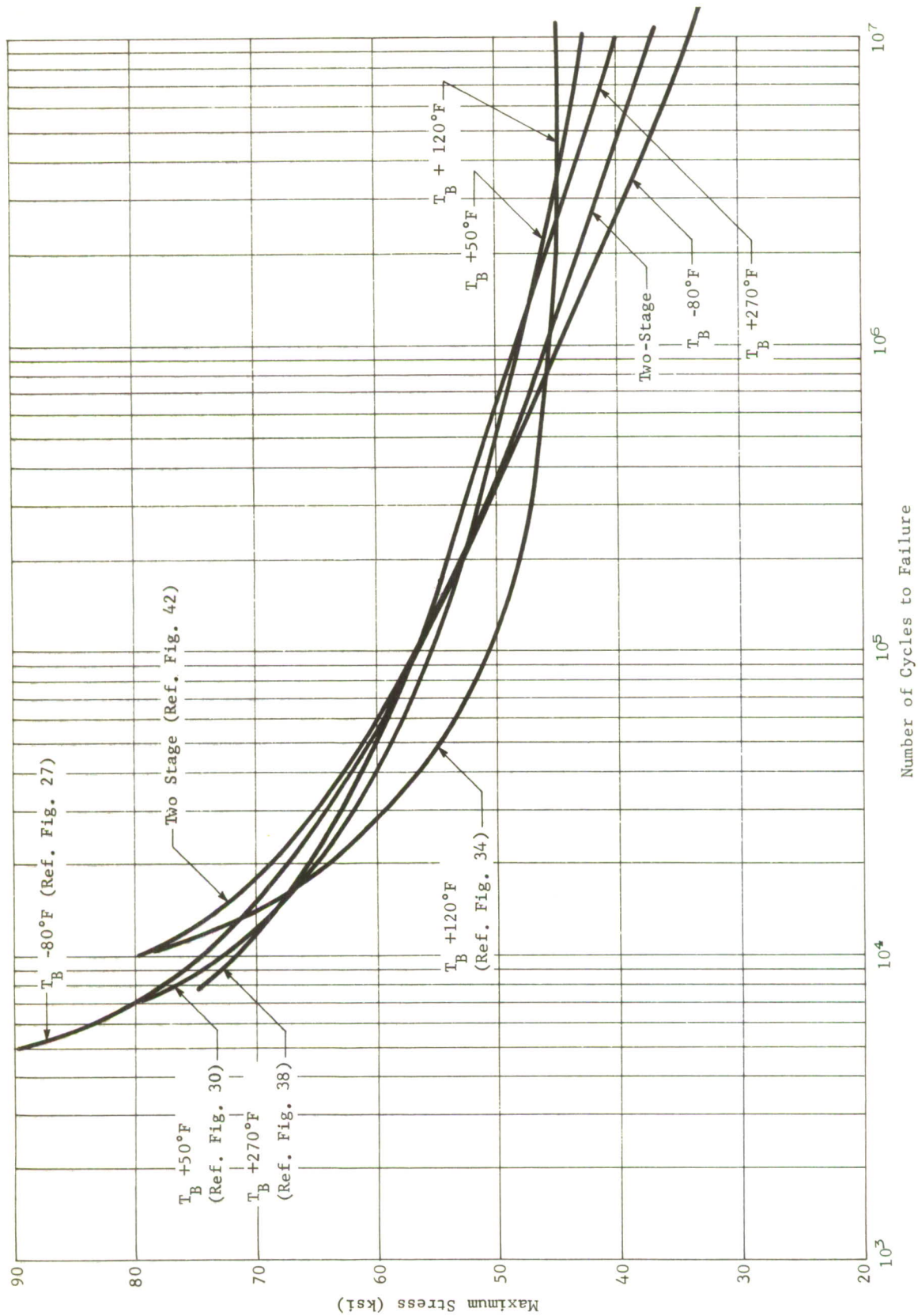


Figure 52 Summary of Forging Temperature Effects on Notched Fatigue Strength of 6Al-4V Titanium Alloy ($K_t = 3.0$, $A = 0.9$)

Another interesting trend that can be observed from Table IV is that a higher forging temperature reduces the fatigue limit of the unnotched specimens. This detrimental effect is most apparent if one compares the material forged at 1880°F with material forged at 2100°F, or the two-stage forged material. Although the long-term fatigue strength was greatest for the material forged at $T_B + 50^\circ\text{F}$, the material forged at $T_B + 120^\circ\text{F}$ was nearly as strong; this trend was reversed for the notched specimen data. Since the long-term fatigue strength is more important for most design applications, the choice of an optimum beta-forging temperature seemed to be between 1880°F and 1950°F.

A higher forging temperature offers the advantages of improved forgeability and longer forge-die life. Less force is required to forge parts and shape definition is improved because the material's resistance to plastic flow is reduced. Since the two forging temperatures produced material with similar tensile and fatigue properties, the higher forging temperature, $T_B + 120^\circ\text{F}$, was selected on the basis of better forgeability.

After selection of the optimum forging temperature, more fatigue testing was performed to determine the effect of stress ratio on the optimum beta-forged ($T_B + 120^\circ\text{F}$) and two-stage-forged material. These results are summarized in the constant life diagrams, Figure 49 and 50, and in Table V. Examination of Table V shows that the beta-forged material is stronger for $A = 0.9$ or 0.33 , but is weaker for reversed loading. The two-stage-forged material offers no particular advantage at any stress ratio. The data are also very consistent between smooth and notched fatigue results, e.g., if the beta-forged material is strongest in smooth condition it is also strongest in notched fatigue. The two-stage-forged material does not seem to be quite as sensitive to reversed loading (especially notched) as the beta-forged material.

The S-N curves for 6Al-4V titanium alloy in STA condition are presented in Figures 45 and 46. Since no conventional-forged STA material was evaluated in this program, a representative S-N curve was obtained from a previous testing program conducted at Martin Marietta and is presented in Figure 47. The STA material tested in both programs have similar chemistry and tensile properties but vary in product form, the previous testing being performed on 0.100-in. sheet.

Comparison of these two S-N curves (Figure 46 and 47) reveals that the beta-forged STA material is significantly stronger than the conventional-forged STA material at life times of 10^5 , 10^6 , and 10^7 cycles. Therefore, heat treating subsequent to beta-forging has not eliminated the improved fatigue properties that were realized from the annealed material.

The S-N curve for annealed beta-forged ($T_B + 50^\circ\text{F}$) material is shown as a dashed line in Figure 46. The effect of heat treatment can be observed by comparing the two curves in this figure and values in Table IV. Notice that the strengthening mechanism of heat treating has significantly improved shorter lifetime fatigue properties. This is to be expected from the differences in tensile properties between the two conditions. However, the fatigue limit is apparently unaffected by heat treating. This may indicate the fracture toughness of the material in these two conditions is similar.

2. SURFACE EFFECTS

The same heat of material was used for surface effect studies as for forging effect studies. The material, 6Al-4V titanium, was evaluated in conventional ($T_B - 80^\circ\text{F}$) and beta ($T_B + 120^\circ\text{F}$) - forged condition and subsequently annealed. The fatigue data for these two materials in the various surface conditions are presented as S-N curves in Figures 53 through 61 and are summarized in Table VI and Figures 62 and 63.

Examining Figures 62 and 63 reveals several data trends. The chemically milled material generally has the lowest fatigue strength at either forging condition. This is probably the result of complete removal of all worked material from the surface of these specimens. Conventionally forged material in Figure 62 showed significant improvement in fatigue strength as a result of grinding or lathe turning. When these surface preparations are followed by shot peening, an improvement is noticed in short time fatigue properties, but the material is more prone to fracturing and has the lowest fatigue strength at 10^7 cycles of all surface preparations. Fatigue data for conventional-forged polished specimens (from forging effect studies) showed little improvement over chemical milled specimens. This is possibly the result of smaller compressive surface layer stresses imposed during polishing as compared to other mechanical material removal techniques. Pronounced grain distortion was visually observed in polished and etched sections from lathe-turned material (Figure 16). Fatigue strength is often enhanced by creating a compressive surface layer (generally accomplished in industry by shot peening). Machining techniques such as grinding or turning will create stress concentrations which are detrimental to fatigue strength. Thus there are the two factors present in a surface preparation procedure, one helpful and the other deleterious, working against each other to produce the end result. These effects coupled with the two material conditions with their different susceptibility to fracture make comparison of the surface preparation effects between the two materials difficult.

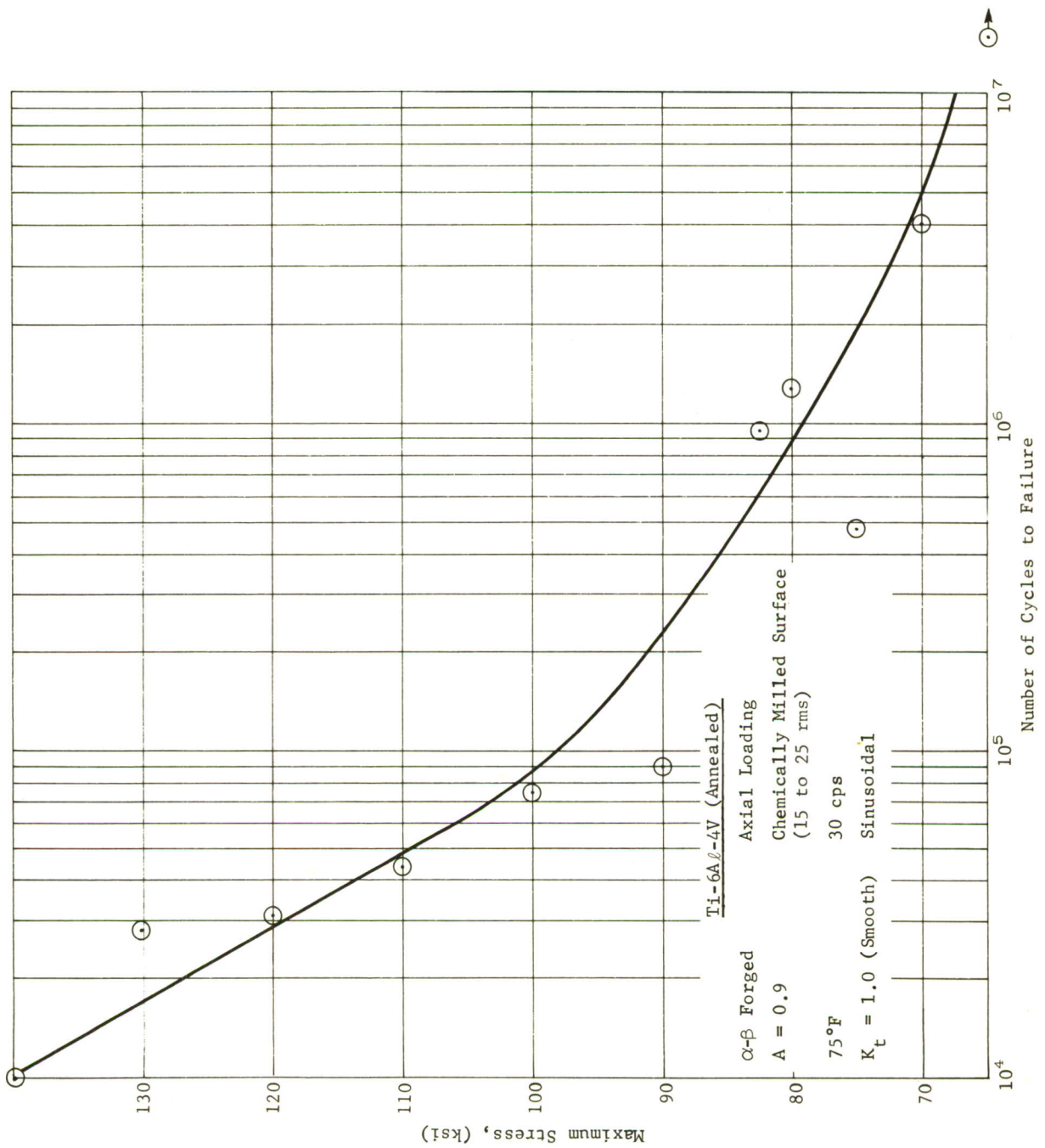


Figure 53 S-N Curve for Chemically Milled 6Al-4V Titanium Alloy
Finish Forged at 1750°F ($T_B - 80^\circ\text{F}$)

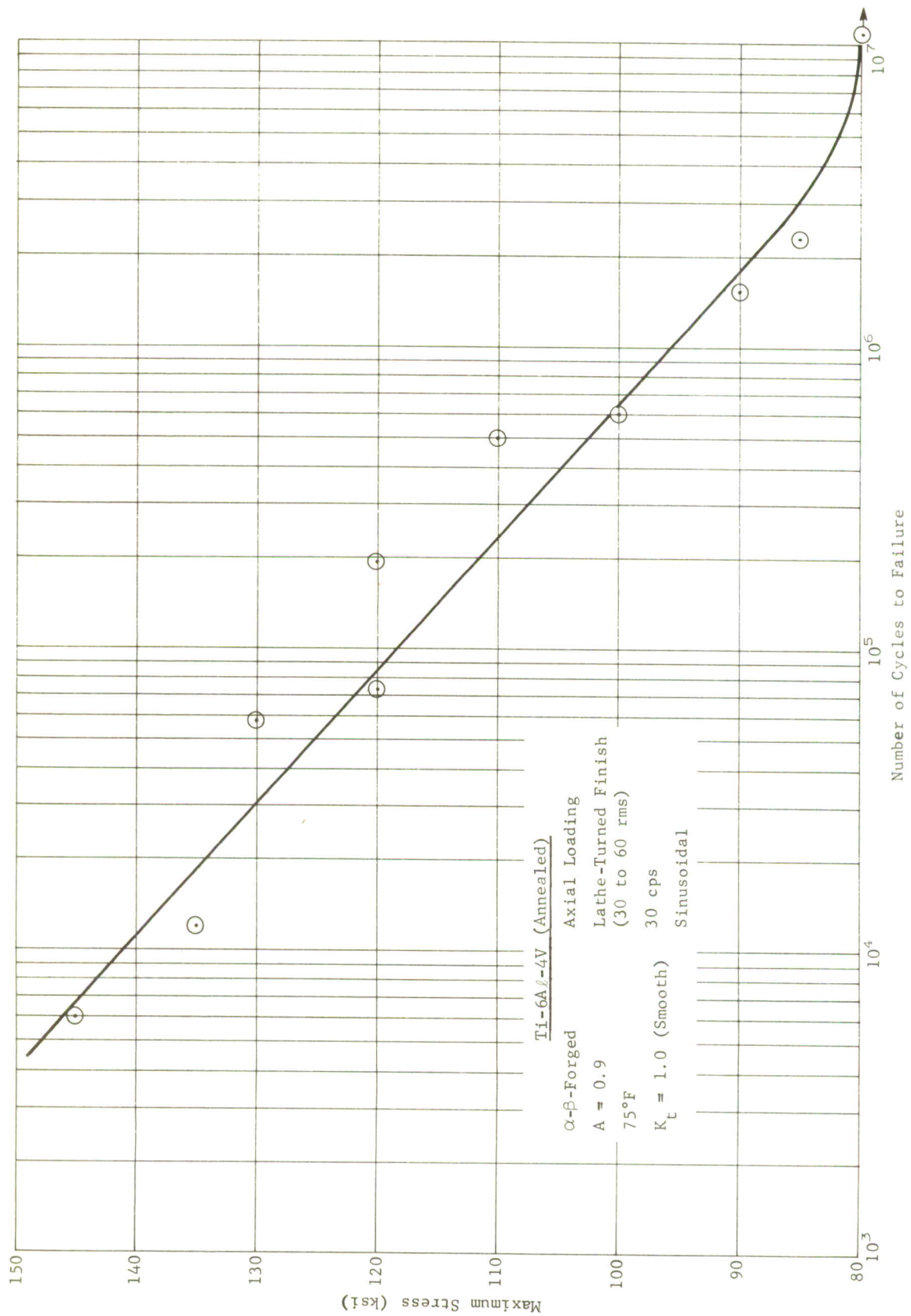


Figure 54 S-N Curve for Lathe-Turned 6Al-4V Titanium Alloy
Finish Forged at 1750°F ($T_B - 80^\circ F$)

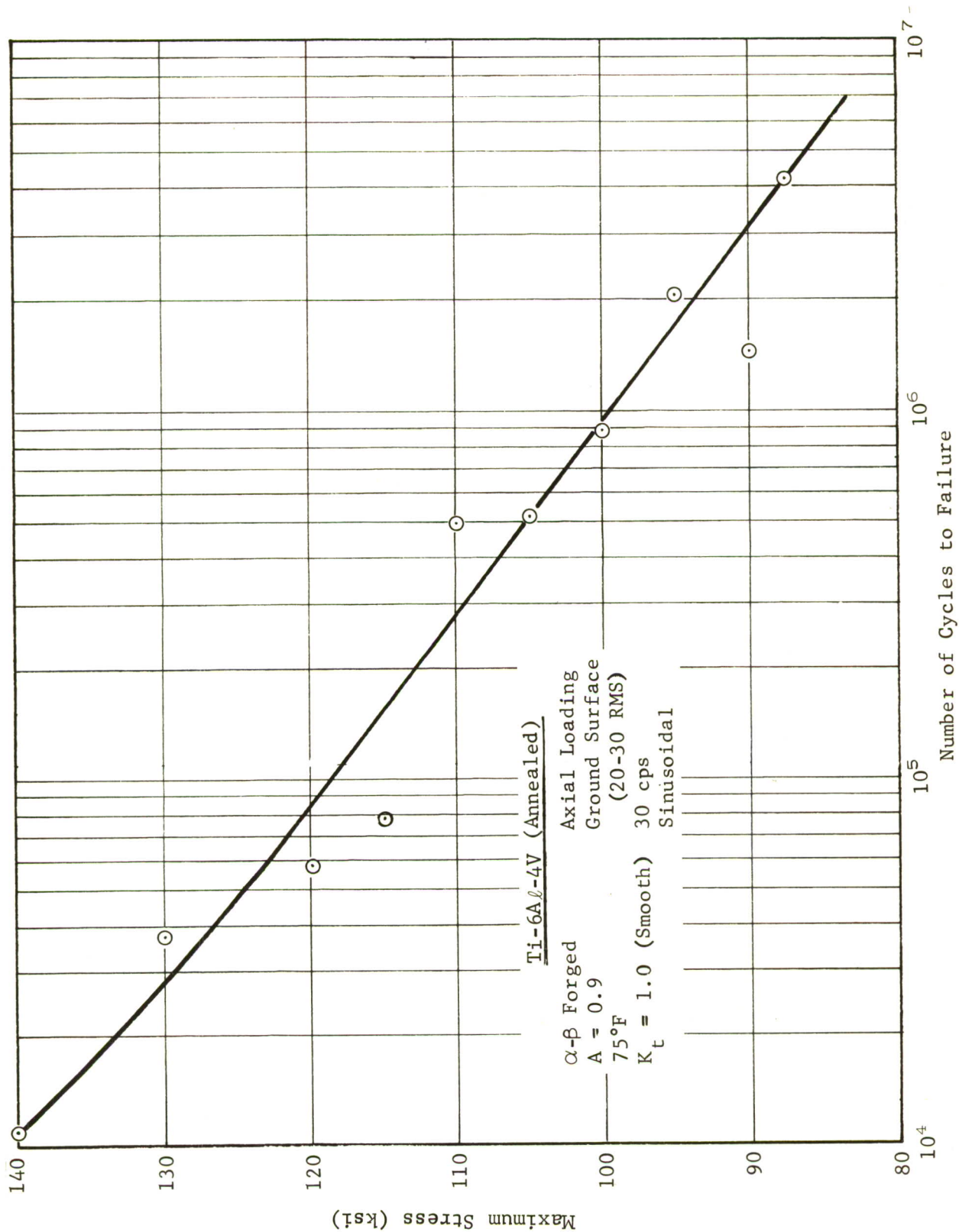


Figure 55 S-N Curve for Ground 6Al-4V Titanium Alloy Finish Forged at 1750°F ($T_B - 80^{\circ}\text{F}$)

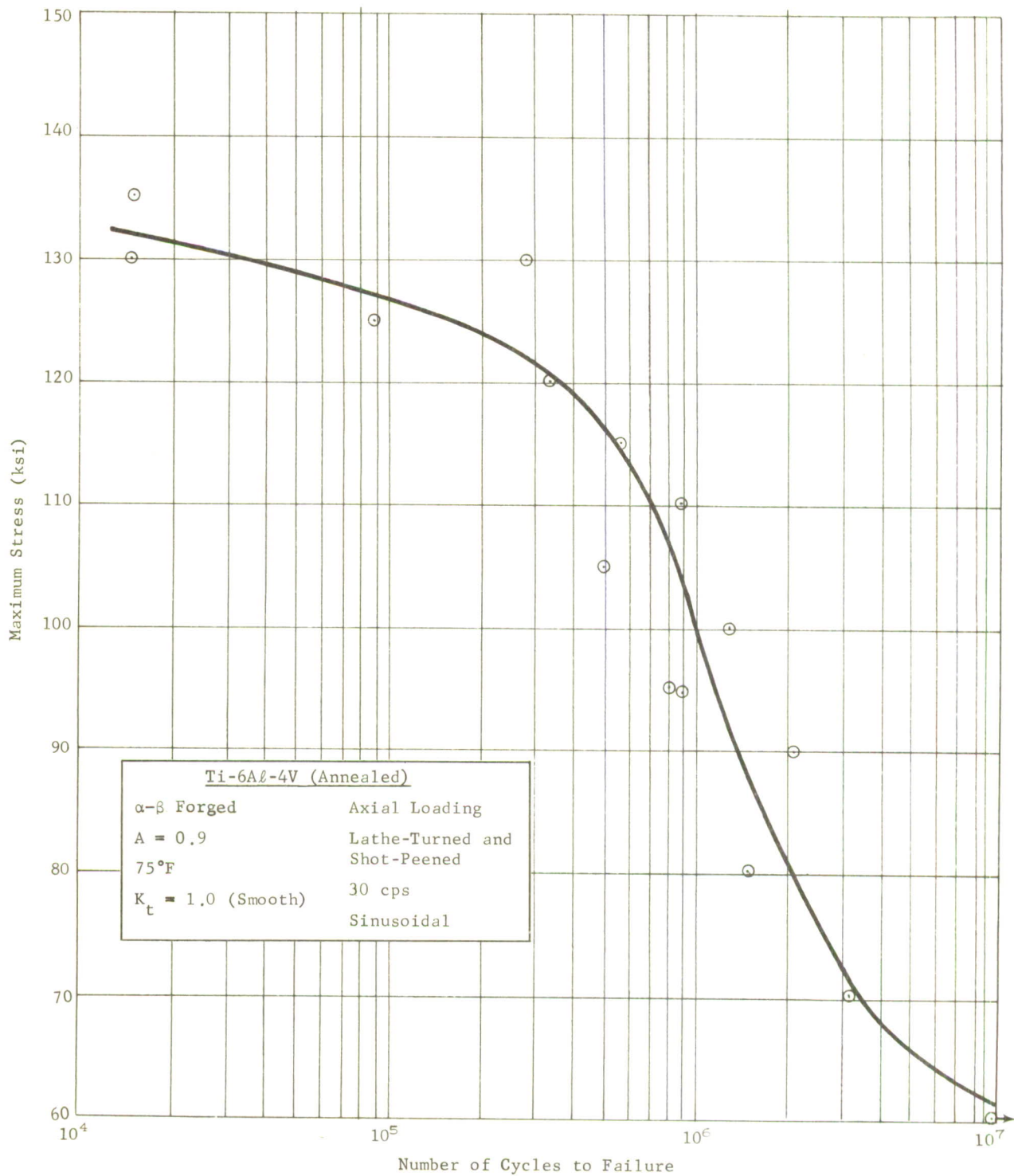


Figure 56 S-N Curve for Lathe-Turned and Shot-Peened 6Al-4V Titanium Alloy
Finish Forged at 1750°F ($T_B - 80^\circ\text{F}$)

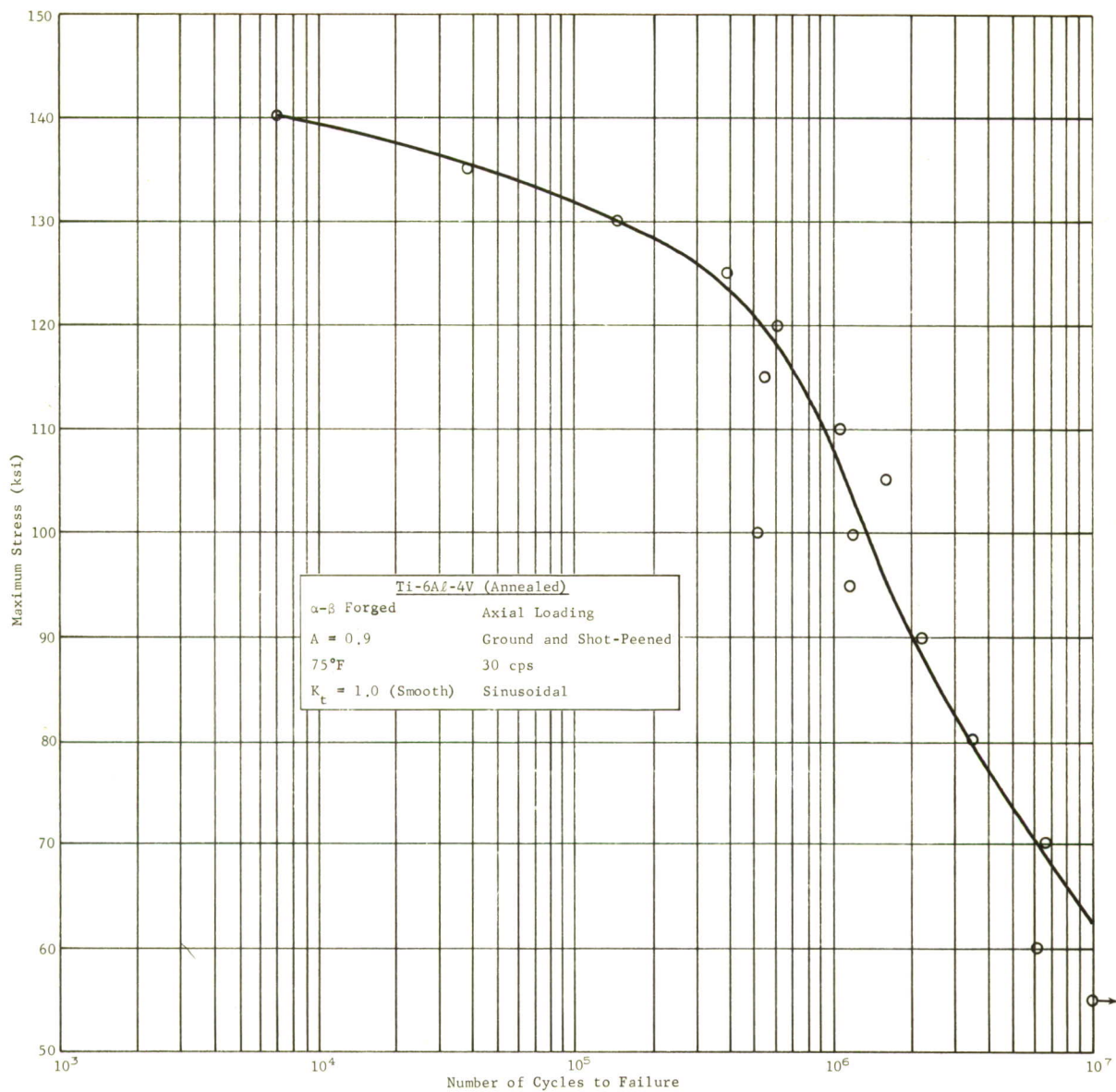


Figure 57 S-N Curve for Ground and Shot-Peened 6Al-4V Titanium Alloy Finish Forged at 1750°F ($T_B - 80^\circ\text{F}$)

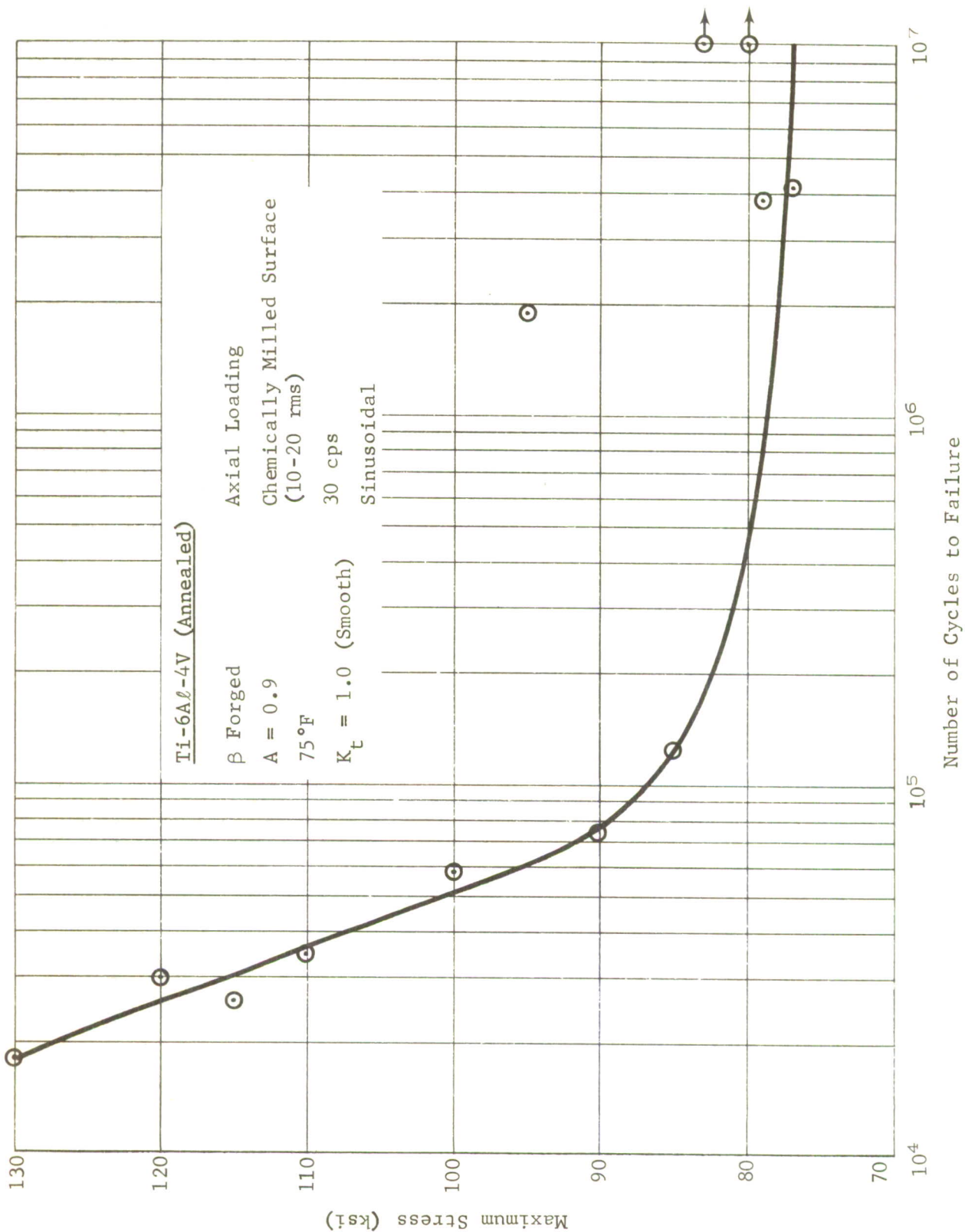


Figure 58 S-N Curve for Chemically Milled 6Al-4V Titanium Alloy Finish Forged at 1950°F
 $(T_B + 120^\circ\text{F})$

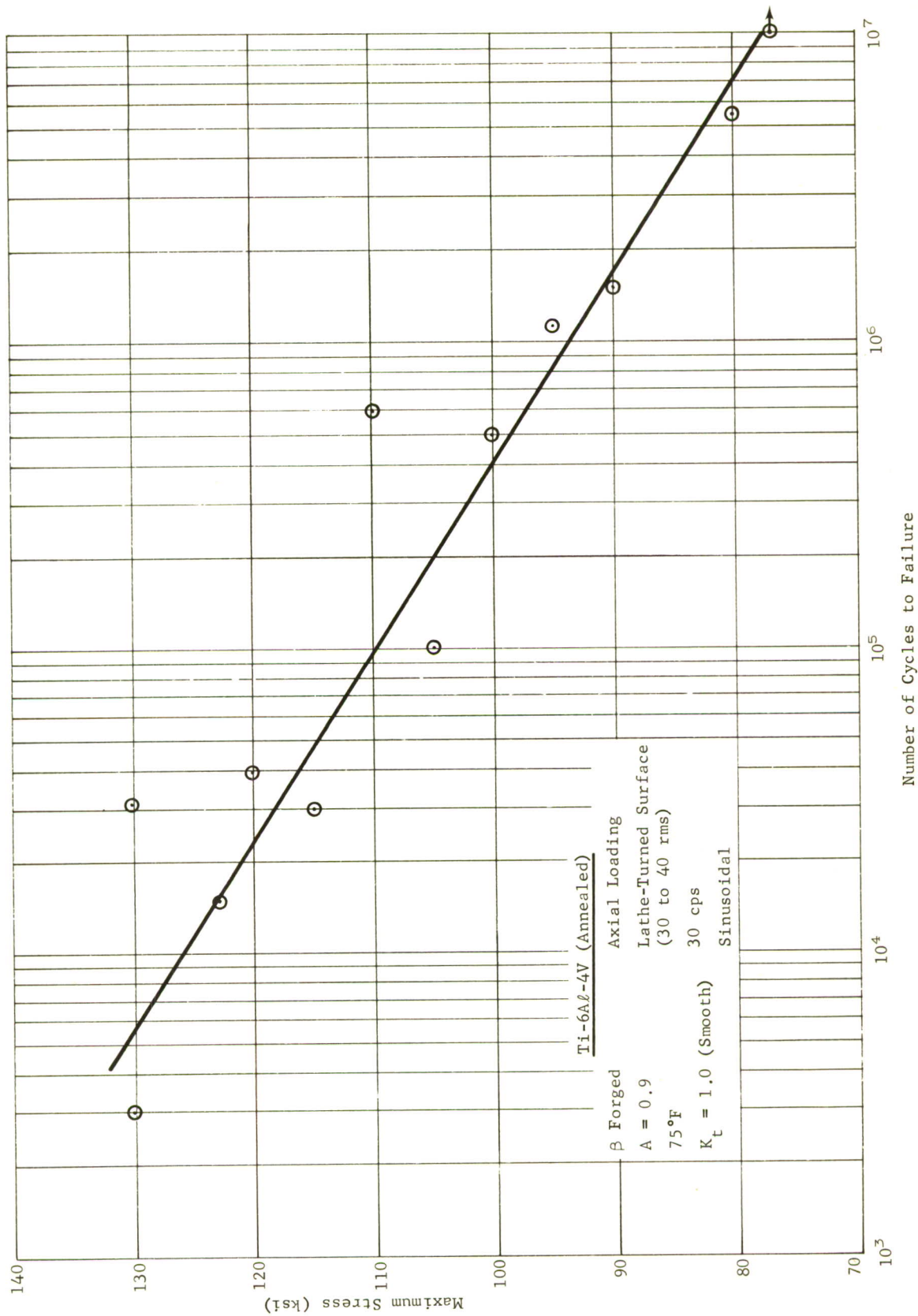


Figure 59 S-N Curve for Lathe-Turned 6Al-4V Titanium Alloy Finish Forged at 1950°F ($T_B + 120^\circ\text{F}$)

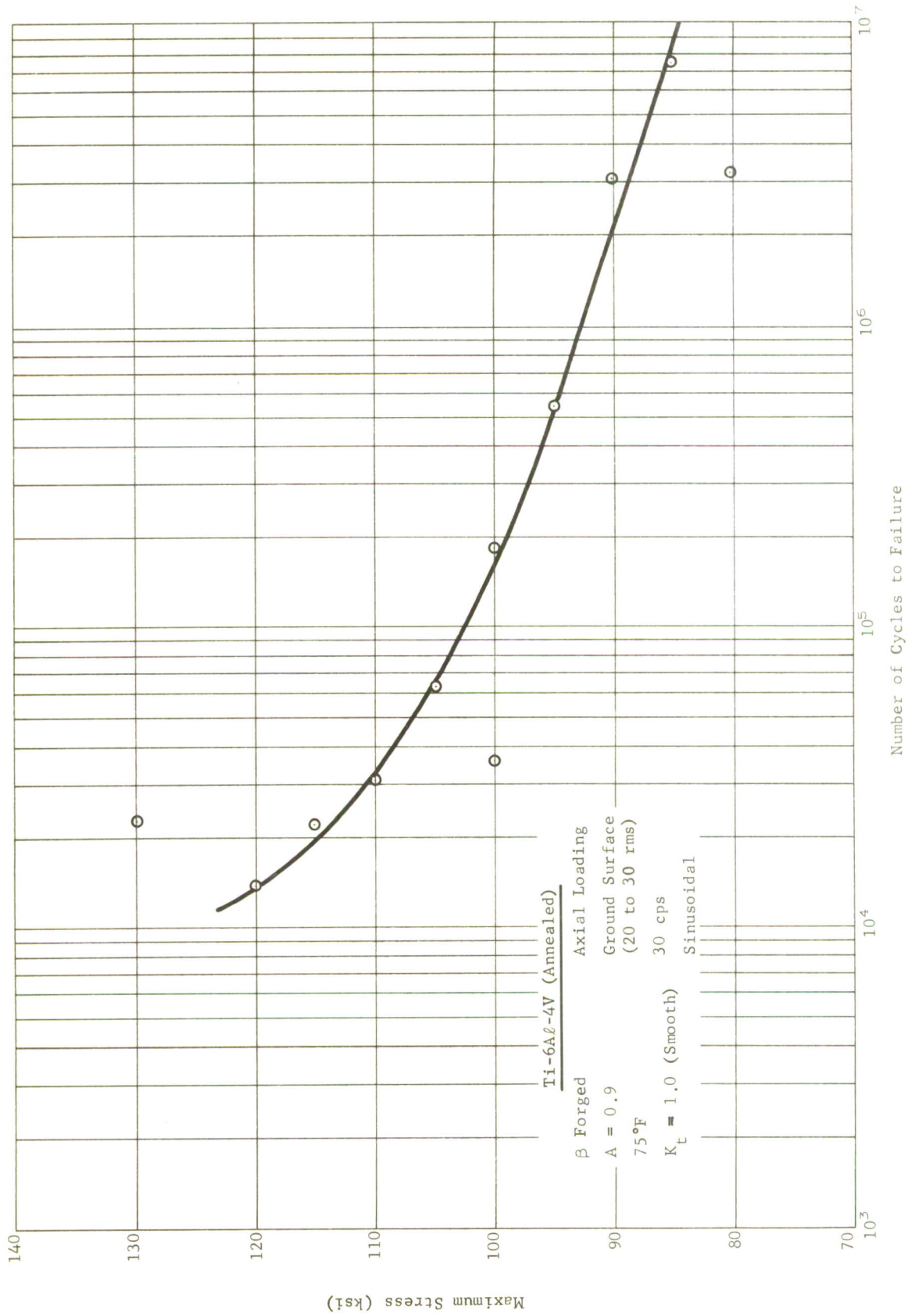


Figure 60 S-N Curve for Ground 6Al-4V Titanium Alloy Finish Forged at 1950°F ($T_B + 120^\circ\text{F}$)

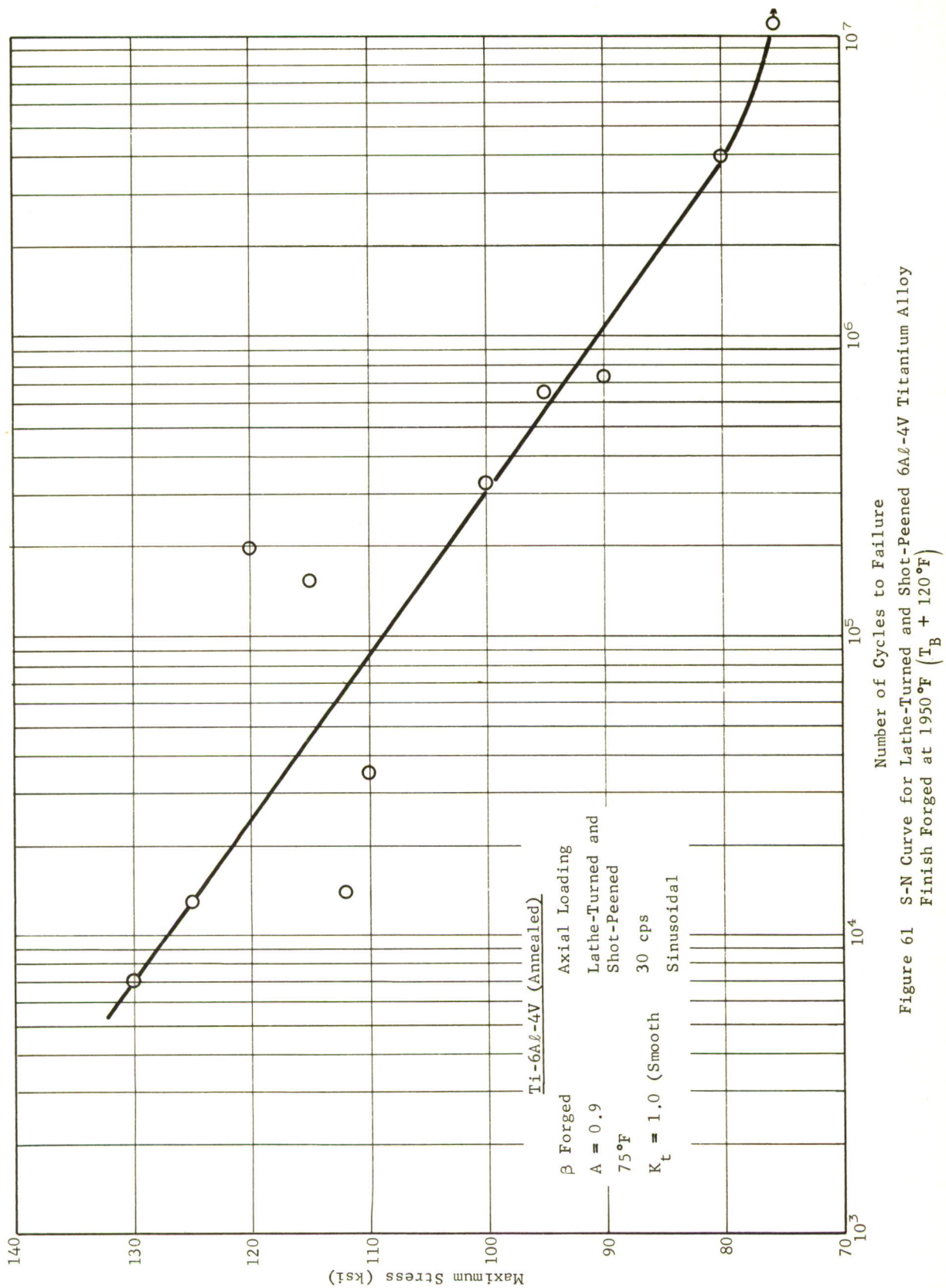


Figure 61 S-N Curve for Lathe-Turned and Shot-Peened 6Al-4V Titanium Alloy
 Finish Forged at 1950°F ($T_B + 120^\circ\text{F}$)

Table VI Summary of Fatigue Data* for Surface Effect Studies of Conventional and Beta-Forged 6Al-4V Titanium Alloy

Surface preparation technique	Fatigue strength (ksi) of indicated material and number of cycles							
	Conventional forged ($T_B - 80^\circ\text{F}$) material				Beta forged ($T_B + 120^\circ\text{F}$) material			
	Number of cycles							
	10^4	10^5	10^6	10^7	10^4	10^5	10^6	10^7
Chemical milled	140	98	79	67	---	87	79	76
Polished	138	116	93	71	136	103	94	85
Lathe turned	141	118	96	81	126	109	94	78
Ground	141	118	99	---	126	103	93	85
Lathe turned and shot peened	133	127	101	61	127	109	91	76
Ground and shot peened	139	132	108	63	---	---	---	---

*A = 0.9.

*A = 0.9.

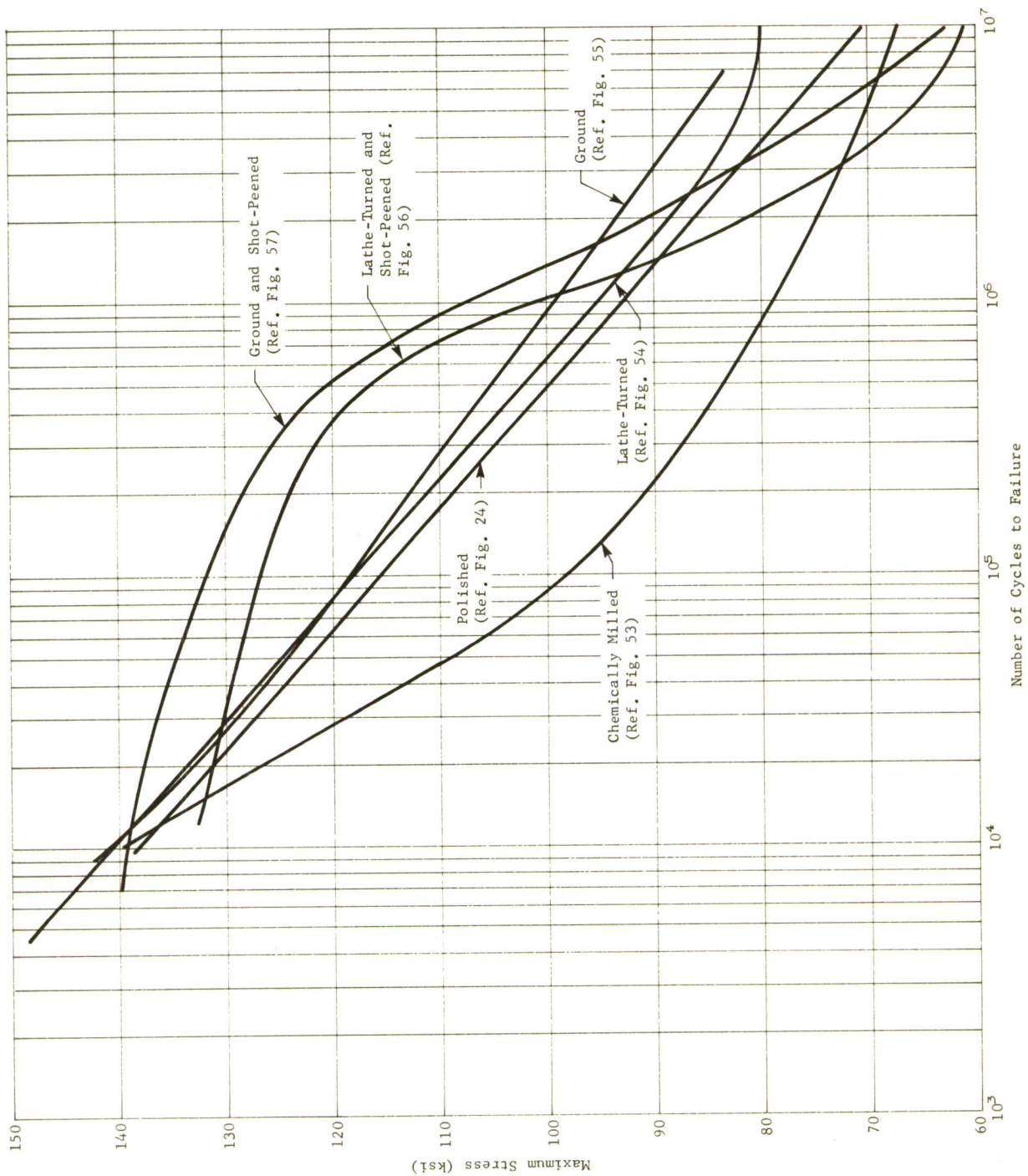


Figure 62 Summary of Surface Effects on Fatigue Strength of 6Al-4V Titanium Alloy Finish Forged at 1750°F (T_B -80°F, $A = 0.9$)

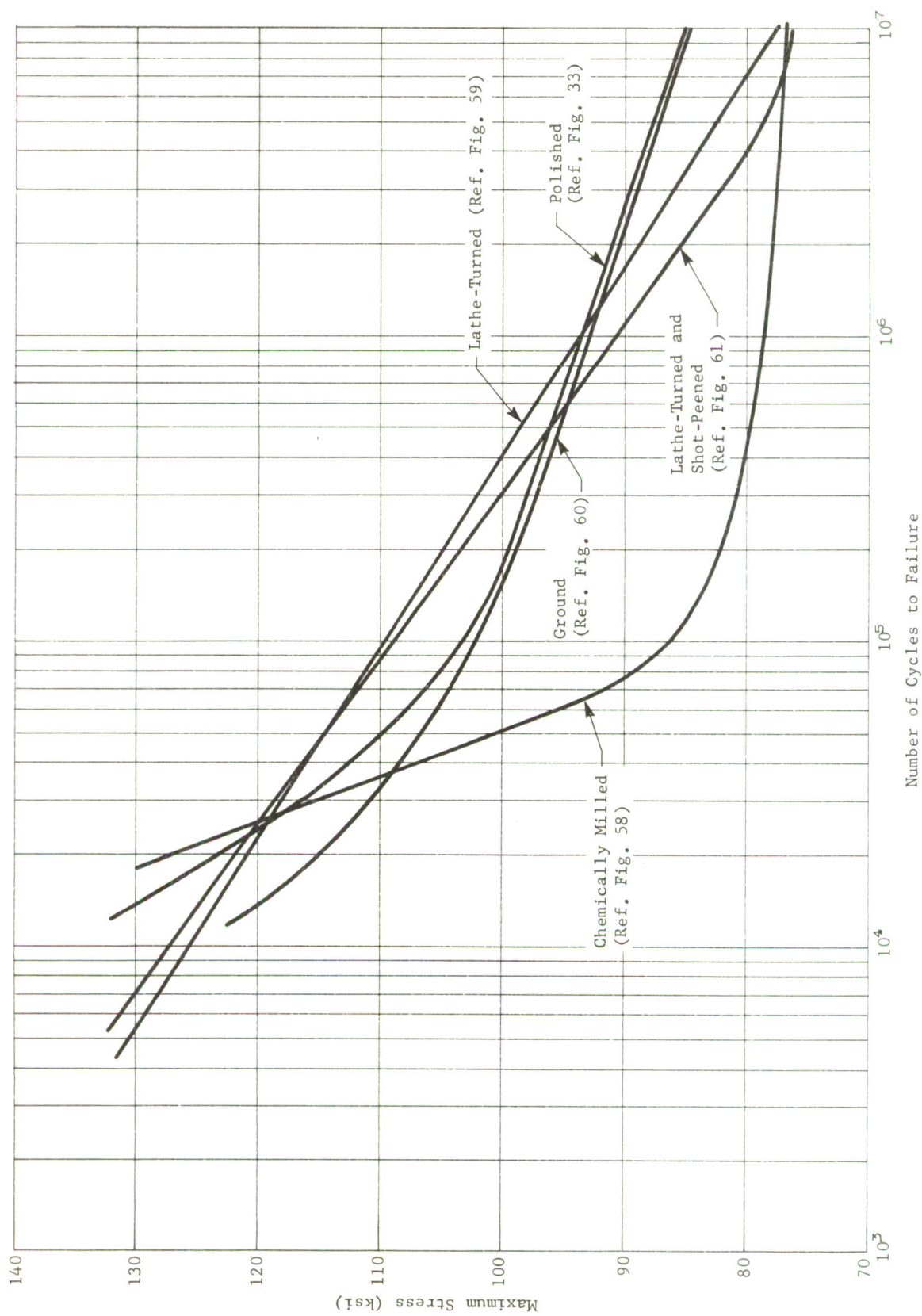


Figure 63 Summary of Surface Effects on Fatigue Strength of 6Al-4V Titanium Alloy Finish Forged at 1950°F ($T_B + 120^\circ\text{F}$, $A = 0.9$)

With the exception of chemical milling, notice that each materials reaction to a particular surface preparation technique is different, e.g., shot peening. The beta-forged material does not show the initial strengthening from shot peening observed in the conventional-forged material. However, the longer-term fatigue data of beta-forged material show less scatter and detrimental affect* from shot peening than the conventional-forged material. The higher fracture toughness of the beta-forged material⁴ would indicate a higher tolerance for defects imposed during shot peening and contribute to the better long-term fatigue performance of the beta-forged material in this surface condition.

Compared to chemical milling, mechanical material removal of the surface of the specimens was not detrimental to fatigue properties. Perhaps if the shot peened surface had been less irregular (Figure 20) scatter would have been less frequent and long-term fatigue properties would have been enhanced. The irregular surface may have been the result of the shot peening intensity being too high. For 4340 steel, a small change in shot peening intensity causes strong changes in the fatigue limit.⁵ A shot peening intensity of 0.006-0.008A produced failure of 4340 specimens between $1.5 - 2.5 \times 10^6$ cycles while a higher intensity of 0.010-0.012A caused failure under 0.5×10^6 cycles, all tests being conducted with the same loading cycle.

*(i.e., the fatigue limit at 10^7 cycles for shot peened samples is the same as for chemical milled samples.)

⁴ "Boeing Model 2707 Airframe Design Report, Part D, Materials and Processes," Report V2-B2707-8, Contract FA-SS-66-5, The Boeing Company (Sept. 6, 1966).

⁵ A. Pomp and M. Hempel: Comparative Investigation of Nickel and Nickel-Free Steels Concerning their Mechanical Characteristics, Especially with Respect to their Behavior During Fatigue Tests. Mitt. Kaiser-Wilhelm-Inst. Eisentorsch Dusseldorf, Vol. 19, pp. 221-236, 1937.

SECTION VI

CONCLUSIONS AND RECOMMENDATIONS

The fatigue strength of annealed beta-forged ($T_B + 120^\circ\text{F}$) 6Al-4V titanium alloy was superior to the conventional-forged material at the two stress ratios, $A = 0.33$ and 0.90 . This trend was reversed at $A = \infty$ (reversed loading), i.e., the conventional-forged material had a higher fatigue limit than the beta-forged material, although there was an overlapping of data points. This apparent sensitivity to a tension-compression cycle in the beta-forged material should be examined more thoroughly by obtaining more data at intermediate stress ratios. The conventional forged material cannot be overlooked in such a test program, because it provides a baseline of comparison. An examination of the constant-life diagrams for these two materials (Figure 48 and 49) indicates that the data from conventional-forged material was less uniform with the stress-ratio parameter, and the possibility of making an invalid comparison on the basis of this limited test program is more likely to occur. With the advantages of increased forgeability, fracture toughness, and limited improvement in fatigue strength, the design engineer should consider the beta-forging process superior to conventional forging.

The two-stage-forged material yielded fatigue properties that were intermediate between properties obtained from conventional forging and from complete beta forging ($T_B + 120^\circ$). If the two forging temperatures and the amount of finish forging reduction were optimized this procedure could very likely produce a material with superior properties. Fracture toughness properties are also needed for this forging condition.

The limited fatigue data obtained from beta-forged STA 6Al-4V titanium show that the improvement in fatigue properties is retained even with subsequent heat treatment. Good representative baseline data are required to determine if the improvement changes with stress ratio or surface condition.

Examining all of the fatigue results for a possible effect of forging location revealed that there was some tendency for fatigue results to be higher from beta-forged ($T_B + 120^\circ\text{F}$) specimens machined from position Number 1 in the forging block, e.g., see Figures 33, 59, 60, and 61. This is possibly the result of slightly more flow and beta-grain working at that position in the forging.

Surface effect studies indicated that polishing, lathe-turning, or grinding, if carefully controlled, improved fatigue strength over the chemical milled specimens. Chemical milling was used as a baseline for comparison since this process removes residual surface stresses formed during processing, thus resulting in essentially an energy-free surface.

The broad range of fatigue results obtained from this study would indicate a strong need for standardization of specimen surface preparation technique. It would also seem logical to suggest a technique shunning mechanical material removal in favor of chemically milling. Chemically milling, as a final step before testing, can be controlled much more easily than mechanical removal, which has a multitude of variables, each requiring a control and an effect relationship which is undoubtedly different for each material. Chemically milling has two major variables: rate of removable, depending primarily on solution strength and temperature, and amount or thickness of material that must be removed to dissipate effects of prior machining. These variables would be somewhat dependent on material, but could be evaluated in a relatively brief program.

The effect of glass shot peening on fatigue behavior for the two forged materials was somewhat disappointing, i.e., the fatigue limit was not improved. A shot peening intensity of 0.010A is within the specifications (MIL-S-13165B) recommended for titanium, but may have been excessive for titanium in this annealed condition. A rather extensive fatigue evaluation of shot peening parameters for titanium is indicated. Such an evaluation should include a two-step process, steel shot followed by glass shot, where the steel shot can be used at a higher intensity, if needed, without breakage and the glass shot is used to remove contamination. Such a process has been reported by others to significantly improve the fatigue strength of titanium.⁶

The chemically milled beta-forged material gave some indication of an aging phenomena, i.e., fatigue strength increased with time. Six additional tests conducted on this material did not provide sufficient evidence of aging behavior. More extensive testing would be required to establish this.

⁶ AFML discussion with Steel Improvement Corporation.

APPENDIX

TABLES

Table VII Cross Reference between Forging Serial Number and Material Condition

Forging serial number	Forging condition	Heat treatment
1 thru 7, 20, 21, 22, 26, 27	Conventional ($T_B - 80^\circ\text{F}$)	Annealed*
8, 9, 10, 30	Beta ($T_B + 50^\circ\text{F}$)	Annealed
11, 12, 13, 31 thru 38	Beta ($T_B + 120^\circ\text{F}$)	Annealed
14, 15, 16	Beta ($T_B + 270^\circ\text{F}$)	Annealed
17, 18, 19, 20a, 23, 24, 25	Two Stage ($T_B + 270^\circ\text{F}$ and $T_B - 80^\circ\text{F}$)	Annealed
28, 29	Beta ($T_B + 50^\circ\text{F}$)	STA [†]
*1300°F for 2 hr, AC.		
[†] 1725°F for 1 hr, W.Q., 1000°F for 4 hr, AC.		

Table VIII Fatigue Data for Conventional-Forged ($T_B - 80^\circ F$) and Annealed 6Al-4V Titanium Alloy

Stress ratio								
A = ∞			A = 0.9			A = 0.33		
Specimen ID no.	Maximum stress (ksi)	Cycles to failure	Specimen ID no.	Maximum stress (ksi)	Cycles to failure	Specimen ID no.	Maximum stress (ksi)	Cycles to failure
1-1	99.0	1.00×10^4	2-10	125.0	3.20×10^4	4-10	140.0	2.35×10^4
4-12	90.0	3.10×10^4	1-3	120.0	6.10×10^4	4-11	135.0	4.40×10^4
1-2	80.0	3.60×10^4	2-11	120.0	6.90×10^4	4-4	130.0	1.30×10^5
1-5	75.0	3.80×10^4	2-5	115.0	1.12×10^5	4-3	120.0	3.10×10^5
5-10	75.0	5.60×10^4	2-9	115.0	5.27×10^5	4-2	110.0	4.90×10^5
7-5	72.5	1.16×10^5	1-11	110.0	7.40×10^4	4-1	100.0	1.38×10^6
2-6	70.0	5.51×10^5	1-10	100.0	3.00×10^5	4-5	95.0	2.19×10^6
2-12	70.0	1.09×10^6	1-6	95.0	1.21×10^6	4-6	90.0	2.76×10^6
7-9	68.0	4.09×10^5	1-12	90.0	1.83×10^6	4-7	85.0	1.68×10^6
2-7	65.0	9.21×10^6	1-9	85.0	2.22×10^6	4-8	85.0	3.55×10^6
1-4	60.0	9.86×10^6 *	1-7	75.0	5.59×10^6	4-9	80.0	$1.03 \times 10^{7*}$

*Test discontinued.

Table IX Notched* Fatigue Data for Conventional-Forged ($T_B - 80^\circ F$) and Annealed 6Al-4V Titanium Alloy

Stress ratio								
A = ∞				A = 0.9				
Specimen ID no.	Maximum stress (ksi)	Cycles to failure	Specimen ID no.	Maximum stress (ksi)	Cycles to failure	Specimen ID no.	Maximum stress (ksi)	Cycles to failure
6-1	50.0	9.0 × 10 ³	3-1	90.0	5.0 × 10 ³	5-3	90.0	2.40 × 10 ⁴
6-9	45.0	1.40 × 10 ⁴	3-2	70.0	1.50 × 10 ⁴	5-2	80.0	4.10 × 10 ⁴
6-8	45.0	1.50 × 10 ⁴	3-4	60.0	3.60 × 10 ⁴	5-1	70.0	2.10 × 10 ⁵
6-2	40.0	6.60 × 10 ⁴	3-6	57.5	5.50 × 10 ⁴	5-4	60.0	5.07 × 10 ⁵
6-10	35.0	1.36 × 10 ⁵	3-5	55.0	4.79 × 10 ⁵	6-7	55.0	2.61 × 10 ⁵
7-10	32.5	1.20 × 10 ^{7†}	3-3	50.0	7.24 × 10 ⁵	7-2	52.5	7.18 × 10 ⁵
6-3	30.0	2.47 × 10 ⁵	3-7	45.0	2.00 × 10 ⁶	5-5	50.0	3.03 × 10 ⁵
5-9	30.0	2.26 × 10 ⁶	3-8	42.5	1.88 × 10 ⁶	5-6	45.0	2.81 × 10 ⁶
7-6	27.5	1.02 × 10 ^{7†}	3-10	40.0	1.68 × 10 ⁶	5-7	40.0	4.32 × 10 ⁶
6-12	25.0	1.69 × 10 ^{7†}	3-12	40.0	2.14 × 10 ⁶	5-8	35.0	1.02 × 10 ⁷
6-5	20.0	1.05 × 10 ^{7†}	3-11	35.0	1.57 × 10 ⁶			
			6-11	35.0	4.32 × 10 ⁶			
			3-9	30.0	1.28 × 10 ^{7†}			
*K _t = 3.0.								
†Test discontinued.								

Table X Fatigue Data* for Beta-Forged ($T_B + 50^\circ\text{F}$) and Annealed 6Al-4V Titanium Alloy

Smooth			Notched ($K_t = 3.0$)		
Specimen ID no.	Maximum stress (ksi)	Cycles to failure	Specimen ID no.	Maximum stress (ksi)	Cycles to failure
8-7	130.0	6.0×10^3	10-5	80.0	7.0×10^3
8-11	125.0	2.30×10^4	8-4	71.0	2.30×10^4
9-5	120.0	4.70×10^4	10-1	70.0	1.50×10^4
9-1	120.0	4.35×10^5	10-3	60.0	1.90×10^4
9-2	115.0	2.47×10^5	10-6	60.0	3.20×10^4
9-6	110.0	3.12×10^5	10-4	55.0	1.20×10^5
9-10	105.0	2.64×10^5	10-2	50.0	7.10×10^5
9-8	100.0	8.72×10^5	10-11	47.5	2.07×10^5
9-7	95.0	1.24×10^6	10-12	47.5	1.06×10^6
8-3	92.5	1.16×10^6	10-7	45.0	9.40×10^4
9-4	90.0	8.21×10^6 †	10-10	45.0	1.73×10^7 †
			10-9	40.0	1.47×10^7 †
* A = 0.9.					
† Test discontinued.					

Table XI Fatigue Data for Beta-Forged ($T_B + 50^\circ\text{F}$) and Solution-Treated and Aged 6Al-4V Titanium Alloy

Stress ratio					
A = ∞			A = 0.9		
Specimen ID no.	Maximum stress (ksi)	Cycles to failure	Specimen ID no.	Maximum stress (ksi)	Cycles to failure
29-5	110.0	6.0×10^3	28-7	140.0	2.00×10^4
29-9	100.0	2.10×10^4	28-5	135.0	3.10×10^4
29-1	90.0	2.70×10^4	28-1	130.0	1.23×10^5
29-6	85.0	5.30×10^4	28-9	125.0	2.72×10^5
29-11	80.0	7.27×10^5	28-11	120.0	3.71×10^5
29-2	80.0	7.81×10^5	28-4	115.0	5.55×10^5
29-7	75.0	2.79×10^5	28-10	110.0	1.63×10^6
29-4	72.5	6.43×10^6	28-2	105.0	8.40×10^5
29-10	70.0	3.60×10^6	28-3	100.0	2.53×10^6
29-12	70.0	7.50×10^6	28-6	95.0	3.31×10^6
			28-12	90.0	1.00×10^7 †
† Test discontinued.					

Table XII Fatigue Data for Beta-Forged ($T_B + 120^\circ F$) and Annealed 6Al-4V Titanium Alloy

Stress ratio								
A = ∞				A = 0.9			A = 0.33	
Specimen ID no.	Maximum stress (ksi)	Cycles to failure	Specimen ID no.	Maximum stress (ksi)	Cycles to failure	Specimen ID no.	Maximum stress (ksi)	Cycles to failure
32-11	100.0	9.0×10^3	11-12	130.0	1.40×10^4	32-8	140.0	4.90×10^4
32-1	90.0	2.80×10^4	11-3	120.0	2.40×10^4	31-3	135.0	5.30×10^4
32-3	85.0	5.00×10^4	11-2	120.0	2.80×10^4	31-2	130.0	1.02×10^5
32-4	80.0	4.40×10^4	11-5	115.0	3.60×10^4	31-8	125.0	1.28×10^5
32-6	70.0	4.40×10^4	11-6	110.0	4.30×10^4	31-6	122.5	1.34×10^5
32-5	70.0	8.20×10^4	11-1	110.0	1.30×10^5	31-5	120.0	1.27×10^5
32-7	65.0	1.04×10^5	11-9	105.0	6.90×10^4	31-10	120.0	1.13×10^5
32-10	60.0	1.58×10^5	11-7	100.0	3.45×10^5	31-12	117.5	3.12×10^5
13-1	59.0	8.4×10^4	11-10	95.0	9.11×10^5	31-7	115.0	1.59×10^5
38-5	59.0	1.29×10^5	11-11	90.0	1.25×10^5	31-11	115.0	2.06×10^5
38-10	58.0	5.90×10^5	11-12	85.0	1.03×10^7 *	31-1	110.0	1.03×10^7 *
31-9	57.5	1.08×10^7 *						
32-11	55.0	1.02×10^7 *						

*Test discontinued.

Table XIV Fatigue Data* for Beta-Forged ($T_B + 270^\circ F$) and Annealed 6Al-4V Titanium Alloy

Smooth			Notched ($K_t = 3.0$)		
Specimen ID no.	Maximum stress (ksi)	Cycles to failure	Specimen ID no.	Maximum stress (ksi)	Cycles to failure
16-9	125.0	1.80×10^4	14-11	75.0	8.0×10^3
15-2	120.0	1.00×10^4	14-10	70.0	1.20×10^4
15-7	115.0	1.36×10^5	14-6	65.0	3.40×10^4
15-6	110.0	2.59×10^5	14-3	60.0	3.50×10^4
15-4	105.0	6.90×10^4	14-4	55.0	9.50×10^4
16-4	105.0	2.86×10^5	14-1	53.0	4.51×10^5
15-9	100.0	4.20×10^4	14-12	50.0	1.29×10^6
15-3	100.0	5.00×10^4	14-5	45.0	8.90×10^4
16-8	100.0	8.93×10^5	14-8	45.0	4.32×10^6
15-12	95.0	1.68×10^6	14-2	40.0	7.03×10^6
15-8	90.0	2.20×10^6	14-11	35.0	$1.01 \times 10^{7\dagger}$
15-11	85.0	1.59×10^6			
16-1	85.0	3.14×10^6			
16-12	80.0	5.02×10^6			
*A = 0.9.					
†Test discontinued.					

Table XV Fatigue Data for Two-Stage-Forged and Annealed 6Al-4V Titanium Alloy

Stress ratio							
A = ∞				A = 0.9			
Specimen ID no.	Maximum stress (ksi)	Cycles to failure	Specimen ID no.	Maximum stress (ksi)	Cycles to failure	Specimen ID no.	Maximum stress (ksi)
17-3	100.0	2.50 x 10 ⁴	19-2	125.0	1.60 x 10 ⁴	18-1	145.0
17-12	95.0	8.00 x 10 ³	19-6	120.0	5.60 x 10 ⁴	18-9	140.0
17-4	90.0	1.60 x 10 ⁴	19-8	115.0	4.02 x 10 ⁵	18-6	130.0
17-9	85.0	2.40 x 10 ⁴	19-10	110.0	4.80 x 10 ⁴	17-2	125.0
17-6	80.0	4.30 x 10 ⁴	19-4	105.0	6.97 x 10 ⁵	19-7	125.0
17-8	75.0	6.60 x 10 ⁴	19-8	100.0	4.70 x 10 ⁵	18-3	120.0
17-10	70.0	6.00 x 10 ⁴	19-9	90.0	1.49 x 10 ⁶	18-10	115.0
17-7	70.0	1.33 x 10 ⁶	18-2	85.0	1.58 x 10 ⁶	18-7	115.0
20a-1	65.0	5.70 x 10 ⁴	18-4	80.0	2.78 x 10 ⁶	18-11	110.0
17-11	65.0	6.40 x 10 ⁴	18-8	75.0	1.31 x 10 ⁷ *	18-1	100.0
20a-5	65.0	2.45 x 10 ⁶					
18-12	60.0	5.63 x 10 ⁶					
18-4	56.0	1.00 x 10 ⁷ *					
*Test discontinued.							

Table XVI Notched* Fatigue Data for Two-Stage-Forged and Annealed 6Al-4V Titanium Alloy

Stress ratio								
A = ∞			A = 0.9			A = 0.33		
Specimen ID no.	Maximum stress (ksi)	Cycles to failure	Specimen ID no.	Maximum stress (ksi)	Cycles to failure	Specimen ID no.	Maximum stress (ksi)	Cycles to failure
24-2	60.0	4.0×10^3	23-11	80.0	1.00×10^4	25-11	100.0	1.60×10^4
24-4	50.0	1.10×10^4	23-10	70.0	2.10×10^4	25-10	95.0	2.10×10^4
24-11	47.5	1.30×10^4	23-9	65.0	2.80×10^4	25-8	90.0	2.70×10^4
24-8	45.0	2.70×10^4	23-8	61.0	2.20×10^4	25-7	85.0	3.20×10^4
24-3	40.0	5.20×10^4	23-7	55.0	1.03×10^5	25-4	80.0	4.50×10^4
24-10	37.5	1.04×10^5	23-5	50.0	9.40×10^5	25-5	75.0	4.20×10^4
24-6	35.0	2.04×10^5	23-12	50.0	1.01×10^6	25-3	70.0	1.52×10^5
24-9	32.5	3.15×10^5	23-2	45.0	1.42×10^6	25-2	65.0	1.55×10^5
24-7	30.0	5.22×10^6	23-1	40.0	3.93×10^6	25-1	60.0	1.78×10^6
25-6	27.5	1.00×10^7 [†]	23-3	35.0	1.02×10^7 [†]	25-12	55.0	3.52×10^6
*K _t = 3.0.								
†Test discontinued.								

Table XVII Fatigue Data* for Conventionally Forged 6Al-4V
Titanium Alloy with the Indicated Surface Condition

Surface condition								
Lathe turned			Ground			Chemically milled		
Specimen ID no.	Maximum stress (ksi)	Cycles to failure	Specimen ID no.	Maximum stress (ksi)	Cycles to failure	Specimen ID no.	Maximum stress (ksi)	Cycles to failure
20-12	145.0	6.0×10^3	21-2	140.0	1.10×10^4	22-12	140.0	1.00×10^4
20-10	135.0	1.20×10^4	21-9	130.0	3.70×10^4	22-5	130.0	2.80×10^4
20-9	130.0	5.80×10^4	21-7	120.0	5.80×10^4	22-3	120.0	3.10×10^4
20-6	120.0	7.30×10^4	21-6	115.0	7.80×10^4	22-6	110.0	4.40×10^4
20-2	120.0	1.96×10^5	21-5	110.0	4.97×10^5	22-2	100.0	7.40×10^4
20-5	110.0	4.99×10^5	21-3	105.0	5.21×10^5	22-7	90.0	8.90×10^4
20-7	100.0	5.97×10^5	21-1	100.0	8.80×10^5	22-8	82.5	9.48×10^5
20-4	90.0	1.54×10^6	21-8	95.0	2.04×10^6	22-9	80.0	1.29×10^6
20-11	85.0	2.30×10^6	21-11	90.0	1.43×10^6	22-11	75.0	4.81×10^5
20-12	80.0	$1.11 \times 10^{7\dagger}$	21-12	87.5	4.21×10^6	22-10	70.0	4.00×10^6
						22-12	65.0	$1.54 \times 10^{7\dagger}$

*A = 0.9.

†Test discontinued.

Table XVIII Fatigue Data* for Conventionally Forged 6Al-4V
Titanium Alloy with the Indicated Surface Condition

Surface condition					
Lathe turned and shot peened			Ground and shot peened		
Specimen ID no.	Maximum stress (ksi)	Cycles to failure	Specimen ID no.	Maximum stress (ksi)	Cycles to failure
26-5	135.0	1.50×10^4	27-6	140.0	7.0×10^3
26-6	130.0	1.50×10^4	27-5	135.0	3.80×10^4
26-4	130.0	2.96×10^5	27-3	130.0	1.44×10^5
26-3	125.0	9.20×10^4	27-2	125.0	3.85×10^5
26-1	120.0	3.46×10^5	27-1	120.0	6.17×10^5
26-2	115.0	5.78×10^5	27-4	115.0	5.44×10^5
26-7	110.0	9.22×10^5	27-7	110.0	1.05×10^6
26-8	105.0	5.09×10^5	27-9	105.0	1.60×10^6
26-9	100.0	1.34×10^6	27-10	100.0	5.05×10^5
26-10	95.0	8.42×10^5	27-8	100.0	1.18×10^6
26-11	95.0	9.21×10^5	27-11	95.0	1.14×10^6
26-12	90.0	2.18×10^6	27-12	90.0	2.18×10^6
6-6	80.0	1.51×10^6	21-4	80.0	3.49×10^6
20-13	70.0	3.38×10^6	22-4	70.0	6.84×10^6
5-11	60.0	$1.00 \times 10^{7\dagger}$	21-10	60.0	6.08×10^6
			22-1	55.0	$1.03 \times 10^{7\dagger}$
*A = 0.9.					
[†] Test discontinued.					

Table XIX Fatigue Data* for Beta-Forged ($T_B + 120^\circ\text{F}$) 6Al-4V
Titanium Alloy With the Indicated Surface Condition

Surface condition					
Lathe turned			Ground		
Specimen ID no.	Maximum stress (ksi)	Cycles to failure	Specimen ID no.	Maximum stress (ksi)	Cycles to failure
38-7	130.0	3.0×10^3	37-1	130.0	2.30×10^4
36-4	130.0	3.10×10^4	37-2	120.0	1.40×10^4
36-5	123.0	1.50×10^4	37-3	115.0	2.20×10^4
36-3	120.0	4.00×10^4	37-5	110.0	3.10×10^4
36-6	115.0	3.00×10^4	37-4	105.0	6.40×10^5
36-1	110.0	5.96×10^5	37-6	100.0	3.60×10^4
36-7	105.0	1.02×10^5	37-11	100.0	1.84×10^5
36-2	100.0	4.97×10^5	37-9	95.0	5.45×10^5
36-8	95.0	1.10×10^6	37-8	90.0	3.08×10^6
32-12	90.0	1.49×10^6	37-10	85.0	7.50×10^6
38-6	80.0	5.44×10^6	37-7	80.0	3.22×10^6
38-7	77.0	$1.01 \times 10^{7\dagger}$			
*A = 0.9.					
\dagger Test discontinued.					

Table XX Fatigue Data* for Beta-Forged ($T_B + 120^\circ\text{F}$) 6Al-4V Titanium Alloy
with the Indicated Surface Condition

Surface condition					
Chemically milled			Lathe turned and shot peened		
Specimen ID no.	Maximum stress (ksi)	Cycles to failure	Specimen ID no.	Maximum stress (ksi)	Cycles to failure
33-9	130.0	1.80×10^4	35-2	130.0	7.0×10^3
33-12	120.0	3.00×10^4	35-3	125.0	1.30×10^4
38-9	115.0	2.60×10^4	35-1	120.0	1.97×10^5
32-6	110.0	3.50×10^4	35-4	115.0	1.54×10^5
33-5	100.0	5.90×10^4	35-5	112.0	1.40×10^4
38-8	95.0	1.90×10^6	35-6	110.0	3.50×10^4
33-6	90.0	7.40×10^4	35-7	100.0	3.24×10^5
33-8	85.0	1.24×10^5	35-9	95.0	6.47×10^5
37-12	83.0	$1.01 \times 10^{7+}$	35-10	90.0	7.40×10^5
33-9	80.0	$1.06 \times 10^{7+}$	35-11	80.0	4.00×10^6
33-7	79.0	3.81×10^6	35-12	75.0	$1.23 \times 10^{7+}$
33-10	77.0	4.15×10^6			
*A = 0.9.					
†Test discontinued.					

DISTRIBUTION LIST

AFML (MAAE/D. C. Watson) (9 Cys)	AFML (MAMC/J. Krochmal)
AFML (MAAE/A. Olevitch)	AFML (MAY)
AFML (MAA/W. P. Conrardy/J. Teres)	AFML (MAS)
AFML (MAAA/D. Shinn)	AVTM
AFML (MAAM)	ASD (ASNPD-30)
AFML (MAMP/P. Hendricks)	APT
AFML (MATB/G. W. Trickett)	ASEP
AFML (MAAM/Technical Library)	SEPS
AFML (MAMP/Dr. Pierce)	BWFRR (4 Cys)
AFML (MAMD/R. Donat)	AFAPL (STINFO)
AFML (MAAA/H. Zoeller)	ARZ
AFML (MAC)	FDT
AFML (MAN)	AFAPL (APRP/C. Donaldson)
AFML (MAMP/K. Elbaum)	AFAPL (APFT/C. Elrod)
AFML (MAMN/A. M. Adair)	AFSC (SEFSA/F. A. Hannon)
	ASD (ASNPD/Library)

SAMSO
AF Unit Post Office
Attn: P. M. Propp
Los Angeles, Calif. 90045

Hq USAF (AFCSAI)
Washington, D. C. 20330

Air University Library
Maxwell AFB, Alabama 36112

AFRPL
6593 Test Group
Edwards AFB, Calif. 93523

AFSC STLO(SCTL-5)
26 Federal Plaza, Suite 1313
New York, N. Y. 10003

AFSC STLO(SCTL-10)
AF Unit Post Office
Los Angeles, Calif. 90045

AFSC STLO(SCTL-9)
Dept of the Navy
Munitions Bldg.
Washington, D. C. 20360

AFSC STLO(SCTL-1)
424 Trapelo Road
Waltham Federal Center
Waltham, Mass. 02154

AFSC STLO(SCTL-7)
c/o The Boeing Company
Seattle, Washington 98124

AFSC STLO(SCTL-2)
O'Hara Office Center
3166 Des Plaines Ave.
Des Plaines, Ill. 60018

Hq AFSC (SCAP)
Andrews AFB, Wash., D. C. 20331

AFSC STLO(SCTL-3)
227 Federal Office Bldg.
1240 East 9th Street
Cleveland, Ohio 44199

AFSC STLO(SCTL-4)
500 S. Ervay Street
Dallas, Texas 75201

AFSC STLO(SCTL-11)
Building 309
Aberdeen Proving Ground, Md. 21005

AFSC STLO(SCTL-13)
P. O. Drawer 942
APO New York 09827

AFSC STLO(SCTL-16)
US Naval Army Dev. Center
Johnsville, Warminster, Pa. 18974

AFSC STLO(RTSNM/Maj. L. Marlow)
Naval Missile Center
Bldg 36, Rm. 1074
Point Mugu, Calif. 93041

AFSC STLO (SCTL-19)
Naval Research Lab.
Washington, D. C. 20390

AFSC STLO(SCTL-23)
Lewis Research Center (NASA)
21000 Brookpark Road
Cleveland, Ohio 44135

AFSC STLO(SCTL-21)
Langley Research Center (NASA)
Langley AFB, Va. 23365

AFSC STLO(SCTL-20)
Ames Research Center (NASA)
Moffett Field, Calif. 94035

AFSC STLO (SCTL-12)
Bldg 5101
Edgewood Arsenal, Md. 21010

AFSC STLO(SCTL-6)
363 South Taaffe Ave., Suite 104
Sunnyvale, Calif. 94086

Federal Aviation Agency
Attn: B. Grochal
Washington, D. C. 20390

Dept of the Navy
Bureau of Weapons
Attn: Mr. N. Promisel
21st & Constitution Avenue
Washington, D. C. 20025

Dept of the Navy
Naval Air Systems Command
Attn: R. Schmidt
AIR-520311, Rm. 2W96
Washington, D. C. 20360

Mechanical Properties Data Center
Attn: A. J. Belfour
Belfour Stulen, Inc.
13919 West Bay Shore Drive
Traverse City, Mich. 49684

AFFIC (FTAT-2/Tech Library)
Edwards AFB, Calif. 93523

Naval Research Labs.
Mechanics Dept.
Attn: G. Irwin
Washington, D. C. 20390

SAMSO (SMSDI, J. Dougherty)
AF Unit Post Office
Los Angeles, Calif. 90045

Office of Supersonic Transport Div.
Federal Aviation Agency
Washington, D. C. 20590

Naval Air Engineering Center
Aeronautical Structures Lab (S-3)
Attn: M. Rosenfeld
Philadelphia, Pa. 19112

US Naval Research Library
Attn: Librarian
Washington, D. C. 20390

Commander
Naval Air Development Center
Attn: Tech Library
Johnsville, Pa. 18974

Air Force Machinability Data Center
Attn: J. Maranchik, Jr.
Metcut Research Associates, Inc.
3980 Rosslyn Drive
Cincinnati, Ohio 45209

US Army Weapons Command
Rock Island Arsenal
Attn: G. Reinsmith
Rock Island, Ill. 61202

US Army Transportation Research Command
Attn: J. Daniel, Group Leader
Aeronautical Systems Group
Fort Eustis, Va. 23604

Watertown Arsenal
Attn: Tech Library
Watertown, Mass. 02172

NASA
Materials Research
Attn: R. Raring
600 Independence Ave.
Washington, D. C. 20546

National Aeronautics & Space Adm.
Attn: M. G. Rosche
(Adv. Research Programs Structures)
1512 H. St., N. W.
Washington, D. C. 20390

US Army Materials Research Agency
AMXMR-TMS (T. E. Dunn, Jr.)
Watertown, Mass. 02172

NASA
Lewis Research Center
Attn: W. Brown, Jr.
21000 Brookpark Road, Mail Stop 105-1
Cleveland, Ohio 44130

NASA
Goddard Space Flight Center
Attn: Technical Library
Greenbelt, Maryland 20770

NASA
George Marshall Space Flight Center
Materials Branch
Attn: Dr. R. Lucas
Huntsville, Ala. 35812

NASA
Manned Spacecraft Center
Attn: C. M. Grant
Technical Info. Center
Houston, Texas 77058

Defense Documentation Center
Cameron Station, Bldg. 5
5010 Duke Street
Alexandria, Va. 22314 (20 Cys)

Advanced Technology Labs.
Attn: Library
P. O. Box 370
Mt. View, California

Depts of the Navy & Air Force
Aeronautical Standards Group
Attn: M. J. Crane
8719 Colesville Road
Silver Spring, Maryland 20910

Aerojet-General Corp.
Attn: Tech Library
Downey, Calif. 90241

Aerojet-General Corp.
Attn: Tech Library
P. O. Box 1947
Sacramento, Calif 95809

Aerospace Corporation
Attn: Library
2400 E. El Segundo Blvd
El Segundo, Calif 90245

Aerospace Industries Assoc.
Attn: J. P. Reese
1725 DeSales St., N. W.
Washington, D. C. 20036

Aluminum Co. of America
Attn: N. H. Orr, Jr.
1200 Ring Bldg
Washington, D. C. 20036

Armco Steel Corp.
Attn: M. E. Carruthers
Research Labs
Middletown, Ohio 45042

Allvac Metal Co.
P. O. Box 759
Monroe, N. C.

Alcoa Application & Engineering Div.
Attn: C. L. Burton
2210 Harvard Ave.
Cleveland, Ohio 44105

Allegheny Ludlum Steel Co.
Research Center
Attn: R. A. Lula
Brackenridge, Pa. 15014

Avco Corporation
Avco Space Systems Div.
Attn: Dr. R. P. Murro
Lowell Industrial Park
Lowell, Mass. 01851

Avco Corporation
Attn: Tech Library
550 South Main Street
Stratford, Conn. 06497

Battelle Memorial Institute
Attn: A. F. Anderson
Structural Materials Engineering
Columbus, Ohio 43201

Battelle Memorial Institute
Attn: W. H. Hyler
Dept of Mechanical Eng.
505 King Avenue
Columbus, Ohio 43201

DMIC
Attn: R. J. Runck
c/o Battelle Memorial Institute
505 King Avenue
Columbus, Ohio 43201

Bell Aircraft Corporation
Attn: Tech Library
P. O. Box 1
Buffalo, N. Y. 14205

Bell Aircraft Corporation
Attn: N. MacKenzie
Chief Tech. Eng.
Fort Worth, Texas 76101

Bendix Aerospace Div.
Attn: C. S. Ades
717 Bendix Drive
South Bend, Ind. 46620

Bendix Aviation Corp.
Utica Division
Attn: H. A. Alexanderson
Utica, N. Y. 13503

The Bendix Corporation
Pioneer-Central Division
Attn: R. E. Pearson
Staff Engineer - Titanium
P. O. Box 707
Renton, Wash. 98055

Bendix Energy Controls Div.
717 North Bendix Drive
Attn: J. Grodrian
South Bend, Ind. 46620

Boeing Company
Aerospace Division
Attn: O. T. Ritchie
P. O. Box 3707, MS 45-83
Seattle, Wash. 98124

Boeing Company
Commercial Airplane Div.
Attn: R. V. Carter
P. O. Box 3733
Seattle, Wash. 98124

Boeing Company
Vertol Division
Attn: W. Lieberman
100 Woodland Ave.
Morton, Pa. 19070

Borg-Warner Corp.
Byron Jackson Div.
Attn: F. R. Srahas
P. O. Box 2017, Terminal Annex
Los Angeles, Calif. 90045

Case Institute of Technology
Dept of Metallurgical Engrg.
Metals Research Lab.
Cleveland, Ohio 44106

Cessna Aircraft Co.
Attn: J. Dussault
Chief of Structures
Wichita, Kansas 67201

Chrysler Corp. Missile Div.
Attn: Tech Info Center
P. O. Box 2628
Detroit, Mich. 48231

Cleveland Pneumatic Industries
Attn: J. A. Hakkio
3781 E. 77th Street
Cleveland, Ohio 44103

Continental Aviation & Eng. Corp.
Attn: J. W. Kinnucan, Vice Pres.
1500 Algonquin Avenue
Detroit, Mich. 48214

Consolidated Western Steel Div.
US Steel Corporation
Attn: W. A. Saylor
P. O. Box 2015, Terminal Annex
Los Angeles, Calif. 90045

Curtiss-Wright Corporation
Curtiss Division
Attn: Engineering Library
Caldwell, N. J. 07006

Curtiss-Wright Corporation
Wright Division
Attn: Library
Woodridge, N. J. 07075

Dow Chemical Co.
Metal Products Dept.
Attn: A. A. Moore
Hopkins Bldg.
Midland, Mich. 48640

Douglas Missiles & Space Div.
Attn: P. E. Denke
3000 Ocean Park Blvd.
Santa Monica, Calif. 90406

Fairchild Aircraft Division
Fairchild Engine & Airplane Corp.
Attn: E. Williams
Chief of Process & Materials
Hagerstown, Md. 21740

Ford Motor Company
Aeronutronic Division
Attn: W. M. Fassell
Newport Beach, Calif. 92660

Fairchild Hiller Corp.
Attn: W. C. Travis, Jr.
Republic Aviation Div.
Farmingdale, L.I., N. Y. 11735

Fifth Sterling Inc.
3113 Forbes Avenue
Pittsburgh, Pa. 15230

The Garret Corporation
Airesearch Manufacturing Co. Div.
Attn: Tech Library
9851-9951 Sepulveda Blvd.
Los Angeles, Calif. 90009

General Dynamics/Gen. Atomics
Attn: J. F. Watson
P. O. Box 608
San Diego, Calif. 92112

General Dynamics/Convair Div.
Attn: C. J. Kropp
P.O. Box 1128
Mail Zone 572-10
San Diego, California 92112

General Dynamics/Pomona
Structures & Materials Sec.
Pomona, Calif. 91766

General Dynamics/Fort Worth
Attn: O. N. Thompson
P. O. Box 748, Mail Zone T112
Fort Worth, Texas 76101

General Electric Company
Re-Entry Systems Dept.
Attn: A. W. Dickens
P. O. Box 8661 (CC&F2)
Philadelphia, Pa. 19101

General Electric Co.
Flight Propulsion Div.
Attn: E. L. Dunn
1 Jimson Road
Cincinnati, Ohio 45215

General Motors Corp.
Allison Div.
Attn: D. K. Hanink
Indianapolis, Ind. 46206

General Electric Co.
Attn: J. S. Mosier
Materials Dev. Lab
Main Drop M-88
Cincinnati, Ohio 45215

Goodyear Aircraft Corp.
Attn: R. S. Ross, Mgr.
Aeromechanics R&D
1210 Massillon Road
Akron, Ohio 43315

Grumman Aircraft Engr. Corp.
Attn: C. J. Shaver
Plant 5, Dept 690
Bethpage, N. Y. 11714

Hughes Aircraft Co.
Attn: Tech Document Center
Florence and Teale Street
Culver City, Calif. 90232

International Nickel Co., Inc.
Attn: K. M. Spicer
Tech Serv. Section
Huntington, West Va. 25717

Joliet Metallurgical Lab.
Attn: W. F. Carow
205 N. Republic Ave.
Joliet, Ill. 60435

Hi-Shear Corp.
Attn: M. M. Schuster
2600 W. 247th Street
Torrance, Calif. 90409

IIT Research Institute
35 West 33rd Street
Chicago, Ill. 60616

Kaiser Alum. & Chem. Corp.
Attn: L. J. Barker
300 Lakeside Dr.
Oakland, Calif.

Ladish Company
Attn: R. P. Daykin
Research & Metallurgy
Cudahy, Wisc. 53110

Ling-Temco-Vought Aerospace Corp.
Attn: G. A. Starr, Chief
Applied Research & Dev.
P. O. Box 5907
Dallas, Texas 75222

Lockheed Missiles & Space Co.
Attn: D. M. Lorimer
P. O. Box 504, Dept. 55-55
Sunnyvale, Calif. 94088

Lockheed California Co.
Attn: M. A. Melcon
Structural Methods Dept.
P. O. Box 551
Burbank, Calif. 91502

Lockheed California Co.
Attn: R. F. Simenz
P. O. Box 551
Burbank, Calif. 91503

Lockheed Aircraft Corp.
Attn: E. J. Bateh
Dept 72-26, Zone 263
86 So. Cobb Drive
Marietta, Ga. 30060

Marquardt Corporation
Attn: Technical Library
16555 Saticoy Street
Van Nuys, Calif. 91406

Martin Co/Denver Div.
Attn: Library Section
P. O. Box 179
Denver, Colorado 80201

Martin Orlando Corporation
Attn: C. N. Odell
Sand Lake Road
Orlando, Fla.

McDonnell Aircraft Corp.
Attn: R. Schoppman
P. O. Box 516
St. Louis, Missouri 63116

Metcut Research Associates, Inc.
Attn: Dr. J. F. Kahles
3980 Rosslyn Drive
Cincinnati, Ohio 45209

Midwest Research Institute
Attn: P. Bidstrup
425 Volker Blvd.
Kansas, City, Mo.

Narmco Research & Dev.
Attn: E. P. Carmichael
3540 Aero Court
San Diego, Calif. 92123

National Research Corp.
Tech, Info. Center
Attn: PC692JL, Mrs. Spitzer
70 Memorial Drive
Cambridge, Mass. 02139

New England Materials Lab., Inc.
Attn: Dr. R. Widman
35 Commercial Street
P. O. Box 128
Medford, Mass. 02155

North American Aviation, Inc.
4300 East Fifth Avenue
Attn: P. E. Ruff
Columbus, Ohio 43216

North American Aviation, Inc.
Attn: N. Klimmek
International Airport
Los Angeles, Calif. 90009

North American Aviation, Inc.
Space & Info Systems Div.
Attn: C. W. Haynes
12214 Lakewood Blvd.
Downey, Calif. 90241

National Screw & Manuf. Co.
Attn: Joseph Massa
2440 E. 75th Street
Cleveland, Ohio 44116

Northrop/Norair Division
Attn: D. R. Apodaca (3963-32)
3901 East Broadway
Hawthorne, Calif. 90250

Northrop/Ventura Division
Attn: Library
Materials Engineering
1515 Rancho Conejo
Newbury Park, Calif. 91320

Office of Research Analysis
Attn: Tech Library
Holloman AFB, N. Mexico 88330

Pratt & Whitney Aircraft Corp.
Attn: Library
362 S. Main St.
East Hartford, Conn. 06108

Pratt-Whitney Aircraft
Attn: Tech Library
P. O. Box 2691
West Palm Beach, Fla. 33402

Rand Corporation
Attn: Library
1700 Main Street
Santa Monica, Calif. 90406

Reactive Metals, Inc.
Attn: Walter Herman
1000 Warren Avenue
Niles, Ohio 44446

Republic Steel Corp.
Attn: J. A. Rinebolt
Massillon, Ohio 44117

Reynolds Metals Co.
Metallurgical Research Lab.
Attn: Research Library
Richmond, Va. 23200

Reynolds Metals Co.
Attn: W. E. Kelly
Richmond, Va. 23200

Rocket Propulsion Laboratory
Attn: DGRP (Maj. Arpke)
Edwards AFB, Calif. 93523

Ryan Aeronautical Company
Attn: L. J. Hull, Chief Metallurgist
Materials & Process Lab.
San Diego, Calif. 92212

Rosan Inc.
Headed Product Division
Attn: D. W. Schonfield
2901 W. Coast Highway
Newport Beach, Calif. 92663

Standard Pressed Steel Co.
SPS Laboratories
Technical Library
Jenkintown, Pa. 19046

Sikorsky Aircraft
333 W. First Street
Dayton, Ohio 45402

Solar, Div. of International Harvester
Attn: J. V. Long
Director of Research
2200 Pacific Highway
San Diego, Calif. 92101

Space Technology Labs., Inc.
Attn: Engr. Data Control
One Space Park
Redondo Beach, Calif. 90278

Space Technology Labs., Inc
Attn: Tech Library
P. O. Box 4277
Patrick AFB, Fla. 32925

Temco Missile & Aircraft
Materials & Processes
Attn: F. Jacobs, Group Eng.
P. O. Box 6191
Dallas, Texas 75222

Texas Instruments Inc.
Materials R&D Labs
13500 N. Central Expressway
Dallas, Texas 75222

Thiokol Chemical Corp.
Attn: Tech Library
Wasatch Division
Brigham City, Utah 84302

Thiokol Chemical Corp.
Attn: Library
Reaction Motors Div.
Danville, N. J. 07834

Thompson Ramo-Wooldridge, Inc.
Attn: E. A. Steigerwald
23555 Euclid Avenue
Cleveland, Ohio 44117

Sundstrand Aviation
Attn: W. G. Gibbons
4747 Harrison Avenue
Rockford, Ill. 61101

Titanium Metals Corporation
Attn: W. W. Minkler
V.P. Marketing
195 Clinton Road
West Caldwell, New Jersey 07006

Titanium Metals Corp. of America
Attn: R. G. Broadwell
195 Clinton Rd.
W. Cardwell, N. J. 07066

Titanium Metals Corp. of America
Attn: R. R. Vogel
6565 Corvette Street
Los Angeles, Calif. 90022

Williams Research Corp.
Attn: G. W. Rourke
2280 W. Maple Road
P. O. Box 95
Walled Lake, Mich. 48088

United Aircraft Corp.
Missiles & Space Systems Div.
Attn: Tech Library
440 Main Street
East Hartford, Conn. 06108

U.S. Steel Corporation
Attn: Library
P. O. Box 2015, Terminal Annex
Los Angeles, Calif. 90054

Westinghouse Research Labs.
Attn: Tech Library
Beulah Road, Chruchill Borough
Pittsburgh, Pa. 15235

B.F. Goodrich Aerospace & Defense Products
Attn: Engineering Librarian
P.O. Box 340
Troy, Ohio 45373

Wyman-Gordon Company
Attn: J. E. Coyne
Research & Dev. Dept.
Worcester, Mass. 01601

Sundstrand Corp/Aviation Div.
Attn: E. Erikson, Chief Eng.
Rockford, Ill. 61105

U.S. Steel Corporation
Attn: R. M. Buck
525 Wm. Penn Place
Pittsburgh, Pa. 15213

Voi-Shan Manuf. Co.
Attn: F. Tisch
8463 Higuere
Culver City, Calif 90230

Union Carbide Metals Co.
Attn: Tech Library
4625 Royal Ave.
P. O. Box 580
Niagra Falls, N. Y. 14202

Universal Cyclops Steel Corp.
Bridgeville Div.
Attn: Library
Station Street
Bridgeville, Pa. 15017

Douglas Aircraft Co.
Attn: R. J. Sutton, Dept CL-260
3855 Lakewood Blvd.
Long Beach, Calif. 90801

Douglas Aircraft Company
Attn: G. E. Bockrath
Dept A2-260
3000 Ocean Park Blvd.
Santa Monica, Calif. 90406

General Dynamics/Convair
Attn: D. E. Diller
P. O. Box 1128, Dept 587-30
San Diego, Calif. 92112

North American Aviation, Inc.
Attn: L. R. Spalding
Section Head, Materials
International Airport
Los Angeles, Calif. 90009

Unclassified

Security Classification

DOCUMENT CONTROL DATA - R&D

(Security classification of title, body of abstract and indexing annotation must be entered when the overall report is classified)

1. ORIGINATING ACTIVITY (Corporate author) Martin Marietta Corporation PO Box 179 Denver, Colorado 80201		2a. REPORT SECURITY CLASSIFICATION Unclassified	
		2b. GROUP	
3. REPORT TITLE EFFECT OF BETA PROCESSING AND FABRICATION ON AXIAL LOADING FATIGUE BEHAVIOR OF TITANIUM			
4. DESCRIPTIVE NOTES (Type of report and inclusive dates) 1968 April 01 thru 1969 March 31			
5. AUTHOR(S) (Last name, first name, initial) Beck, Emory			
6. REPORT DATE May 1969		7a. TOTAL NO. OF PAGES 108	7b. NO. OF REFS 7
8a. CONTRACT OR GRANT NO. F33615-68-C-1351		9a. ORIGINATOR'S REPORT NUMBER(S) MCR-69-140	
b. PROJECT NO 7381			
c. Task No. 738106		9b. OTHER REPORT NO(S) (Any other numbers that may be assigned this report) AFML-TR-69-108	
d.			
10. AVAILABILITY/LIMITATION NOTICES This document is subject to special export controls and each transmittal to foreign governments or foreign nationals may be made only with prior approval of the Air Force Materials Laboratory (MAAE), Wright-Patterson Air Force Base, Ohio 45433			
11. SUPPLEMENTARY NOTES		12. SPONSORING MILITARY ACTIVITY Air Force Materials Laboratory Air Force Systems Command Wright-Patterson Air Force Base, Ohio	
13. ABSTRACT <p>A single heat of 6Al-4V titanium has been die forged at conventional and beta forging temperatures. These forgings have been annealed, sectioned, and subsequently machined into tensile and fatigue test specimens. Notched and smooth fatigue specimens were tested in axial-loading fatigue machines at room temperature using three stress ratios. The data presented show that beta-forged material exhibits better fatigue strength than conventionally forged material, while tensile properties are nearly unaffected. A forging temperature at 120°F above the alpha-beta/beta transus was selected as the optimum forging temperature based on initial fatigue results at a single A-ratio of 0.9. This temperature was selected as a compromise between improved forgeability and the superior fatigue results realized for forging near the transus temperature. More extensive fatigue testing at various stress ratios revealed that the beta-forged material had a lower tolerance for the reversed load cycle ($A = \infty$) than the conventional forged material. Surface effect studies for the same heat of 6Al-4V titanium indicated that mechanical material removal in a controlled manner was not detrimental to fatigue strength but was of considerable benefit. Shot peening at an intensity of 0.010A did not improve the fatigue limit of conventional or beta-forged material.</p> <p>This document is subject to special export controls and each transmittal to foreign governments or foreign nationals may be made only with prior approval of the Air Force Materials Laboratory (MAAE), Wright-Patterson Air Force Base, Ohio 45433.</p>			

14. KEY WORDS	LINK A		LINK B		LINK C	
	ROLE	WT	ROLE	WT	ROLE	WT

INSTRUCTIONS

1. **ORIGINATING ACTIVITY:** Enter the name and address of the contractor, subcontractor, grantee, Department of Defense activity or other organization (*corporate author*) issuing the report.

2a. **REPORT SECURITY CLASSIFICATION:** Enter the overall security classification of the report. Indicate whether "Restricted Data" is included. Marking is to be in accordance with appropriate security regulations.

2b. **GROUP:** Automatic downgrading is specified in DoD Directive 5200.10 and Armed Forces Industrial Manual. Enter the group number. Also, when applicable, show that optional markings have been used for Group 3 and Group 4 as authorized.

3. **REPORT TITLE:** Enter the complete report title in all capital letters. Titles in all cases should be unclassified. If a meaningful title cannot be selected without classification, show title classification in all capitals in parenthesis immediately following the title.

4. **DESCRIPTIVE NOTES:** If appropriate, enter the type of report, e.g., interim, progress, summary, annual, or final. Give the inclusive dates when a specific reporting period is covered.

5. **AUTHOR(S):** Enter the name(s) of author(s) as shown on or in the report. Enter last name, first name, middle initial. If military, show rank and branch of service. The name of the principal author is an absolute minimum requirement.

6. **REPORT DATE:** Enter the date of the report as day, month, year; or month, year. If more than one date appears on the report, use date of publication.

7a. **TOTAL NUMBER OF PAGES:** The total page count should follow normal pagination procedures, i.e., enter the number of pages containing information.

7b. **NUMBER OF REFERENCES:** Enter the total number of references cited in the report.

8a. **CONTRACT OR GRANT NUMBER:** If appropriate, enter the applicable number of the contract or grant under which the report was written.

8b, 8c, & 8d. **PROJECT NUMBER:** Enter the appropriate military department identification, such as project number, subproject number, system numbers, task number, etc.

9a. **ORIGINATOR'S REPORT NUMBER(S):** Enter the official report number by which the document will be identified and controlled by the originating activity. This number must be unique to this report.

9b. **OTHER REPORT NUMBER(S):** If the report has been assigned any other report numbers (*either by the originator or by the sponsor*), also enter this number(s).

10. **AVAILABILITY/LIMITATION NOTICES:** Enter any limitations on further dissemination of the report, other than those

imposed by security classification, using standard statements such as:

- (1) "Qualified requesters may obtain copies of this report from DDC."
- (2) "Foreign announcement and dissemination of this report by DDC is not authorized."
- (3) "U. S. Government agencies may obtain copies of this report directly from DDC. Other qualified DDC users shall request through _____."
- (4) "U. S. military agencies may obtain copies of this report directly from DDC. Other qualified users shall request through _____."
- (5) "All distribution of this report is controlled. Qualified DDC users shall request through _____."

If the report has been furnished to the Office of Technical Services, Department of Commerce, for sale to the public, indicate this fact and enter the price, if known.

11. **SUPPLEMENTARY NOTES:** Use for additional explanatory notes.

12. **SPONSORING MILITARY ACTIVITY:** Enter the name of the departmental project office or laboratory sponsoring (*paying for*) the research and development. Include address.

13. **ABSTRACT:** Enter an abstract giving a brief and factual summary of the document indicative of the report, even though it may also appear elsewhere in the body of the technical report. If additional space is required, a continuation sheet shall be attached.

It is highly desirable that the abstract of classified reports be unclassified. Each paragraph of the abstract shall end with an indication of the military security classification of the information in the paragraph, represented as (TS), (S), (C), or (U).

There is no limitation on the length of the abstract. However, the suggested length is from 150 to 225 words.

14. **KEY WORDS:** Key words are technically meaningful terms or short phrases that characterize a report and may be used as index entries for cataloging the report. Key words must be selected so that no security classification is required. Identifiers, such as equipment model designation, trade name, military project code name, geographic location, may be used as key words but will be followed by an indication of technical context. The assignment of links, rules, and weights is optional.